ANL/OEPM-82-5

ANL/OEPM-82-5

DEVELOPMENT OF AQUEOUS BATTERIES FOR ELECTRIC VEHICLES

Summary Report
October 1980 – September 1981

ARGONNE NATIONAL LABORATORY, ARGONNE, ILLINOIS

Prepared for the U. S. DEPARTMENT OF ENERGY
under Contract W-31-109-Eng-38

Distribution Category:
Energy Storage—Electrochemical--
Near-Term Batteries (UC-94ca)

ANL/OEPM-82-5

ANL/OEPM--82-5

DE83 012459

ARGONNE NATIONAL LABORATORY
9700 South Cass Avenue
Argonne, Illinois 60439

DEVELOPMENT OF AQUEOUS BATTERIES FOR ELECTRIC VEHICLES

Summary Report
October 1980—September 1981

by

The Office for Electrochemical Project Management
Chemical Engineering Division

May 1982

Previous reports

ANL/OEPM-80-5	October 1977—September 1979
ANL/OEPM-81-5	October 1979—September 1980

TABLE OF CONTENTS

LIST OF FIGURES

LIST OF TABLES

FOREWORD

This ongoing work is performed by the Argonne National Laboratory (ANL) under contract W-31-109-Eng-38 for the Department of Energy. The work is part of DOE's Electric and Hybrid Vehicle (EHV) Program being conducted in response to Public Law 94-413, mandated by the Congress in September 1976 and amended later by Public Law 95-238 in March 1978. The overall objective of the DOE's EHV Program is to carry out the R&D required in EHV components and systems so as to accelerate the widespread use of EHV's, thus resulting in reduction of petroleum use in the transportation sector. Toward these objectives, four program elements have been established by the DOE. They are the (1) Electric Vehicle Project (2) Hybrid Vehicle Project (3) Advanced Vehicle Development Project and (4) Testing and Evaluation. The current aqueous mobile battery development and testing effort is in support of the Electric Vehicle Project.

The Office for Electrochemical Project Management (OEPM) at ANL is the Project Field Office responsible for the development and testing of aqueous mobile batteries amenable to production in the late 1980's. The battery candidates are improved lead-acid, nickel/iron and nickel/zinc systems. The ANL/OEPM battery project utilizes an industry-based approach whereby industry carries out the major part in the battery technology development and ANL/OEPM provides technical management and in-house support for battery verification testing and relevant support research.

ANL/OEPM initiated eight major industrial contracts for the battery technology development early in 1978: three in lead-acid, two in nickel/iron and three in nickel/zinc. Each contractor pursued a parallel, but differing technical approach offering promise of meeting the project objectives. The ANL National Battery Test Laboratory (NBTL) provides technology verification testing of the full-size cells, modules, and batteries delivered by the industrial contractors on a scheduled basis. ANL/OEPM also provides timely research support on those topics that are critical or applicable to the advancement of the technologies.

This summary report represents an interim progress report for the period of October 1980 through September 1981. The report summarizes the approach and results of the industrial contractor research and development, the verification testing at NBTL, the support research activities, the research and development in battery components, the battery/vehicle system integration activities, and an assessment of the hybrid vehicle battery requirements. As the contractors' efforts are detailed in their individual annual reports, a larger fraction of this summary report relates to in-house activities at ANL.

The Aqueous Mobile Battery Research Program is implemented at ANL through a team composed of management technical staff and support personnel. Each team member provides a focused and expert contribution to the project. Members of the ANL/Aqueous Mobile Battery Program Team responsible for specific management and task leadership areas are:

Dr. N. P. Yao, Project Manager and Director, OEPM
Mr. C. C. Christianson, Deputy Project Manager
Mr. F. Hornstra, Manager, NBTL
Dr. T. Lee, Technical Monitor, Lead-Acid Contracts
Mr. J. Rajan, Technical Monitor, Nickel/Iron Contracts
Dr. J. Miller, Technical Monitor, Nickel/Zinc Contracts
Dr. G. Cook, Group Leader, Battery Support Research
Mr. W. DeLuca, Group Leader, Battery Components
Mr. F. Foster, Contract Administrator
Mr. J. Geller, Quality Assurance Engineer

ACKNOWLEDGEMENTS

Support of this work was provided by DOE's Electric and Hybrid Vehicle (EHV) and Energy Storage (STOR) Divisions within the Office of Deputy Assistant Secretary for Conservation and Solar Energy. The DOE Headquarters Program Manager is Dr. A. R. Landgrebe.

Major technical contributions were made by ANL's industrial contractors, namely Exide, Globe Division of Johnson Controls, Eltra, Westinghouse, Eagle-Picher, Gould, and Energy Research Corporation.

Members of the OEPM team who contributed sections of this report are N. P. Yao, J. B. Rajan, T. S. Lee, J. F. Miller, F. Hornstra, G. M. Cook, W. DeLuca, J. Klinger, D. Poa, J. Waters, J. Lee and J. J. Barghusen. The section on modeling of materials supply/demand relationships was provided by L. G. Hill of the EES Division at Argonne National Laboratory.

This report was compiled and edited by J. B. Rajan under the direction of and with input from C. C. Christianson.

ABSTRACT

This report summarizes the results and status of activities in the Aqueous Mobile Battery Research Program of the Argonne National Laboratory (ANL) for FY 1981. This program, under ANL's Office for Electrochemical Project Management (OEPM), conducts R&D on lead-acid, nickel/iron and nickel/zinc batteries for electric vehicles. The bulk of the R&D is performed by eight industrial contractors. Performance verification testing of contractor supplied cells, modules, and batteries is performed by ANL's National Battery Test Laboratory (NBTL). Various supporting research activities in specific areas of critical need are conducted by ANL. Since contractor R&D progress is detailed in separate annual reports, this report stresses the progress of ANL in-house activities.

Key results of the R&D indicate major technology advancements since the project inception in FY 1978 and achievement of most of FY 1981 performance goals. In the lead-acid system, the specific energy was increased from less than 30 Wh/kg to 41 Wh/kg at the C/3 rate; the specific peak power improved from 96 W/kg to 104 W/kg at the 50% state of charge; and a cycle life of over 481 deep-discharge cycles in continuing tests has been demonstrated. In the nickel/iron system, a specific energy of 48 Wh/kg, a peak power of 103 W/kg, and a life of over 740 cycles in ongoing tests was obtained. In the nickel/zinc system, specific energies of up to 68 Wh/kg, peak powers of 131 W/kg, and a life of 179 cycles was measured. Future R&D will emphasize increased specific energy and cycle life for lead-acid batteries, and improved specific energy and reduced costs for nickel/iron batteries. Future R&D on nickel/zinc batteries will be directed at solving the present problem of limited cycle life.

Testing of 555 cells was completed by NBTL as of the end of FY 1981. In addition, post-test analysis of failed batteries was carried out during FY 1981. Significant advances in testing capability were implemented during FY 1981, including the installation of a peak power test station, three environmental chambers, and computer-controlled load banks which simulate the power profiles imposed on a battery by an electric vehicle.

In technology-supporting research at ANL, detailed charging and discharging studies have identified improved charging procedures which optimize battery capacity and efficiency. In fundamental electrode studies, neutron diffraction experiments on lead-acid battery active materials have revealed chemical changes in addition to electrochemical transformations; a relationship between charge efficiency and state-of-charge was established for nickel electrodes; and a model describing mass transfer characteristics at vibrating electrodes was developed. Models for predicting the thermal and electrical behavior of batteries were also developed. An evaluation of the availability and cost of critical battery materials was made. A preliminary assessment of the battery requirements for the electric hybrid vehicle was completed.

EXECUTIVE SUMMARY

The Electric and Hybrid Vehicle Research, Development and Demonstration Act of 1976 (PL 94-413), later amended in March 1978 by PL 95-238, provides for the development of improved batteries for electric vehicle propulsion. This activity is performed as part of the Department of Energy's Electric Vehicle (EV) Project. The EV Project's objective is to maximize the national petroleum savings potential of the electric vehicle by accelerating the advancement of related technologies to levels that are conducive to significant market penetration. This would lead to a reduction in petroleum use by the transportation sector. The development of improved battery technology is a major part of the EV Project. The Office for Electrochemical Project Management (OEPM) at Argonne National Laboratory (ANL) was assigned project management responsibility by DOE for the development of those improved battery systems considered to be suitable for late 1980's application in electric vehicles. Three battery systems were identified by OEPM as likely candidates for improvement and incorporation in electric vehicles by the late 1980's. These are the lead-acid, nickel/iron and nickel/zinc batteries. The bulk of the R&D efforts on these batteries is carried out on a cost sharing basis by industrial organizations who were competitively selected by OEPM in 1977-1978. These contractors follow a pre-established statement-of-work and submit regular progress reports to OEPM. They also send cells, modules and batteries to the National Battery Test Laboratory (NBTL) at Argonne for test verification of their technical progress.

Associated program activities by OEPM include several interactive tasks collectively aimed at the development of aqueous battery technology. These technical activities include:

- Verification testing of contractor fabricated cells and batteries at the NBTL
- Battery analysis and optimization studies
- Support research in areas of critical need
- Post-test analysis of cells and batteries
- Development of supporting technologies such as separators
- Techniques for charging and state of charge monitoring
- Preparation of battery application information for vehicle/system developer use
- Support and/or monitoring of in-vehicle engineering tests of experimental batteries that incorporate technology from this program
- Support of battery/vehicle system integration studies to ensure compatibility of R&D goals with vehicle needs
- Assessment of battery requirements for the hybrid vehicle

Progress from program initiation through FY 1980 is provided in two earlier reports.[17,18] The progress in FY 81 is summarized in this report. The R&D efforts of the contractors have been presented in technical reports.[10-16] Thus, this report provides only a brief overview of contractor activities and gives much greater emphasis to the in-house ANL activities which in many cases have not been published elsewhere. For completeness, a brief summary is also included of relevant non-ANL research activities such as those at Lawrence Berkeley Laboratory (LBL) and other laboratories.

Battery Contractor Research Development

Each of the three lead-acid battery contractors is pursuing a different technical approach which is aimed at developing batteries having improved specific energy, specific power, and life at an acceptable cost. For example, Eltra emphasized low cost and minimum maintenance through use of expanded lead-calcium metal alloy grids which reduce self-discharge rates and exhibit high corrosion resistance. Although specific energies of 40 Wh/kg were verified, the cycle life remained below 100 cycles, and the contract was terminated in March 1981. A second contractor, Exide, is pursuing definition of the optimum cell construction through use of factorial experiments which evaluate several construction combinations and design parameter variations. These include both flat-plate and tubular-plate positive electrodes. A third contractor, Globe, emphasizes cell design optimization by means of a sophisticated computer model, and the use of a unique intracell electrolyte mixing system.

R&D objectives for FY 1981 for the lead-acid system were the achievement of a specific energy of 42 Wh/kg, a specific power of 110 W/kg, and a cycle life of 450 cycles. A specific energy improvement from pre-contract values of less than 30 Wh/kg to over 41 Wh/kg at the 3-hour rate was demonstrated at NBTL. Peak specific power increased from pre-contract values of 96 W/kg to over 104 W/kg for a 30 second pulse with the battery at 50% state-of-charge. Cycle life at an 80% depth of discharge was demonstrated to be greater than 481 cycles. These improvements were all demonstrated by the end of FY 1981 in the technology available from Globe.

The two nickel/iron battery contractors, Westinghouse and Eagle-Picher Industries are also pursuing differing technical approaches. Westinghouse is emphasizing low initial cost through minimization of the amount of nickel used while still maintaining good performance. This is effected by the use of pressed, sintered steel wool electrode substrates in both electrodes thereby substantially limiting the nickel to that required as the active material. In the case of the nickel electrode the substrate is nickel-plated. A central electrolyte circulation system achieves thermal management, gas management, and easy electrolyte maintenance. Eagle-Picher is stressing high performance through use of a nickel electrode having a sintered nickel substrate and a proprietary iron electrode developed by the Swedish National Development Company.

Nickel/iron R&D objectives for FY 1981 were a specific energy of 54 Wh/kg, a specific power of 110 W/kg, and a cycle life of 400 cycles. Both contractors achieved a specific energy of about 48 Wh/kg and a specific power of about 100 W/kg in modules. Life cycle tests are continuing with over 740 cycles having been demonstrated by September 30, 1981.

In the case of the nickel/zinc batteries, each of the three contractors is also pursuing a different technical approach. The Energy Research Corporation (ERC) is emphasizing low initial cost through use of plastic-bonded electrodes which reduce the quantity of nickel needed. Exide is developing a battery with a unique vibrating zinc electrode in order to overcome the life limiting dendritic growth and shape change problems. Gould pursued a high performance battery based on the use of sintered nickel electrodes.

The nickel/zinc R&D objectives for FY 1981 were a specific energy of 65 Wh/kg, a specific power of 120 W/kg, and a cycle life of 250 cycles. These objectives were achieved in Gould's modules, except for cycle life where the best life demonstrated in NBTL was 179 cycles through September 1981.

In order to focus available resources on the development of the promising technologies, a first major decision point of the ANL Aqueous Mobile Battery Program was implemented in September 1981, and involved reducing the number of contractors. The decision was based on three major criteria covering (a) battery performance achieved, (b) battery application compatibility, and (c) performance, commitment and commercialization intent of the contractor. A document describing the decision plan was formulated by ANL and approved by DOE in FY 1980. An evaluation of the contractors was completed in FY 1981. Recommendations were made to DOE to continue three contractors, namely Globe (lead-acid), Westinghouse (nickel/iron) and Eagle-Picher (nickel/iron).

Battery Verification Testing at NBTL

A key part of the program is the performance verification testing at NBTL of contractor supplied cells, modules, and batteries. Standard test procedures have been defined for measuring specific energy, sustained peak specific power for a specific duration, self-discharge rate, performance with a simulated power profile (based on an electric passenger car driven on the SAE J227a/D urban cycle), effects of partial depths of discharge, and battery cycle life. Contractor modules are subjected to these standard tests thus providing a common evaluation basis. As of the end of FY 1981, 555 cells from eight battery contractors had been tested. Specific energies measured were 41 Wh/kg for improved lead-acid batteries, 48 Wh/kg for nickel/iron batteries and up to 68 Wh/kg for nickel/zinc batteries. Corresponding vehicle ranges based on simulated urban driving (J227a/D cycle) in an improved version of the DOE Electric Test Vehicle (ETV-1) with regenerative braking are up to 80 miles for improved lead-acid batteries, 96 miles for the nickel/iron battery and 138 miles for the Ni/Zn battery. By comparison, the pre-contract state-of-the-art lead-acid battery (ESB EV-106) gives a simulated range of 51 miles. Comparative simulated vehicle range testing with and without regenerative braking indicates range increases of over 20% with regenerative braking. All batteries tested show excellent charge acceptance of the regenerative braking current.

Measurements of peak specific power capability for a 30 second duration at a 50% DOD indicate values of over 104 W/kg for improved lead-acid batteries, 103 W/kg for nickel/iron batteries, and 131 W/kg for nickel/zinc batteries. The peak power capability decreases as the battery becomes discharged. At any given depth of discharge the peak power for a duration of 15 seconds

is not appreciably higher than for a 30-second duration. Comparison of sustained peak power data from selected Ni/Zn, Ni/Fe and lead-acid batteries shows that even at an 80% DOD all of them provide more peak specific power than the 47 W/kg required to accelerate a well designed electric passenger car during the SAE J227a/D urban driving schedule.

Advances in NBTL Testing Capability

As of the end of FY 1981, 42 test stations (39 for modules, 3 for full-sized battery packs) were operational in NBTL with work underway to expand to 50 test stations. A typical cell/module test station has current capability of ± 500 amps and a voltage range of 0-12 volts. Capability of a battery test station is (+)350 amps, (-)500 amps and 10-120 volts. Advances in testing capabilities in FY 1981 include the installation of a peak power test station, three environmental chambers, and computer-controlled load banks which can simulate the power profile imposed on a battery by an electric vehicle. The hydrogen ventilation system was rendered operational, and the CAMAC data acquisition and control system was expanded to the environmental annex. A solid state voltage scanner was assembled and the equipment and facilities of the battery components test laboratory were made operational for specialized charge/discharge testing.

Battery Charge and Discharge Studies

An important task is the definition of improved techniques for charging and measuring the state of charge for various aqueous batteries. Proper charging techniques are vital in achieving good battery life and efficiency, minimizing battery servicing needs, and attaining acceptable recharge times within reasonable AC power limitations. Methods of monitoring battery state-of-charge are needed to provide information to the electic vehicle operator on the remaining distance that may be driven before battery charge depletion.

In tests with lead-acid batteries, constant current/constant voltage charging techniques revealed that the total time required to fully charge a lead-acid battery from a state of deep discharge is limited by the battery charge acceptance, but in general, this time can be reduced by increasing the initial constant current component of the charge. Battery discharge capacity was found to be independent of the initial charge rate within the examined limits of 25-250A. In constant voltage charging only a limited voltage range provided reproducible and efficient battery operation. For the EV-106 the optimum voltage was 2.49 volts per cell; this charge voltage was independent of the constant current charge levels employed.

Pulsed current discharges of lead-acid batteries on a 50% duty cycle tested in the frequency range of 50-1000 Hz showed that the discharge capacity, output power and average voltage were constant to ±0.3% for all the frequency levels tested. The internal power losses were also constant. Loss of output power and available energy was about 3.5% when compared with equivalent constant current discharges. When the duty cycle was varied from 25% to 100% at a fixed 200 Hz frequency the output power of the battery dropped linearly by 11% because of the increased I^2R losses as the value of the

current was increased. Under a constant 50% duty cycle at a fixed frequency of 200 Hz, discharge capacity dropped with increasing discharge rate. Overall pulsed current discharge provided no benefits in battery discharge performance.

ANL Technical Support Activities

The support research activities at ANL consisted of basic and applied research in specific areas of critical need which complement the research activities of the contractors. These ANL activities included post-test analyses, research efforts on improving performance and predicting failure modes by experimental studies and mathematical modeling, an assessment of hybrid vehicle battery requirements, and an evaluation of materials supply/demand relationships.

Post-Test Battery Analyses

Post-test analysis of contractors batteries which had failed during testing was carried out through FY 81. Twenty-five contractor-fabricated modules were examined. In the lead-acid battery, failure modes identified included incomplete formation of the active material, abnormalities in both electrodes, and extensive corrosion of the positive grid. In the nickel/iron modules, the primary failure mode was swelling of the nickel electrode. In the nickel/zinc batteries, the failures were due to separator penetration by dendrites and hard shorts caused by massive shape change in the zinc electrodes.

Fundamental Electrode Studies

Zinc electrode studies during the past year included investigations of the hydrodynamics and mass transfer characteristics at a vibrating electrode as used in the Exide Vibrocel™. A mathematical model was developed to describe the mass transfer and electrochemical processes that occur at the surface of a vibrating electrode. Based on experiments conducted using a well defined copper sulfate electrolyte system, the average mass transfer coefficients for various electrode lengths and vibrational amplitudes and frequencies were correlated by a relationship for a quasi steady-state model. The results from this model agreed within 14% of actual experimental values. The model indicates that the mass transfer characteristics of vibrating electrodes provides no basis for improved deposit morphology. Another area of work related to the zinc electrode was the use of electrolyte additives. It was found that a dendrite-free zinc deposit could be achieved in the presence of organic additives. A cathodic sweep technique was established to determine the presence of effective additives in the electrolyte.

In work on the nickel electrode, a relationship was identified between the state of charge of the electrode and the charging efficiency. Assuming that the charge efficiency decreases with increasing state of charge and that there is a maximum discharge capacity when the overall charge efficiency goes to zero, and using a normalized capacity, the data for all types of nickel oxide electrodes could be correlated using a single expression. This relationship could provide useful information to estimate thermal effects and water losses by gas evolution during cell operation at various states of charge.

In the lead-acid system, studies of β-PbO_2 have indicated that the chemically produced species is less active than that produced electrochemically in cells. Attempts to identify the difference in the two species using neutron diffraction techniques revealed that the battery active lead dioxide is lead deficient and contains a significant amount of hydrogen in contrast to earlier reports which indicate an oxygen deficiency. Spectra of chemically prepared β-PbO_2, however, indicate a stoichiometric amount of oxygen. This finding could be used to improve the utilization of the active material by modifying the structure of β-PbO_2.

Nickel/Zinc Battery Separators

Battery separator activities during FY 1981 included identification of the mechanism of failure caused by zinc penetration on two different separator materials, the effects of separator arrangement and phase boundary layer resistivity on the diffusion flux of KOH, in-cell cycle life performance testing and subsequent characterization. Zinc penetration tests indicate that the zinc penetration factor of a separator can be improved by about 50% by a single layer of metallic coating. By the method of the modified Wilson plot, it was determined that in a KOH concentration of 40-60%, the true membrane resistance for RAI Permion P2291 40/30 is about twice that of Dupont 193 PUDO cellophane and independent of concentration changes within the range specified. The phase boundary resistance was the same for both materials but was dependent on the electrolyte concentration.

In a subcontracted activity, Prof. D. Bennion of Brigham Young University conducted a literature review of separator materials. His suggestions for improved performance of Ni/Zn batteries include several modifications such as engineering design improvements for zinc electrode composition and structure, and bipolar electrodes.

Battery Application Model Development

In order to portray the electrical and thermal behavior of batteries during in-vehicle use, a thermal model, an equivalent electrical circuit model, and a more general physico-chemical model were developed.

The thermal behavior of full-size batteries was estimated using an iterative time-stepping approach after establishing the temperatures of the different modules at their respective boundaries. The numerical method employed in the model appeared to be stable and the number of iterations required was highly dependent on the rate of heat generation. Further refinements of the model are planned for FY 1982.

The equivalent electrical circuit portraying the static/dynamic electrical behavior of the battery consists of three capacitors and seven resistors. The model provides the voltage-time response of the battery under constant-current charge/discharge cycling or simulated driving profiles with and without regenerative braking. Correlations between voltage-time profiles generated by the model and experimentally measured profiles are extremely good.

An approximate physicochemical battery model was also developed from the basic electrochemical equations that describe cell behavior. This model utilizes seven first order differential equations which relate the timewise behavior of electrode porosities, active-passive interfaces, and electrolyte concentrations. Additional equations describe electrode resistances, current distributions, and overpotential, as well as average diffusivity and conductivity. Numerical solution of these equations yields terminal voltage as a function of battery current and time. Preliminary results are promising but much additional evaluation is needed to verify the utility of this model.

In-Vehicle Test Monitoring Support

In-vehicle battery testing was conducted by JPL on two full-sized lead-acid battery packs from Globe and on nickel/iron batteries from Eagle-Picher and Westinghouse. JPL will issue separate reports on the test data gathered on these batteries.

Reports from the DOE EV Test and Evaluation Program indicate that the site operators are experiencing many problems with the state-of-art batteries as used in their vehicles. These problems may be classified into four general areas: a) inability of chargers to return the battery to the prescribed capacity, b) battery thermal problems - battery temperatures >130°F during charge/ discharge operations, c) malfunction, corrosion, and meltdown of battery terminals and interconnecting cables and d) abuse of the battery by discharging beyond specified limits on a day by day basis and poor maintenance. Lessons learned from these site operator experiences are being factored into the aqueous battery development. In addition the site operators are showing interest in evaluating prototype batteries from this battery R&D. As of September 1981, Northrop Corporation, General Telephone and Electronics Corporation and AT&T have entered into agreements to retrofit electric vehicles with nickel/iron batteries.

Hybrid Vehicle Battery Requirements Assessment

A preliminary assessment of the battery development design goals for a hybrid electric vehicle was made at ANL as part of the hybrid vehicle battery project. Desirable values for the battery specific power, specific energy, life and cost were determined by means of a computer study which investigated the effect on the petroleum consumption of a baseline hybrid vehicle with batteries having various specific energy and specific power characteristics. The baseline hybrid vehicle was the five passenger sedan developed for the DOE by General Electric and known as the Near-Term Hybrid Vehicle (NTHV). Allowable battery cost for each set of battery performance characteristics was determined based on a hybrid vehicle lifetime costs equal to the ICE vehicle lifetime cost and a battery life of 800 cycles. The results of the study indicated that the desirable battery characteristics for the NTHV type of vehicle are a specific energy of 60-70 WH/Kg, a specific power of 150 W/Kg at 50% DOD, and an OEM battery cost of $80/KWH with an 80% DOD cycle life of 800 cycles.

Materials Availability/Cost Studies

The ultimate success of the battery and electric vehicle program also depends on the availability and cost of the required materials. To assess

the impact of material supply-demand constraints on the cost of the battery, a computerized methodology identified as the Materials Economic Technology Assessment Link (METAL) was developed as described in the FY 1980 report. Utilizing METAL to examine the effect of extreme case conditions on the price of nickel, cobalt, lead and zinc revealed that the real cost of nickel in 1978 dollars would be about $34/kWh in the year 2000. The cost of cobalt would be about $8/kWh. The price of lead and zinc would increase to about $32 and $3 per kWh. Distributional flows may be seriously impacted only for cobalt.

Relevant Non-ANL Support Research

These activities included the following: Caulder and Simon identified the cause of loss of capacity in lead-acid batteries as the corralloid structure of the active material formed during cycling. Failure of tubular positives by bursting was caused by large volume corrosion products formed on the lead spine. The effects of pulsed discharge on a lead-acid battery were investigated by Simon, Caulder and Dowgiallo who found that formation of the coralloid inactive structure was enhanced by the pulsed discharge. Corrosion rates of grids were unaffected by pulsed discharge in some of the batteries tested. Efforts on liquid membrane battery separator technology revealed that the activity of the liquid ion exchange resin is unchanged over two months in Ni/Zn cells; no degradation was apparent over 6 weeks at 50°C; hydroxyl ion transport through these membranes was much lower. Study of zinc electrode/electrolyte formations by Charkey have shown that a lower concentration of electrolytes in which the solubility of zinc oxide is limited may be useful to reduce degradation of the zinc electrode. In an assessment of the depletion of hydroxyl ion during discharge Hamby found that the predicted rates were much higher than those actually observed in cells at different rates of discharge. Katan at Lockheed is carrying out fundamental work to aid the development of the zinc/nickel oxide batteries. Accomplishments included the identification of approaches to reduce dendrite formation. Capacity loss in nickel electrodes during cycling was partly attributed by MacDonald to the growth of anodic film on nickel electrodes. He is also developing basic thermodynamic data for concentrated aqueous electrolyte solutions in the temperature range -20°C to 120°C. Non-reproducibility of data in the cycling of nickel electrodes by McKubre was attributed to the effect of carbonates. Wagner has reported that dendritic penetration of Celgard 3401 could be avoided by interrupting the charge current for periods of 150-200 milliseconds while maintaining a maximum pulse interval of 50-60 milliseconds at 3-5 Hz.

Publications

An important ingredient of the program is the dissemination of the knowledge gained from the R&D effort. To that end, a total of 114 publications consisting of reports, papers, and extended abstracts issued through FY 1979 and FY 1980 have been listed in earlier reports. A list of 59 publications released in FY 1981 are included in this report.

I. INTRODUCTION

The increasing reliance on foreign import oil, the interruption of gasoline supply in the United States and the increasing levels of pollutants in urban areas due to automobiles resulted in the enactment by Congress of the Electric and Hybrid Vehicle Research, Development and Demonstration Act of 1976 (PL 94-413) and its amendment, PL 95-238, in March 1978. The Office for Electrochemical Project Manangement (OEPM) at Argonne National Laboratory (ANL) is assisting the Department of Energy (DOE)* in the research and development of aqueous batteries for use in electric and hybrid vehicles being developed under this act. The overall objective of the ANL program is to accelerate the development of aqueous battery technology that could provide performance and cost levels suitable for practical electric vehicle applications. Such batteries are required before electric vehicles with attributes conducive to significant market penetration can be designed and built.

In 1977, design and cost studies[1-9] were conducted by ANL on the specific energy, specific power, lifetime and cost capabilities of various batteries. The lead-acid, nickel/iron and nickel/zinc systems were identified as having potential for electric vehicle application in the late 1980's. The R&D of these three systems is being conducted primarily by industrial firms under cost-sharing contracts with ANL/OEPM. OEPM provides the technical and project management of the contracts. In addition, OEPM provides the following: verification testing of contractor fabricated cells and batteries by the National Battery Test Laboratory (NBTL); post-test analyses of cells and batteries; support research in critical problem areas encountered by the industrial contractors; and development of supporting technologies such as separators and techniques for charging and state-of-charge monitoring. Other efforts at OEPM include support of battery application tasks directed at ensuring compatibility of battery R&D goals with vehicle needs, developing battery application information for use by vehicle system developers and/or monitoring the application performance of these near-term batteries in test vehicles.

The program strategy is to emphasize technology development by industry through cost shared contracts. This ensures a sharp focus by industry on those technical approaches which offer the greatest probability of success. In addition it provides incentive to industry for rapid application and commercialization of the technology developed.

The initial program effort concentrated on R&D exploring promising technical approaches in the three aqueous battery systems. Late in FY 1981 each contractor's progress was evaluated and three were selected for continued DOE support. The selected contractors will emphasize R&D directed at lower cost, longer life and the achievement of technology readiness.

---

*Sponsored by the Electric and Hybrid Vehicle Division and the Division of Energy Storage.

The purpose of this report is to present a description of the program activities and associated key results. The report contains a summary of the battery contractor research and development efforts, results of the battery verification testing at ANL/NBTL, status and results of the support research activities at ANL, results to date in the battery components research and development efforts at ANL, a summary of the major results in the battery application support area, and a preliminary assessment of the hybrid vehicle battery requirements. As the contractor efforts are detailed in their individual annual reports,[10-16] a major portion of this summary describes in-house effort at ANL. The report stresses brevity and conciseness at the expense of completeness in the details presented. A reader desiring additional data or information in a particular area should consult the list of publications listed in Section VII or contact the ANL/OEPM project office.

II. BATTERY CONTRACTOR RESEARCH AND DEVELOPMENT

A. Summary

The major contractors participating in the Aqueous Mobile Battery Research Program are listed in Table II-1. Table II-1 also shows the contract period and contract value including the contractors cost share. The industrial contractors within each battery type are pursuing different technical approaches following their specific areas of expertise.

The electrochemical and thermodynamic characteristics of the three systems are given in Table II-2. Characteristics of major importance in electric vehicle batteries are a high specific energy and specific power, low cost, long cycle life, low maintenance requirements and safety in operation. Battery R&D must be directed at achieving the best combination of all of these characteristics. Each of the three battery types has its own merits and shortcomings.

For example, the state-of-the-art (SOA) lead-acid battery has low cost and acceptable cycle life but low specific energy. The SOA nickel/iron battery however, has good cycle life, medium specific energy, but high cost. High specific energy is the virtue of the nickel/zinc battery, but a major improvement in cycle life is needed while maintaining acceptable cost.

The R&D approaches taken by the contractors are varied as previously stated. For example in the lead-acid area Eltra is using grids made from an expanded lead-calcium metal alloy for both the positive and negative plates. These alloys have lower self discharge and corrosion rates than the conventional lead-antimonial alloys. They have also developed a pilot line for continuous manufacture of expanded metal pasted electrodes. Exide is using their golf cart battery (EV-106) as baseline technology. By means of parametric design evaluation experiments, they are examining several construction combinations directed at increasing the specific energy of the battery to over 40 Wh/kg. Their evaluation includes both flat plate and tubular plate positive electrodes. Globe's approach emphasizes optimization of the cell design, and use of a unique electrolyte mixing system.

Table II-1. Industrial Contractors for Aqueous Mobile Battery Research Program

Battery	Contractors	Contract Period	Contract Value,[a] ($000)
Lead-Acid	Eltra Corporation	04/78-05/81[d]	2,089
	Exide	02/78-01/82	3,386
	Globe	03/78-09/81	4,633
Nickel/Iron	Eagle-Picher Ind., Inc.	03/78-09/81	2,879
	Westinghouse Electric Corporation	12/77-09/81	3,022
Nickel/Zinc	Exide	04/79-01/82	1,200
	Energy Research Corp.	03/78-09/81	3,608
	Gould Inc.	01/78-09/81[c]	6,790
	Yardney Electric Corp.	07/77-09/80[b]	1,000

[a]Includes contractor's share
[b]Contract terminated by mutual agreement in May 1979
[c]Contract terminated by mutual agreement in January 1981.
[d]Contract terminated by mutual agreement in March 1981.

Table II-2

LEAD-ACID, NICKEL/IRON AND NICKEL/ZINC SYSTEM CHARACTERISTICS

	Lead-Acid	Nickel/Iron	Nickel/Zinc
Cathode Reaction	$PbO_2 + SO_4^{=} + 4H^+ + 2e^- \underset{}{\overset{D}{\rightleftharpoons}} PbSO_4 + 2H_2O$	$2NiOOH + 2H_2O + 2e^- \overset{D}{\rightleftharpoons} 2Ni(OH)_2 + 2OH^-$	$2NiOOH + 2H_2O + 2e^- \overset{D}{\rightleftharpoons} 2Ni(OH)_2 + 2OH^-$
Anode Reaction	$Pb + SO_4^{=} \overset{D}{\rightleftharpoons} PbSO_4 + 2e^-$	$Fe + 2OH^- \overset{D}{\rightleftharpoons} Fe(OH)_2 + 2e^-$	$Zn + 2OH^- \overset{D}{} ZnO + H_2O + 2e^-$
Overall Cell Reaction	$PbO_2 + Pb + 2H_2SO_4 \overset{D}{\rightleftharpoons} 2PbSO_4 + 2H_2O$	$2NiOOH + Fe + H_2O \overset{D}{\rightleftharpoons} 2Ni(OH)_2 + Fe(OH)_2$	$2NiOOH + Zn + H_2O \overset{D}{\rightleftharpoons} 2Ni(OH)_2 + ZnO$
Theoretical Cell Voltage	2.09 volts	1.36 volts	1.73 volts
Nominal Cell Voltage	2.1 volts	1.2 volts	1.6 volts
Theoretical Capacity			
$Ni(OH)_2$, or PbO_2	0.224 Ah/g	0.289 Ah/g	0.289 Ah/g
$Fe(OH)_2$, ZnO, or Pb	0.259 Ah/g	0.588 Ah/g	0.645 Ah/g
Theoretical Energy Density	175 Wh/kg	263 Wh/kg	345 Wh/kg
Parasitic Reactions			
at positive electrode	$2H_2O \xrightarrow{C} O_2 + 4H^+ + 4e^-$	$2\ OH^- \xrightarrow{C} 1/2\ O_2 + H_2O + 2e^-$	$2OH^- \xrightarrow{C} 1/2\ O_2 + H_2O + 2e^-$
at negative electrode	$2H^+ + 2e^- \xrightarrow{C} H_2$	$2H_2O + 2e^- \xrightarrow{C} H_2 + 2OH^-$	$2H_2O + 2e^- \xrightarrow{C} H_2 + 2\ OH^-$
Thermodynamic			
ΔG (for cell reaction)	-93.5 Kcal/mole	-63.0 Kcal/mole	-80.0 Kcal/mole
ΔH (for cell reaction)	-90.4 Kcal/mole	-68.5 Kcal/mole	-85.8 Kcal/mole
$T\Delta S$ (at 298K)	+3.1 Kcal/mole	-5.5 Kcal/mole	-5.8 Kcal/mole

The Eagle-Picher nickel/iron approach favors high performance using a sintered nickel positive electrode and an iron electrode from the Swedish National Development Company. Westinghouse is pursuing a low-cost approach in which electrode substrates are prepared from nickel-plated steel wool.

In the nickel/zinc system Exide is developing a battery with a unique vibrating zinc electrode, which overcomes dendritic growth and shape change problems. Gould is developing a high performance battery utilizing sintered nickel electrodes. Much attention is also given to separators and thermal management techniques. Energy Research Corporation (ERC) is emphasizing low initial cost through the use of plastic bonded electrodes and thus reduction in the amount of nickel required.

The pre-contract status, FY 1981 development objectives, FY 1981 accomplishments and the program goals for 1986 are shown in Figures II-1 to II-3. The FY 1981 accomplishments are based on NBTL test data from cells and modules. The program goals for FY 1986 are for full-size batteries. In the three Figures II-1 to II-3, the pre-contract data for the lead-acid and nickel/zinc systems are from cells and modules. The nickel/iron pre-contract data are from a 80-cell battery pack tested at a contractor location. Since the cycle life tests on the pre-contract Ni/Fe battery were discontinued prematurely, the data presented are incomplete and represent the best available results. At the end of FY 1979, DOE established performance and cost objectives for the electric passenger cars to be available in 1986. Characteristics required of these vehicles were a 100 mile urban range, an acceleration comparable to presently available diesel engine sub-compact cars, and an ownership and operating cost competitive with ICE vehicles. The associated battery capabilities required to achieve these vehicle performance and cost objectives are indicated by the 1986 program goals for the batteries.

The details of the varied contractor approaches and accomplishments are provided in the following sections.

B. Lead-Acid Batteries

The three contractors who conducted R&D on lead-acid batteries during FY 1981 were Eltra Corporation (Plymouth Meeting, PA), Exide Management and Technology Co. (formerly named ESB, Inc., Yardley, PA) and Globe Battery Division of Johnson Controls, Inc. (Milwaukee, WI). Prior to the initiation of the Aqueous Mobile Battery R&D Program, lead-acid EV batteries were characterized by limited performance with low specific energies (30 Wh/kg) and short cycle lifetimes (about 200 cycles). As a result of this program, all three industrial contractors for lead-acid batteries have developed improved cells and modules which have met or exceeded 40 Wh/kg. During FY 1981, the principal emphasis has been on improvement of cycle life capability. Progress in lead-acid battery technology development is illustrated in Table II-3 which compares the pre-contract status, FY 1981 accomplishments, and 1986 goals for lead-acid batteries. The FY 1981 accomplishments are verified test results obtained on multicell modules at the NBTL. The 1986 goals are those key battery characteristics established for an electric passenger car to have an urban range of 100 miles and an acceptable performance. A brief description of the research and development programs pursued by each contractor is presented in the following paragraphs.

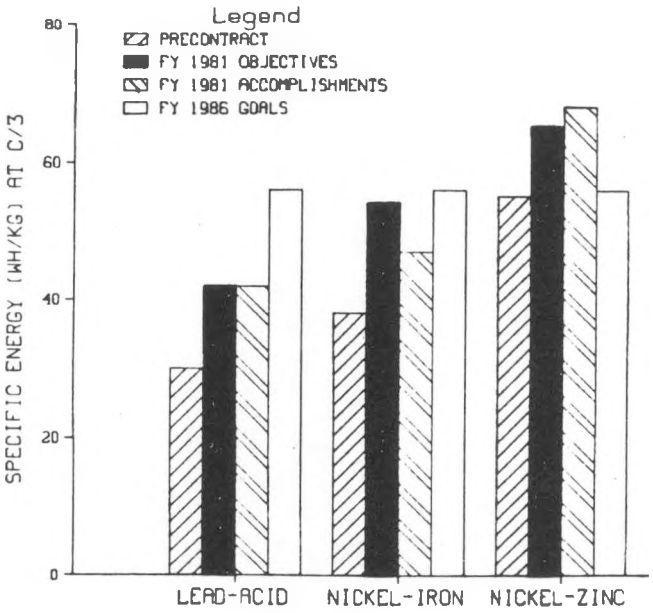

Figure II-1: Specific Energy: Accomplishments and Goals for the Aqueous Batteries

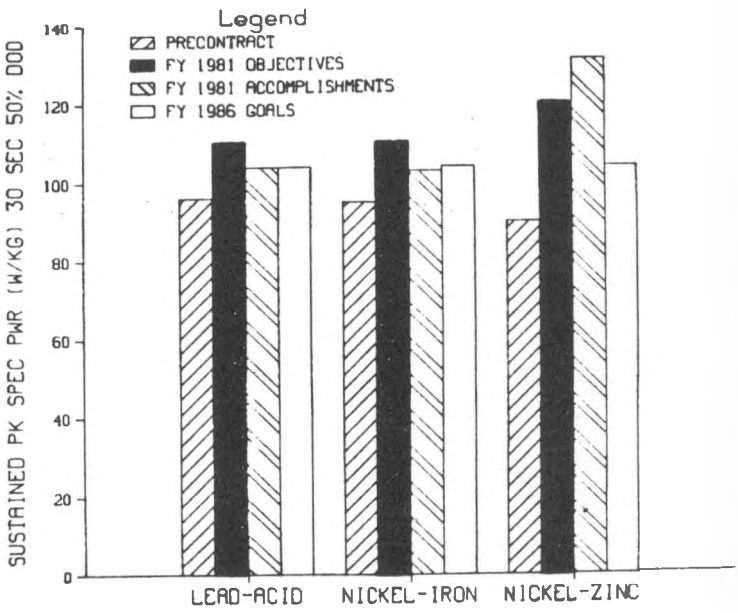

Figure II-2: Specific Power: Accomplishments and Goals for the Aqueous Batteries

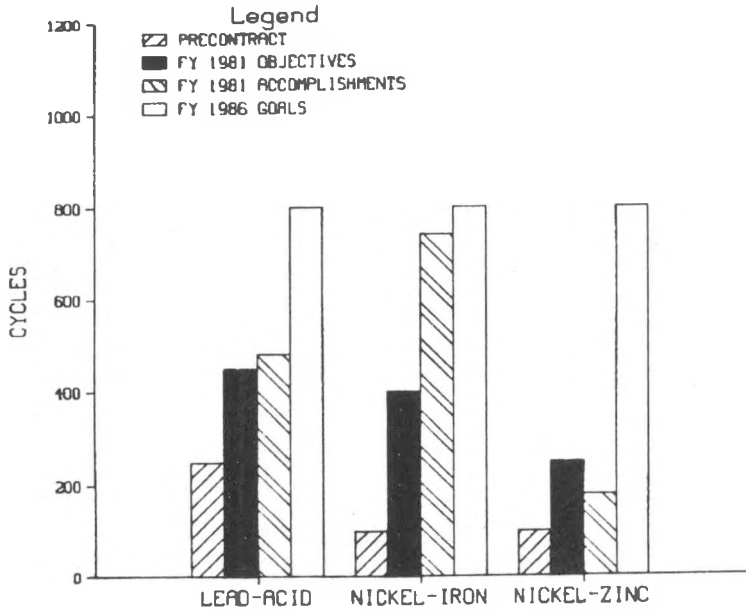

Figure II-3: Cycle Life: Accomplishments and Goals for the Aqueous Batteries

Table II-3. Lead-Acid Battery Progress and Goals

	Pre-Contract Status (1977)	FY 1981 Accomplishments	1986 Goals
Specific Energy, (Wh/kg) (C/3 Rate)	30	41	56
Specific Power, (W/kg) (30 sec. average at 50% DOD)	96	104	104
Cycle Life, (at 80% DOD to 75% retained capacity)	250	>481	800

Globe's improved state-of-the-art (ISOA) activities have emphasized improved cell design, materials selection, and manufacturing processes. This has resulted in the selection of a plate size, plate aspect ratio, number of plates, and an acid concentration best suited for EV application. A low-corrosion grid alloy was identified to enhance cycle life. In addition, Globe has developed an innovative electrolyte mixing pump which has increased both energy density and cycle life.

During FY 1981, Globe delivered two 96-volt, 250-Ah ISOA EV batteries (23.4 kWh) to NBTL for characterizational testing. The batteries were subsequently shipped to the Jet Propulsion Laboratory (JPL) for in-vehicle test and evaluation. NBTL tests of Globe's ISOA twelve-volt modules confirmed a specific energy of up to 41 Wh/kg, a specific power of 104 W/kg at 50% DOD, and a life of up to 481 cycles, with two of the five modules continuing on test. In addition, Globe delivered five prototype cells of smaller capacity (190 Ah) to NBTL for testing. These EV-190 cells incorporate all the ISOA technology advances but yield twelve-volt modules having dimensions that are more amenable to retrofitting of existing EV's.

Globe appears to be capable of achieving the program goals of 800 cycles and an OEM cost of less than $70/kWh (1981 dollars). Globe's long-range development plans will concentrate on increasing the specific energy of lead-acid batteries while maintaining the present long life and low cost. This increase in energy density is expected to be accomplished through two developments. In the Advanced-I design, the use of plastic-lead composites as the grid material instead of lead alloy along with additional design changes, will increase the specific energy to over 45 Wh/kg. In the Advanced-II program, unique design concepts have shown promise of dramatically increasing the active PbO_2 material utilization, thereby permitting the specific energy to approach the 56 Wh/kg goal.

Exide's ISOA program has investigated design variations in both flat-plate and tubular-plate constructions. Modules with flat-plate positive electrodes containing radial-type grid designs have achieved an energy density of 38 Wh/kg and are retaining 86% of rated capacity after 196 cycles in ongoing tests at Exide. Modules with tubular positive plate construction have resulted in somewhat lower energy densities but longer life; modules

with an energy density of 31-33 Wh/kg have exceeded 600 cycles, while other modules with an energy density of 37 Wh/kg are continuing on test at Exide after 450 cycles. Exide's work on advanced cell designs has resulted in the development of plastic-lead and copper-lead composite grid which have permitted increases in energy density up to 40 Wh/kg.

During FY 1981, Exide delivered 15 six-volt modules of various designs and five individual advanced cells to NBTL. NBTL test results have verified 35 Wh/kg and over 400 cycles in ongoing tests for tubular-plate cells; 40 Wh/kg and 295 cycles for flat-plate modules. All lead-acid R&D work under this program at Exide was discontinued in September 1981.

Eltra has pursued an approach to battery development based upon the use of electrodes fabricated from expanded lead-calcium metal mesh instead of conventional cast grids. Although this manufacturing process permits a lower cost battery, the cycle life of batteries of this design has been limited in deep discharge applications. While energy densities of 40 Wh/kg have been verified for Eltra's modules at the NBTL, cycle life has been limited to less than 100 cycles. There were no hardware deliveries during FY 1981, and the R&D effort was stopped in March, 1981.

C. Nickel/Iron Batteries

Two industrial contractors conducting work on the nickel/iron battery development program are Eagle-Picher Industries, Inc. (EPI) (Joplin, MO) and Westinghouse (Pittsburgh, PA). The two contractors are pursuing different approaches. Eagle-Picher has concentrated its efforts on the development of high-performance Ni/Fe batteries. They use a sintered-nickel electrode in combination with a sintered-steel electrode developed by Swedish National, who has also demonstrated the utility of a ribbed sintered PVC separator. Westinghouse is examining low-cost approaches to achieve a nickel/iron battery technology without compromising the inherent long life and performance of which the system is capable.

Both contractors have demonstrated marked progress in nickel/iron battery development as shown in Table II-4. The cycle life of the EPI modules still on test at NBTL has exceeded 740 cycles, while those of Westinghouse have approached the 600-cycle mark. Capacity loss over these cycle-life periods has been less than 16% of their original maximum capacity for EPI and 20% for Westinghouse. The specific energy of the modules have shown significant improvement from their pre-contract level of 38 Wh/kg to over 48 Wh/kg.

Both contractors have made significant progress towards improving performance and reduction of costs. EPI has developed the single-pass nickel electrode technology which is conducive to continuous low-cost production. Along the same lines, Westinghouse has developed the pasted electrode technology for the continuous manufacture of low-cost nickel electrodes using sintered steel wool substrates, which have been nickel plated.

Table II-4. Nickel/Iron Battery Progress and Goals

	Pre-Contract Status (1977)	FY 1981 Accomplishments	1986 Goals
Specific Energy, (Wh/kg) (C/3 Rate)	38	48	56
Specific Power, (W/kg) (30 sec. average at 50% DOD)	95	103	104
Cycle Life, (at 80% DOD to 75% retained capacity)	100	>740	800

EPI has improved roll blending techniques for their single-pass slurry preparation, thus, increasing the homogeneity of their active material. Other benefits of the roll blending technique were better control of the slurry viscosity and density. Further improvements by EPI included substrate modification resulting in reduced nickel requirements and improved substrate conductivity. In low-temperature testing, EPI identified a loss in capacity at -10°C of approximately 11% of the capacity at +20°C. Under ambient-temperature testing, EPI verified over 800 cycles with a minimal loss in capacity.

Westinghouse technology improvements include the implementation of low-cost raw materials and the utilization of established manufacturing processes. Further, Westinghouse has developed a conceptual design of a multicell modular package that can further enhance performance parameters by providing additional 9% weight and 15% volume reductions. Cost-reduction procedures incorporated by Westinghouse include stitched steel fiber metal blanket manufacturing for the electrode substrate, decreased process time and increased process efficiency for the electroprecipitation process nickel electrodes, activation techniques and paste manufacturing process for iron electrodes, and identification of suitable separator systems. Low-temperature performance of batteries has demonstrated a 25% decrease in capacity at 0°C compared to 25°C. Westinghouse has identified that no raw material impact will occur for annual commercial production of 25-kWh batteries at production rates of 100,000 units per year.

Both contractors have actively participated in in-vehicle testing of their batteries. Both EPI and Westinghouse supplied batteries to JPL for in-vehicle testing. The results are being reported on by JPL. EPI has also aggressively looked to industrial fleets for field evaluation of their Ni/Fe battery technology. They have secured contracts with Northrop Inc. to deliver 16 electric vehicles with Ni/Fe batteries for testing at the Northrop facilities in California.

At present, the R&D effort is concentrated on improving packaging to reduce costs, improving the cyclic stability of the electrodes, increasing the charge acceptance of electrodes under various operating modes, and

assessing the impact of varied ambient temperatures on charge acceptance and life. Efforts are also aimed at maximizing the utilization of the electrode materials, and modifying auxiliary equipment to reduce weight, volume and cost.

D. Nickel/Zinc Batteries

The three major industrial subcontractors who conducted R&D on nickel/zinc batteries during FY 1981 were Energy Research Corporation (Danbury, CT), Exide Management and Technology Co. (formerly named ESB Inc.; Yardley, PA), and Gould Inc. (Rolling Meadows, IL). Progress in nickel/zinc battery development is illustrated in Table II-5 which compares pre-contract status, FY 1981 accomplishments and 1986 goals. The FY 1981 accomplishments are verified test results obtained on multi-cell modules at the NBTL. While selected cells have achieved over 250 cycles at two contractor's test facilities, verified accomplishment of this capability in multi-cell modules remains to be demonstrated at NBTL. The following paragraphs describe the three quite different technical approaches being pursued by the nickel/zinc contractors and summarizes the progress achieved and problems encountered by each.

Energy Research Corporation (ERC) is emphasizing the development of a nickel/zinc battery with low initial cost. Efforts are focussed on the nickel electrode which is the most expensive component in the battery. The technical approach is based upon the development of a low-cost plastic-bonded electrode in which graphite replaces the conventional sintered nickel powder substrate as the current collector. ERC's projected selling price of $75/kWh for their Ni/Zn battery (versus their estimate of $120-145/kWh for sintered Ni/Zn batteries) is based upon the use of 35% less nickel than sintered types and production plant capital costs of only one-sixth that of sintered electrodes.

Table II-5. Nickel/Zinc Battery Progress and Goals

	Pre-Contract Status (1977)	FY 1981 Accomplishments	1986 Goals
Specific Energy, (Wh/kg) (C/3 Rate)	55	68	56
Specific Power, (W/kg) (30 sec. average at 50% DOD)	90	131	104
Cycle Life, (at 80% DOD at the C/3 rate)	100	179	800

At ERC, full-size plastic-bonded nickel electrodes are now being routinely manufactured in the pilot plant. It is now apparent that there are no barriers to large-scale production using ERC's non-sintered process. These electrodes have yielded 800 cycles on a 85% DOD test regime. Zinc electrode studies have concentrated on the effect of additives upon shape change and cycle performance, and on the mechanistic processes involved in

zinc dissolution and deposition. Additives have been identified which reduce shape change and lower electrode polarization during cycling. ERC's separator efforts involve both in-house manufactured and commercially available separator materials. The in-house separators, consisting of polymer-blend and filled-polymer films, are produced on a recently installed pilot film-casting machine. Hundreds of formulations have been produced and subsequently screened in laboratory tests and in small cells. Promising formulations are presently being life tested in 250-Ah cells.

Component studies at ERC have led to the development of a basic cell design which includes a cellulose-acetate-coated polypropylene separator (Celgard K-306) and a zinc electrode additive consisting of a mixture of metallic oxides. The integration of these components into tri-electrode 20-Ah Ni/Zn cells using full-size electrodes resulted in a life capability in excess of 240 cycles. Full-size 250-Ah cells have achieved 90-140 cycles under an 80% DOD regime in tests at ERC.

During FY 1981, ERC delivered three 250-Ah modules (4 or 5 cells each) to NBTL for verificational testing. Although there was no improvement over previous ERC modules in the areas of specific energy (46 Wh/kg) and cycle life (79 cycles), specific power was increased from 71 W/kg to 92 W/kg at 50% DOD.

Exide is pursuing a unique cell design based upon vibrating zinc electrodes. When the zinc electrode is vibrated during charging, the life-limiting problems of zinc dendrite formation and electrode shape change are minimized. Although Exide had no hardware deliveries to NBTL in FY 1981, a 300-Ah cell (with energy density of 42 Wh/kg) achieved over 370 cycles (with testing continuing) at Exide, while maintaining 90% of its nominal capacity.

Exide constructed and tested experimental modules based on a design which would match the footprint of the Exide EV-106 commercial lead-acid battery. New features to improve specific energy and volumetric energy density included (1) the reduction of interelectrode spacing from 2.5 mm to 1.5 mm to reduce electrolyte volume and weight and use of special charging techniques to produce the dense zinc deposits necessary with closely-spaced electrodes, (2) the use of higher performance layered-type (CMG) electrodes (instead of sintered nickel electrodes), and (3) an increase in electrolyte concentration from 6 molar to 9 or 10 molar KOH solutions. Although an energy density of 50 Wh/kg had been projected for this design, the modules failed to achieve design capacity which limited their specific energy to 39 Wh/kg.

Exide also investigated the concept of a battery utilizing a moving electrolyte (VIBROLYTE) in place of mechanical vibration of the zinc electrodes. The advantages of this system include:

(1) Electrolyte mixing is more vigorous and equalization of concentration gradients occurs in a very short time.

(2) Internal moving parts are completely eliminated increasing operational reliability.

(3) Energy density of the battery is increased by the elimination of the mechanical vibration hardware.

(4) Since all electrodes are stationary, it is now possible to physically support the nickel electrodes, thereby minimizing many of the problems (swelling, shedding) associated with electrodes in the free-standing conditions.

A 120-Ah cell was constructed to demonstrate this principle. In the 100 cycles imposed to date, the cell has performed well with no apparent problems.

All nickel/zinc battery R&D efforts were discontinued at Exide in September 1981 as the result of Exide's internal business decision.

Gould pursued the development of a high performance nickel/zinc battery based upon the use of sintered nickel electrodes, zinc electrode additives, and membrane-type separators. During FY 1981, Gould delivered two five-cell modules to NBTL for verification testing. Gould's modules displayed good performance with a specific energy of 68 Wh/kg, a specific power of 131 W/kg at 50% DOD, exceeding the FY 1981 goals of 65 Wh/kg and 120 W/kg. However, the verified cycle life of 179 cycles fell short of the 250-cycle goal.

Gould performed a cost analysis for their battery and derived a manufacturing cost projection of $106/kWh for a production volume of 50,000 batteries (25 kWh each) per year. Thus, the relatively high initial battery cost combined with a modest cycle life capability yields a rather high life-cycle-cost projection. Because of the technical risks associated with further development, the uncertainty of a future EV market, and the changing product lines of the corporation, Gould terminated its nickel/zinc battery development program in January 1981.

E. Contractor Evaluation for Future Work

The first major decision point of the ANL Aqueous Mobile Battery Research Program is to reduce the number of developers per battery type. This decision will allow available funds to be concentrated on the most promising technologies beginning in FY 1982. The number of contractors selected for continuing R&D will be dictated by the total funding available, the individual contractor funding requirements, and the evaluation results of individual contractor technology and commitment.

A document entitled, "Major Decision Plan for Reducing the Number of Contractors per Battery Type, Near-Term Electric Vehicle Battery Project" was drafted by ANL and approved by DOE/Headquarters. This document defined the decision criteria and evaluation guidelines to be used in the selection of the preferred contractors. These major areas of evaluation, considered to be of equal importance, were:

a. Battery performance
b. Application compatibility
c. Contractors performance, commitment, and commercialization intent.

Within each of these evaluation areas, specific decision criteria have been defined.

The data and information used for the first evaluation area (battery performance) was based primarily upon the results demonstrated by the contractors hardware in tests performed by the ANL National Battery Test Laboratory (NBTL). In the case of the second evaluation area (application compatibility), the information used consisted of a combination of contractor supplied data and NBTL test results. Information for the third evaluation area (contractors performance, commitment and commercialization intent) included both contractor supplied data and the contractor's contractual performance to date.

To arrive at a ranking of contractors in each battery system, an assessment of each contractor's technology was performed for each decision criteria as defined in the Major Decision Plan. Based upon these assessments, a comparative evaluation of each contractor against other contractors within the same battery type resulted in a ranking of contractors in each of the three major evaluation areas, and an overall ranking within each battery type. In addition, a comparative evaluation of all eight contractors against each other was performed, providing an overall ranking among all contractors.

The contractor evaluation and ranking was completed in August 1981. A briefing covering these results was given to DOE and a report was completed and submitted to DOE, together with a document describing the resultant FY 1982 contractor funding strategy and plans.

Based on the evaluation results, it was recommended that the R&D efforts of three contractors continue to be supported. These contractors were Globe in the lead-acid area and Westinghouse and Eagle-Picher in the nickel/iron area. It was further recommended that future nickel/zinc R&D be limited to solving the present short life problem.

III. BATTERY VERIFICATION AND SPECIALIZED TESTING AT NBTL

The National Battery Test Laboratory (NBTL) was established to provide a facility for the independent testing and evaluation of various batteries. Both cells and batteries developed within DOE-sponsored programs and by private funds are tested at the NBTL. The laboratory is capable of the simultaneous testing of 39 cells or modules and three full-size (30-40 kWh) batteries under simulated driving conditions as well as under normal test conditions. In addition, six test stations are dedicated to specialized tests involving charge optimization studies, pulsed and discharge studies. The laboratory is under computer control to operate unattended continuously around the clock, seven days a week. Graphical displays and tabulations of cell, module or battery performance are directly available through a computer.

A. Standard Test Procedures

Upon arrival at the NBTL, the test battery is labeled, visually inspected, weighed and its physical dimensions measured. The cell voltages are measured, and the electrolyte level determined and, if necessary, adjusted. In some cases, a sample of the electrolyte may be obtained and analyzed for future reference. The battery is then installed in a test station and, if necessary, undergoes conditioning in accordance with the

manufacturer's instructions. Finally, the battery is submitted to a capacity measurement at a 3-hr ($C_3/3$) constant current discharge rate to verify the manufacturer's specifications, establish a baseline capacity for future reference, and qualify it for further testing in the NBTL. As a part of establishing a baseline of performance, the coulombic (Ah) and energetic (Wh) capacities and efficiencies are also measured. Once these steps are completed, the battery is ready for either performance characterization testing or life-cycle testing as described below:

The purposes of characterization testing are as follows:

a. To assess the functional capabilities of a battery over a range of test conditions that are sufficient to permit evaluation of the battery performance in general for vehicle applications.

b. To measure the performance of a battery on a specified simulated load profile (for example, a power profile of a given electric vehicle operated under the "D" driving schedule of the SAE J227a Test Procedure).

c. To perform special charge and discharge studies.

d. To provide data for battery analyses and modeling.

The performance characterization tests consist of the following:

1. Self-Discharge Test. The purpose of this test is to determine the capacity loss over a seven-day period due to self-discharge.

2. Partial Depth of Discharge Test. The response of a battery to a series of shallow (approximately 50%) discharges is used to uncover any so-called memory effects which are manifested by the inability of the battery to achieve its maximum capacity for several cycles following a series of shallow discharges.

3. Energy Density Versus Power Density. This test provides information over a range of test conditions that is suitable for evaluation of battery performance for various applications and for battery modeling. For example, the projected constant-velocity range of a vehicle of known power consumption can be interpolated from the results of this test series. The battery is discharged at 10, 20, and 30 W/kg and the corresponding energy density is measured at each of the following temperatures: -20, 0, 25, and 50°C. In addition, efficiencies and the temperature rise of the battery are measured for each discharge and charge.

4. Simulated Load Profile Tests. The purpose of this test is to measure the performance of a battery discharged under a load profile which simulates vehicle power demands with a specific driving profile. Although almost any profile can be applied, the simulated load profile used as a standard in the NBTL is that originally predicted for the DOE Electric Test Vehicle (ETV-1), both with and

without regenerative braking while traversing the "D" driving cycle of the SAE J227a/D Test Procedure. The actual ETV-1 consumes approximately 15% more energy than originally predicted; however, an improved ETV-1 could be built to achieve the original predictions. Batteries are subjected to this profile using power levels scaled according to the weight of the battery under test. In this manner, a cell, a multi-cell module, or batteries or any arbitrary fraction of a full-size battery can be tested under simulated driving conditions with the power density remaining the same in all cases. During these tests, the number of driving cycles completed during a discharge are counted, the coulombic and energetic capacities and efficiencies recorded, and the temperature rise measured.

5. Peak-Power for Sustained Duration. The purpose of this test is to measure the capability of a battery to deliver power for up to 30 seconds at three states-of-discharge: 20%, 50%, and 80%. Two steps comprise this test. The first step involves a procedure to determine the instantaneous peak-power at the designated state-of-discharge, and the next step involves the measurement of the sustained power for 30 seconds duration at the three states-of-discharge.

The purpose of life-cycle testing is to determine the number of charge/discharge cycles that a battery can achieve before the capacity declines to a given value. In the NBTL tests, the battery is discharged at the 3-hr rate to 80% of its rated capacity. The number of cycles achieved before the battery capacity declines to 75% of rated capacity is the measure of cycle life.

B. Summary of Test Results

Since the National Battery Test Laboratory became operational in 1978, over 555 cells from the eight aqueous battery contractors have been tested. Table III-1 lists the number, type, and capacity of the cells delivered to NBTL from the contractors. Figure III-1 is a photograph of one of the two Globe, 23.4 kWh, 96 V, improved lead-acid electric-vehicle batteries delivered to the NBTL for testing in 1981. The box being examined in the photograph contains the mechanism for the air-induced electrolyte stirring system. Table III-2 shows the ranges of specific energy, efficiency, and cycle-life demonstrated in the testing at the NBTL. Notable achievements in specific energy (up to 41 Wh/kg) of lead-acid cells have been verified. Cycle-lifetimes greater than 480 cycles have been verified in some lead-acid batteries and testing is continuing. Higher specific energies (up to 68 Wh/kg) have been exhibited by some Ni/Zn modules; however, cycle lifetimes no greater than 179 cycles have been achieved by the best Ni/Zn modules. Nickel/iron batteries have exhibited energy densities of up to 48 Wh/kg and cycle life exceeds 740 cycles on one system which is still under test. Although overlapping exists, energetic efficiencies were generally best for the lead-acid and least for nickel/iron batteries.

Figure III-2 is a bar graph showing the results of tests conducted with discharges simulating an improved ETV-1 electric vehicle traversing the J227a/D, urban driving schedule. The Gould Ni/Zn battery achieved the highest projected range of 138 miles. The Ni/Fe modules show a projected range of 95-96 miles. The improved and advanced lead-acid modules show a

Figure III-1: A Globe 23.4 kWh, 96 V, Improved Lead-Acid Electric Vehicle Battery with Air-Induced Electrolyte Stirring System Under Test in the NBTL

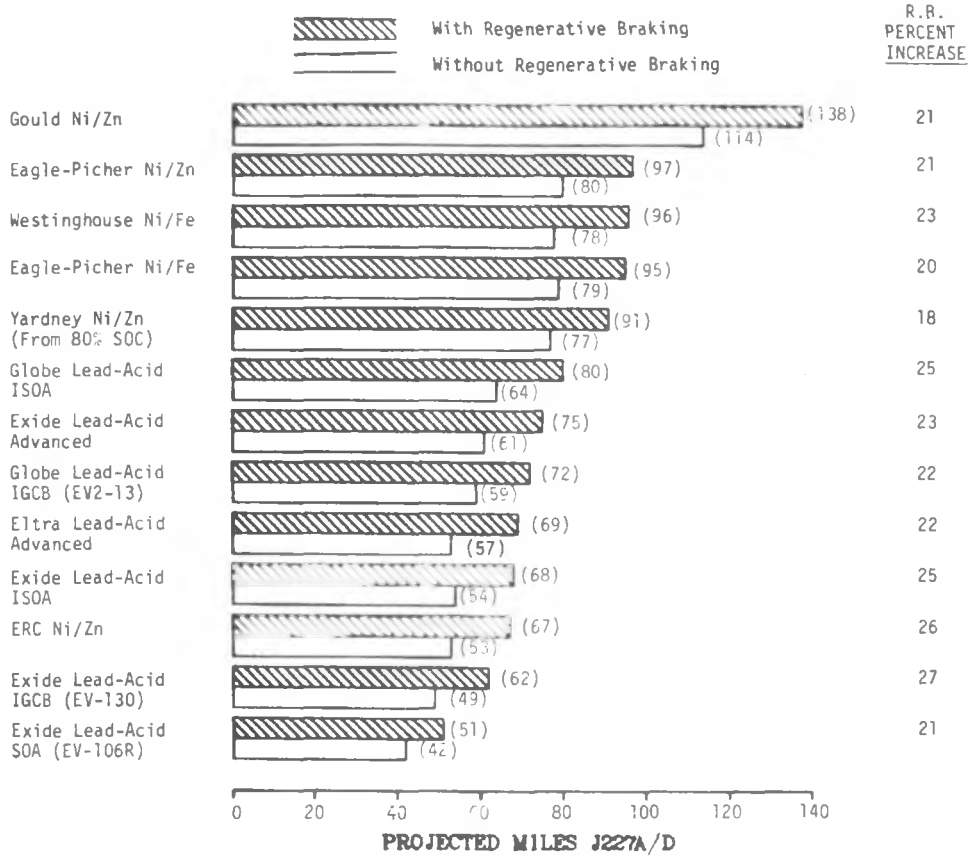

Note: IGCB Represents Improved Golf Cart Battery

Figure III-2: Comparison of Battery Performance (Projected Number Of Miles) Powering an Improved Version of the ETV-1 On the SAE J227a/D Urban Driving Cycle

projected range generally between 70 and 80 miles. In comparison, the state-of-the-art lead-acid battery shows a projected range of 51 miles. These results indicate the relative range of improvements expected from the improved batteries.

Table III-1. Testing of Cells, Modules & Batteries at NBTL for June 1978 to October 1981

Contractor	System	Number of Cells[a]	Nominal Rated Cell Capacity Ah
Eltra, C&D	Lead-Acid	54	165
Exide	Lead-Acid	100	180
Globe/GE	Lead-Acid	36	174
Globe	Lead-Acid	137	249
Eagle-Picher	Ni/Fe	30	270
NIFE	Ni/Fe	10	245
Westinghouse	Ni/Fe	38	220
Eagle-Picher	Ni/Zn	20	225
ERC	Ni/Zn	56	240
Exide	Ni/Zn	4	290
Gould	Ni/Zn	44	400/225
Yardney	Ni/Zn	26	220

[a]These have been tested or are under test at the NBTL in the form of cells, modules or batteries

Table III-2. Performance Data Obtained at NBTL As of September 30, 1981

	Specific Energy (Wh/kg)	Energy Efficiency (%)	Cycle Life
ISOA Lead-Acid			
Eltra	40	71	95
Exide	40	63	295
Globe	41	85	>481
Nickel/Iron			
Eagle-Picher	47	65	>740
NIFE*	38	48	189
Westinghouse	45	49	>582
Nickel/Zinc			
Eagle-Picher*	50	70	38
ERC	46	73	76
Exide	42	48	35
Gould	68	72	179
Yardney	62	80	14

*Direct Purchase

>Indicates Testing is Continuing.

Figure III-3 shows a representative set of characteristics illustrating the peak power capability for sustained discharges of durations of up to 30 seconds. Shown are the data collected for six different depths of discharge on an Eagle-Picher 5-cell, 280 Ah, Ni/Fe module. The values of specific peak power in W/kg at each DOD are plotted as a function of time for up to 30 seconds. As it is evident from these plots, the peak-power decreases as the battery becomes discharged. Also at any given depth of discharge, the peak-power for 15 seconds is not appreciably higher than that for 30 seconds.

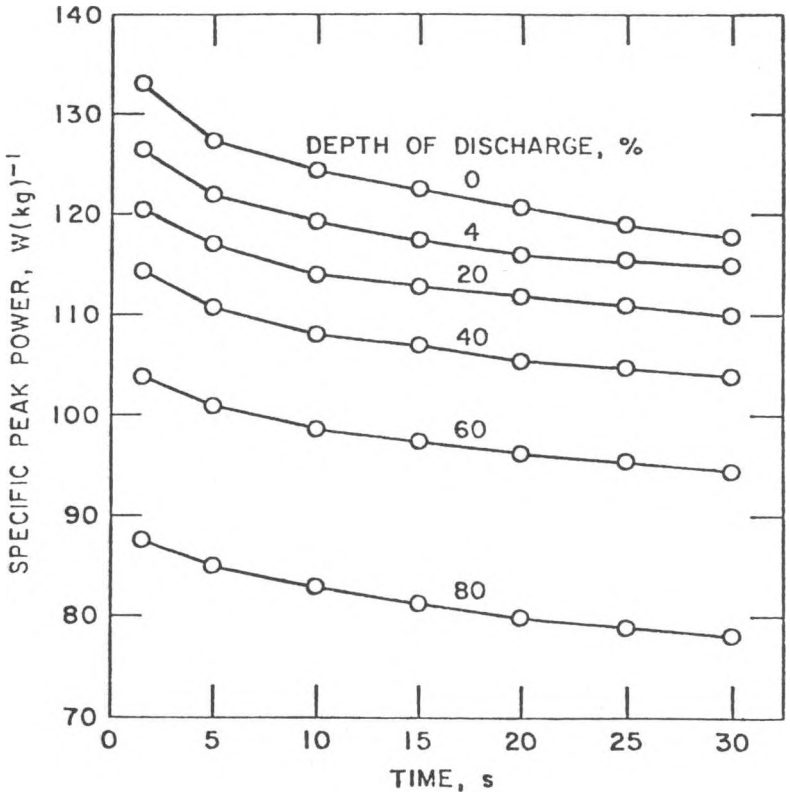

Figure III-3: Sustained Peak-Power Data for Varied Depths of Discharge of an Eagle-Picher, 5-cell, 280 Ah, Nickel/Iron Battery

Figure III-4 is a bargraph of the results of peak-power sustained for 30 seconds at a 50% depth of discharge for each of the battery systems tested. Figure III-5 is a photograph of the electronic regulated, 4000 A, peak power portable test station used for these measurements.

C. Battery Charge and Discharge Studies

The operating conditions imposed by chargers and EV propulsion systems can significantly affect the discharge capacity and energy efficiency of the battery system. Proper selection of the charging procedure and charge parameters is essential in achieving maximum battery performance and life. Excessive over-charging gives rises to increased battery temperatures, high rates of gassing, and increased component corrosion, while consistent under-

charging causes a gradual decrease in battery capacity, which often becomes irreversible. Certain types of current regulators used for EV speed control impose pulsed-current discharge conditions on the battery which increase its internal power losses and thereby lowers the efficiency of the overall propulsion system. In order to optimize propulsion system and charger designs, it is important that those factors wich affect battery performance be understood and characterized.

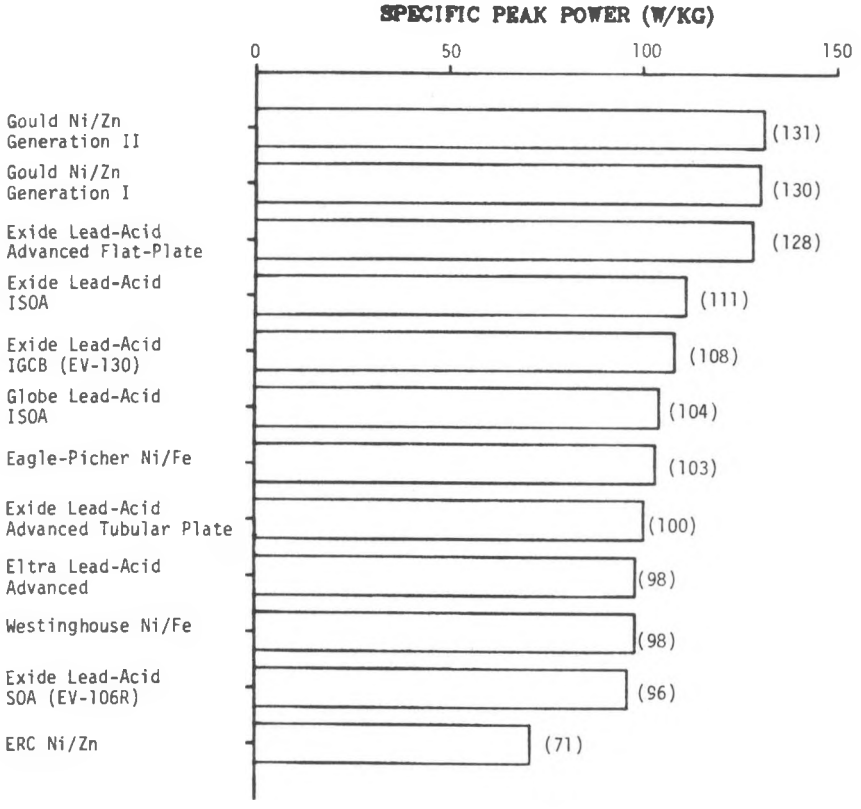

Figure III-4: Specific Peak Power Sustained for a 30 Second Duration at 50% DOD

Studies were, therefore, conducted to quantitatively determine the effects of charge parameters and pulsed-current discharge waveform parameters on the performance of commercial lead-acid batteries. To acquire the necessary data for these studies, a series of tests were performed using a versatile computer-based battery testing system with specialized cycling equipment and instrumentation. In each test, a specific operating parameter such as charge voltage level, discharge current pulse amplitude, etc., was automatically adjusted over a range of predefined values during a continuous charge/discharge cycling sequence while battery performance was quantified and recorded. Because the performance of lead-acid batteries normally varies with cycle life and operating temperature, baseline performance data was obtained by periodically performing reference cycles with fixed operating

conditions during each test and initiating all charges and discharges at a fixed battery operating temperature. The recorded data from series of single parameter tests are then used to analyze battery characteristics, evaluate charging methods and assess discharge conditions imposed to EV propulsion systems.

New 6 V, 3-cell, EV-106 and EE-IV lead-acid golf cart traction batteries (manufactured by Exide Management and Technology), obtained in separate commercially acquired lots, have been used for these tests. The EV-106 and EE-IV batteries have rated capacities of 133 Ah/770 Wh and 120 Ah/690 Wh,

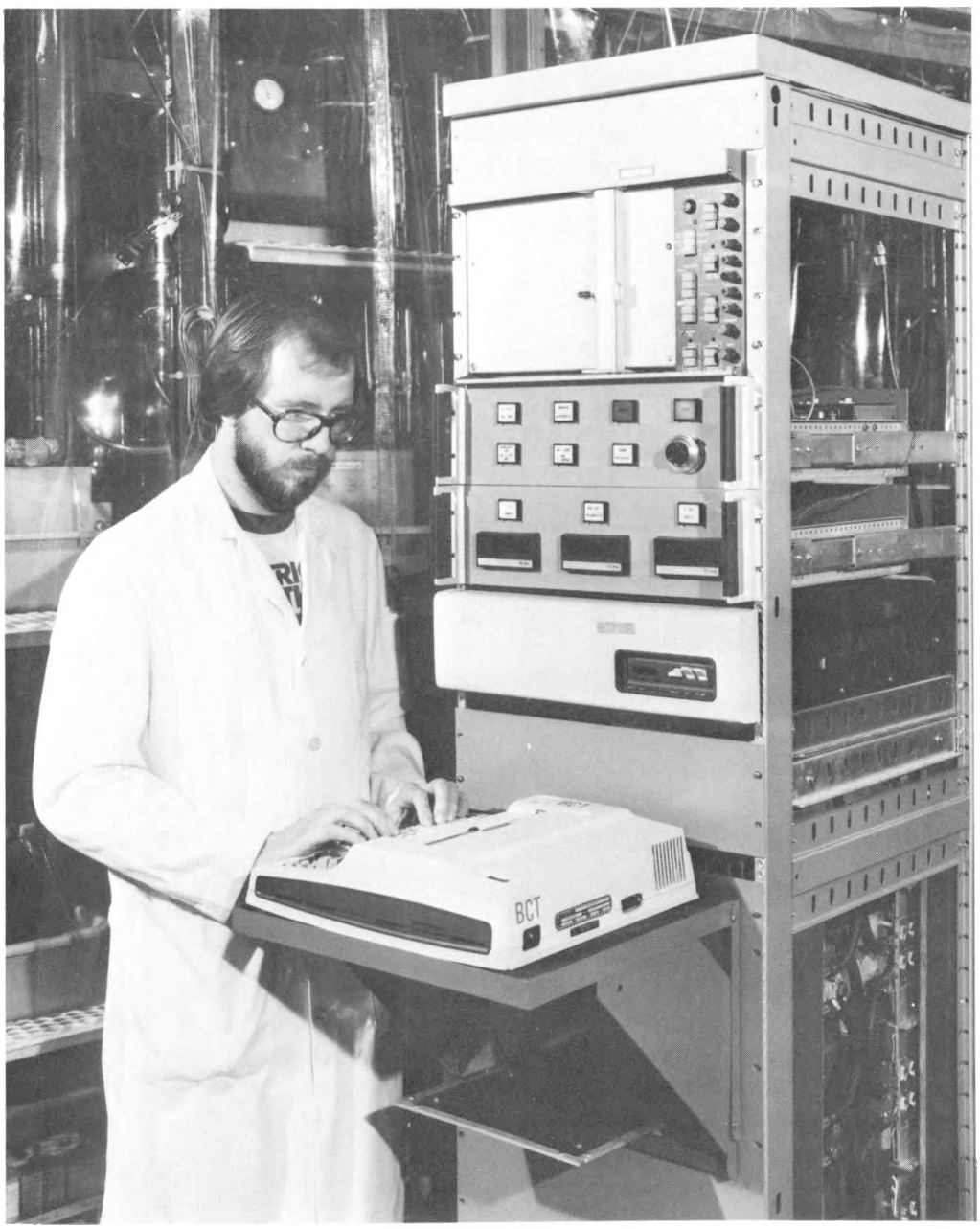

Figure III-5: The 4000-A, Electronically Regulated Peak-Power Portable Test Station in the NBTL

respectively, when discharged at a constant-current rate of 75 A to a minimum battery voltage of 5.25 V. The EV-106 contains a paper separator material while the EE-IV uses a newer rubber separator material.

Battery Charging Studies

The effects of charge-current and charge-voltage levels on lead-acid battery performance have been measured. Constant-current/constant-voltage (CI/CV) charging with its simple and direct method of charge control was used as the basic charging technique for these studies. In this CI/CV charging technique, charging is initiated at the selected constant current level and maintained at this level until the charge voltage reaches the selected CV level. The charge voltage is then maintained at the CV level and the charge current allowed to taper down. For these tests, charging was terminated when the current had tapered to 6.0 amps. In a series of tests, a range of constant-current (25-250 A) and constant-voltage (7.20-7.9 V) charging levels were examined. These tests showed that the total time required to fully charge the lead-acid batteries from a deep-discharged condition is limited by battery charge acceptance, but this time can be reduced by increasing the initial constant-current charge level. A minimum charge time of about 3.0 hours was achieved for EV-106 batteries and about 1.3 hours for EE-IV batteries using a charge rate of 250 A. Battery discharge capacity was independent of the initial charge rates tested (25 to 250 A). The effect of charge-current level on the operating temperature, cycle efficiency and recharge time of an EE-IV battery are shown in Figure III-6. High values of charge-current cause a slight reduction in battery Ah and Wh cycle efficiency due to the increased internal I^2R power losses, operating temperatures and gassing rates encountered during charging. The total charge time, however, is significantly reduced at high values of charge-current. Using a charge-current level of 200 A, about 80% of the total charge is transferred to the EE-IV in the first 0.5 h of the recharge (about 60% is transferred to the EV-106 in the same recharge period).

The effects of charge-voltage level on the discharge capacity (data normalized to the battery's rated values) and cycle efficiency of the EV-106 and EE-IV batteries are shown in Figure III-7. Only a limited voltage range of constant-voltage charging provided reproducible and efficient battery operation. For the EV-106 battery, the voltage range was 7.40 to 7.55 V and for the EE-IV, the range was 7.60 to 7.90 V. At charge-voltage levels below these ranges, a gradual but continuous decline in battery discharge capacity resulted. At charge-voltage levels higher than these ranges, no significant increase in discharge capacity was obtained (only a loss in battery cycle efficiency and a rise in gassing level resulted). Within the charge-voltage range for each battery, discharge capacity was directly related to the constant-voltage charge level while cycle efficiency was inversely related to the constant-voltage charge level. Both battery capacity and efficiency can be maximized with proper selection of the charge-voltage level. The charge-voltage level that provided optimum capacity and efficiency for the EV-106 battery was 7.47 V (2.49 V/cell) and for the EE-IV battery was 7.74 V (2.598 V/cell). When charged to these optimum voltage levels, the EV-106 and EE-IV batteries provided reproducible operation for several accelerated test cycles without the necessity of equalization charges. For a single battery and within the two groups of

batteries tested, the optimum charge voltage level was reproducible and found to be independent of the constant-current charge level employed.

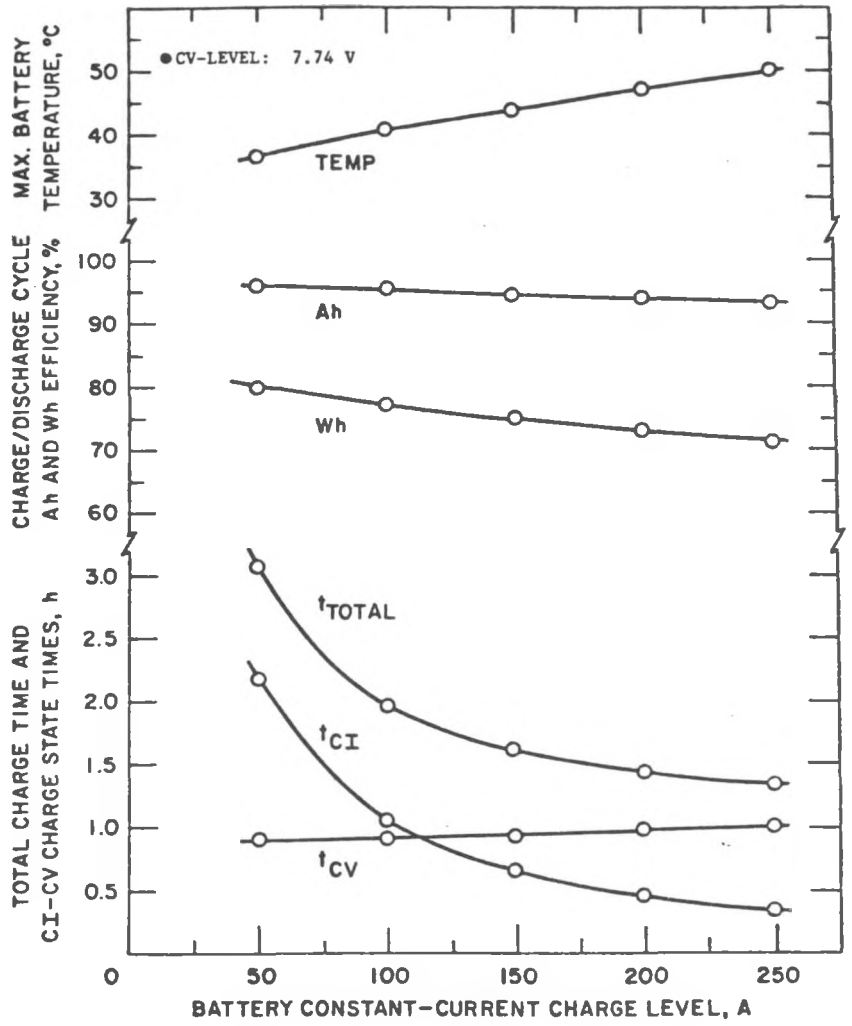

Figure III-6: Effects of Charge Current Level on the Performance of an EE-IV Battery

Battery Discharge Studies

A study was performed to determine the effects of simulated pulsed-current waveforms from a chopper-type controller on battery output power and capacity. A series of tests were developed to quantify the performance of EV-106 and EE-IV batteries with respect to three basic pulsed-current wave-form parameters. The parameters examined were: (1) current-pulsing frequency (F_p); (2) average pulsed-current discharge rate (I_A); and (3) pulse-to-average current level ratio (I_p/I_A). For each test, one parameter was selected as the variable and the other two parameters were maintained at fixed levels. Because the performance of lead-acid batteries varies with cycle life and operating temperature, baseline performance data was obtained by periodically performing equivalent constant-current discharges during each test. In addition, all discharges were initiated at a

fixed battery operating temperature. For the equivalent constant-current discharges, the I_p/I_A ratio is unity, and I_A is the same as that used for the pulsed-current discharges. The recorded data from series of single waveform parameter tests were then used to analyze battery characteristics and performance.

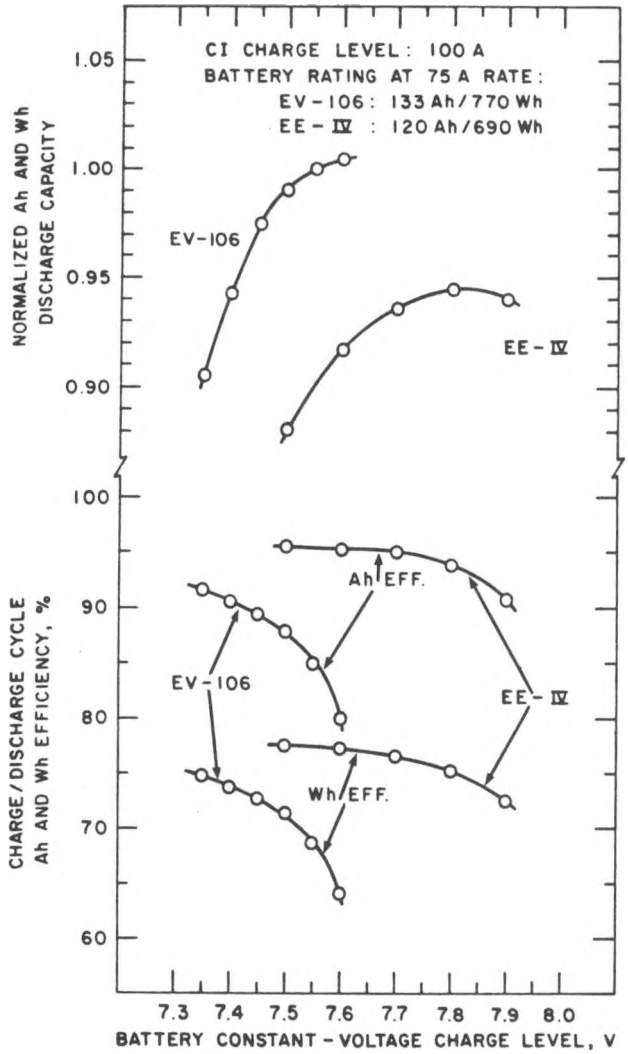

Figure III-7: Effects of Charge Voltage Level on the Performance of an EV-106 and EE-IV Battery

Effect of Pulsed-Current Frequency

Data plots that show the effect of pulsed-current frequency on the discharge performance of an EE-IV battery relative to that obtained for equivalent constant-current discharges are given in Figure III-8. A fixed average-current level (I_A) of 75 A was used for both the pulse and constant-current discharges. A pulse to average current level ratio of two (50% duty cycle) was maintained for all of the frequencies tested (50 to 1000 Hz). The plots in Figure III-8 show that the discharge capacity (Ah

and Wh), output power, and average voltage of the EE-IV battery were constant to within + 0.3% for all of the frequency values tested. Battery operating temperature is also independent of pulsed-current frequency signifying that the internal power losses are constant. Battery output power and available energy were reduced with pulsed-current discharging from that obtained with equivalent constant-current discharging by about 3.5% (14.9 W) and 2.5% (18 Wh), respectively, for all of the frequencies tested. This reduction in power output is directly related to the higher internal battery power loss caused by the pulsed-current waveform structure, I_p/I_A. The higher internal power dissipation with pulsed-current discharging causes the battery to operate at an average discharge temperature that is about 1.4°C higher than that with constant-current discharging. This temperature rise improves battery Ah capacity by about 1%. The loss in battery available energy, (2.5%), is less than that of output power by a level that is equivalent to the increase in battery Ah capacity. The average discharge battery voltage was independent of both the pulsed-current frequencies and different discharge current wave-forms tested. This shows that the values of internal battery voltage and resistance when averaged over the entire discharge period are also independent of these current parameters.

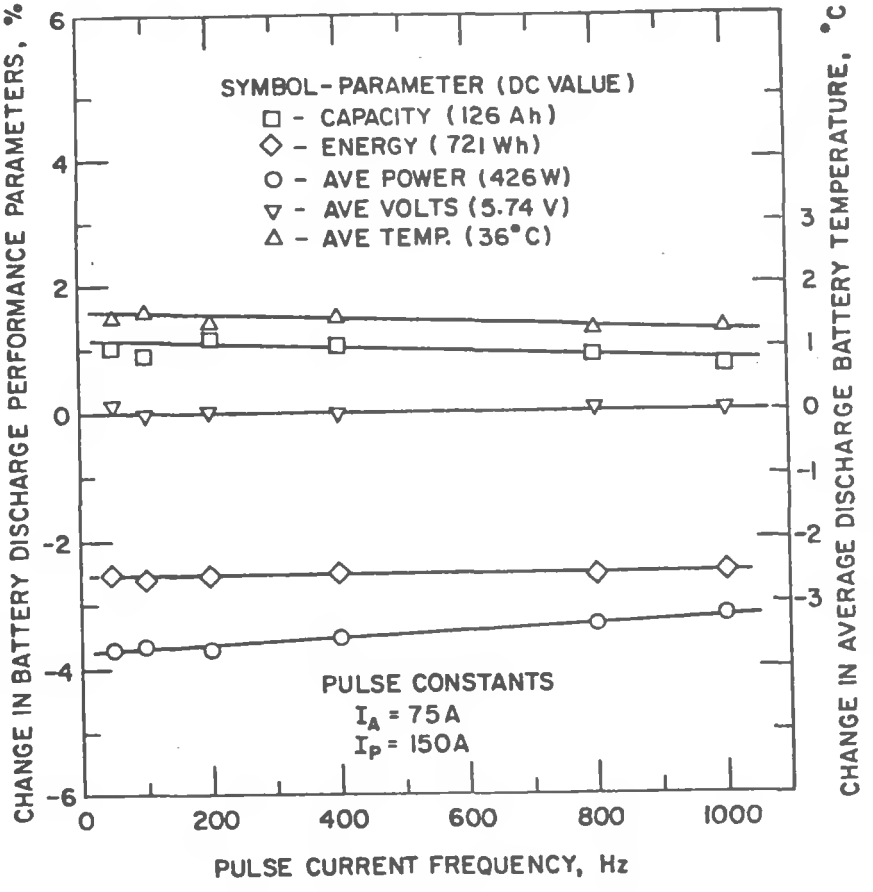

Figure III-8: Effect of Current Pulsing Frequency on the Discharge Performance of an EE-IV Battery Relative to Constant Current Operation

In addition, the effects of pulsed-current frequency were quantified for two average discharge rates, 75 A and 150 A, on the EV-106 battery. In both tests, the I_p/I_A ratio was maintained at a fixed value of 2.0, while frequencies from 30 to 1000 Hz were employed. The test data showed that the performance of the EV-106 was also independent of pulsed-current frequency for all of the values tested. With pulsed-current discharging, the output power and available energy of the EV-106 was also reduced from that obtained with constant current-discharging.

Effect of Pulse-to-Average Current Level Ratio (I_P/I_A)

Tests were conducted to quantify battery performance for current waveform structures that contained pulse-to-average current level ratios (I_p/I_A) of from 1.0 to 4.0 (duty cycles from 100% to 25%). Equivalent constant-current discharges were automatically included in this test sequence when the variable parameter, I_p/I_A, was set to unity. In these tests, the pulsing frequency (F_p) and the average discharge rate (I_A) were maintained at fixed values of 200 Hz and 75 A, respectively. The pulse amplitude was therefore varied from 75 to 300 A to obtain the desired I_p/I_A ratio value while the pulse ON time was adjusted to maintain I_A at 75A. Data plots are given in Figure III-9 which show the effect of the I_p/I_Aratio (I_p variable) on the discharge performance of an EE-IV battery relative to that obtained for the constant-current discharges ($I_p/I_A = 1$) in the test sequence. The plots show that the output power of the EE-IV battery is linearly reduced by up to 11% (46.9 W) because of the higher internal I^2R power loss that occurs as the value of I_p is increased from 75 to 300 A. This increase in internal power dissipation (from about 15.5 to 62.4 W based on a computed average discharge battery resistance of 2.8 ± 0.2 mΩ) causes a 4.5°C rise in the average discharge battery operating temperature at I_p = 300 A and the Ah capacity was increased by about 4% due to the rise in operating temperature. Because of the thermally improved Ah capacity, battery Wh capacity is reduced by only 8%, and not the 11% associated with battery output power, for the 75 to 300A increase with I_P.

To confirm the dependence of battery Ah and Wh capacity on discharge operating temperature, a special test was performed where the average discharge battery operating temperature was maintained at a fixed value of 36°C while a range of current waveform I_p/I_A ratio values were tested. The initial discharge temperature was adjusted in order to provide the fixed 36°C level. When the average operating temperature of the battery was maintained at this fixed level, battery Ah capacity was independent of the pulsed-current I_p/I_A ratio. Battery Wh capacity then responded in the same manner as did the output power for all of the I_p/I_A ratio values tested.

In each of the above tests, the average discharge battery voltage (V_B) was constant to within ± 0.1% indicating that the average discharge internal resistance is independent of the current waveform (pulse frequency and amplitude) for the waveforms tested.

Effect of Average Pulsed-Current Discharge Rate (I_A)

In this test, I_A was varied from 50 to 200 A while the current waveform ratio (I_p/I_A) and the pulsing frequency (F_p) were maintained at fixed values of 2.0 and 200 Hz, respectively. Pulsed and constant current discharges were

consecutively performed at each of the tested values for I_A to determine the relative effect on battery performance. To establish a battery performance baseline, constant-current discharges of 100 A were included at the start, middle and end of the testing sequence. As expected, the test data showed that both battery Ah and Wh discharge capacity decreased as the average discharge rate (I_A) was increased. At each value of I_A tested, the output power and energy obtained from both the EV-106 and EE-IV batteries with pulsed-current discharging was less than that obtained with constant-current discharging due to increased internal power losses.

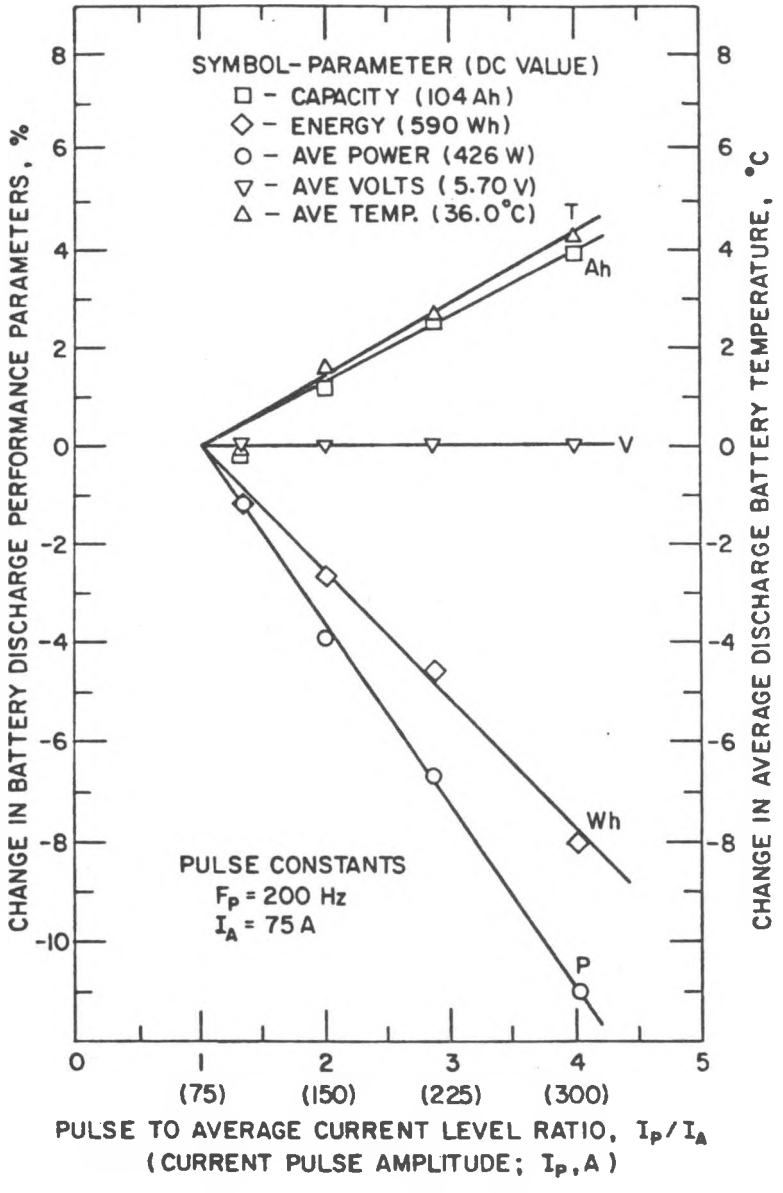

Figure III-9: Effect of Pulse to Average Current Level Ratio on the Discharge Performance of an EE-IV Battery Relative to Constant Current Operation

Figure III-10 shows the average discharge output power and operating temperature of an EE-IV battery as a function of discharge rate (I_A) for both the pulsed and constant current discharges. At each discharge rate, the output power with pulsed-current discharging was reduced from that obtained with constant-current discharging. Thus, if a given output power level is needed, the battery must be discharged at a higher rate with pulsed-current than that needed for constant-current. This higher discharge rate will further reduce the available battery energy. At each value of I_A tested, the relative internal power loss with pulsed-current discharging was twice as large as that with constant-current discharging due to the I_p/I_A ratio value of 2.0. For this reason, the increase in battery operating temperature with pulsed-current discharging is about twice as great as that with constant-current discharging (initial discharge temperature was 35°C). Values of internal (I·R free) battery power output were computed by adding the relative power loss between equivalent pulsed and constant current discharges to the constant-current power level. These internal output power data are also plotted in Figure III-10 and show that the internally generated battery power

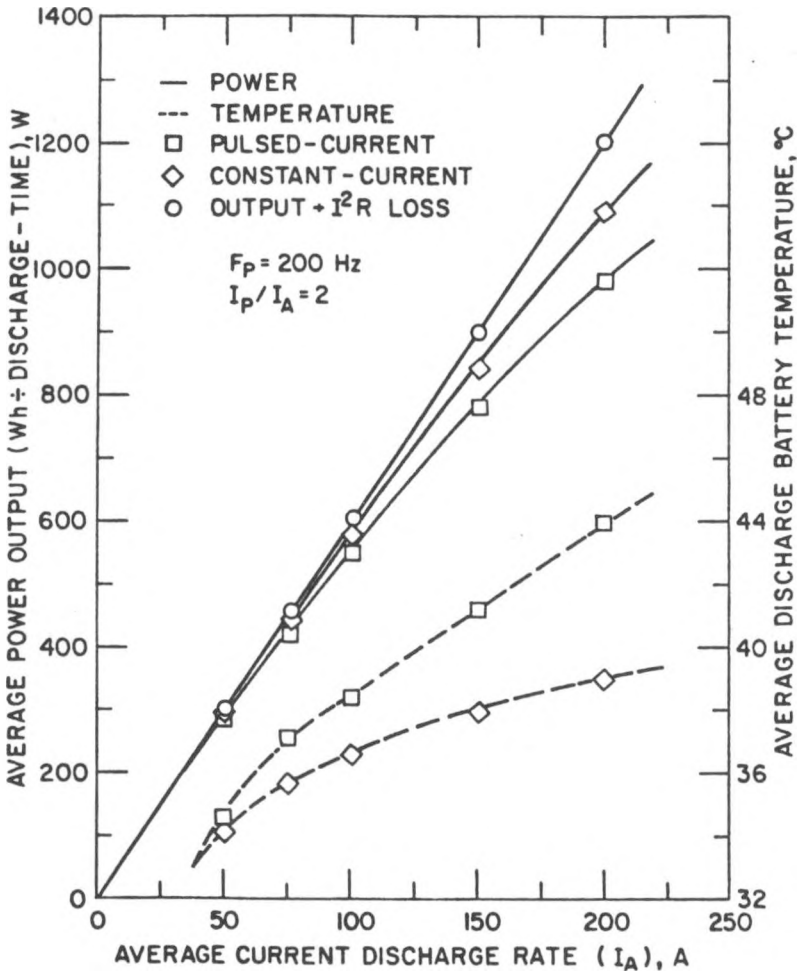

Figure III-10: Effect of Pulsed-Current and Constant-Current Discharge Rates on the Power Output and Temperature of an EE-IV Battery

is directly proportional to the discharge rate (I_A) and independent of the discharge-current waveform. The corresponding average internal "I·R Free" battery voltage is 5.99 ± 0.01 V for all of the discharge rates tested. Values of internal battery resistance were computed for each discharge rate tested by equating the change in measured average discharge output power between the equivalent pulsed and constant current discharges to the change in current RMS level ($R_G = \Delta P/\Delta I^2_{RMS} = \Delta P/I^2_A$). The resistance values computed in this manner were all 2.75 ± 0.05 mΩ.

The response of both the EV-106 and EE-IV batteries to all of the pulsed-current discharge conditions tested was predictable based on the internal resistance and I·R Free voltage of the batteries. Pulsed-current discharging provided no benefit in battery discharge performance.

To perform each of the above tests required special, commercially unavailable instrumentation for parameter detection and computer system control of battery cycling conditions. Interface controllers were designed and developed to generate pulse-current waveform structures by regulating commercially available programmable power supplies and solid state loads. The interface units also facilitate computer control of all operating parameter levels. For the pulsed-current tests, a wideband power and current (for average and RMS levels) detector was developed to obtain signals for computer monitoring. A battery internal resistance detector/meter was also developed to permit computer monitoring of this battery parameter during charge/discharge cycling. The variation in internal resistance of an EV-106 battery for a range of constant-current discharge rates is shown in Figure III-11.

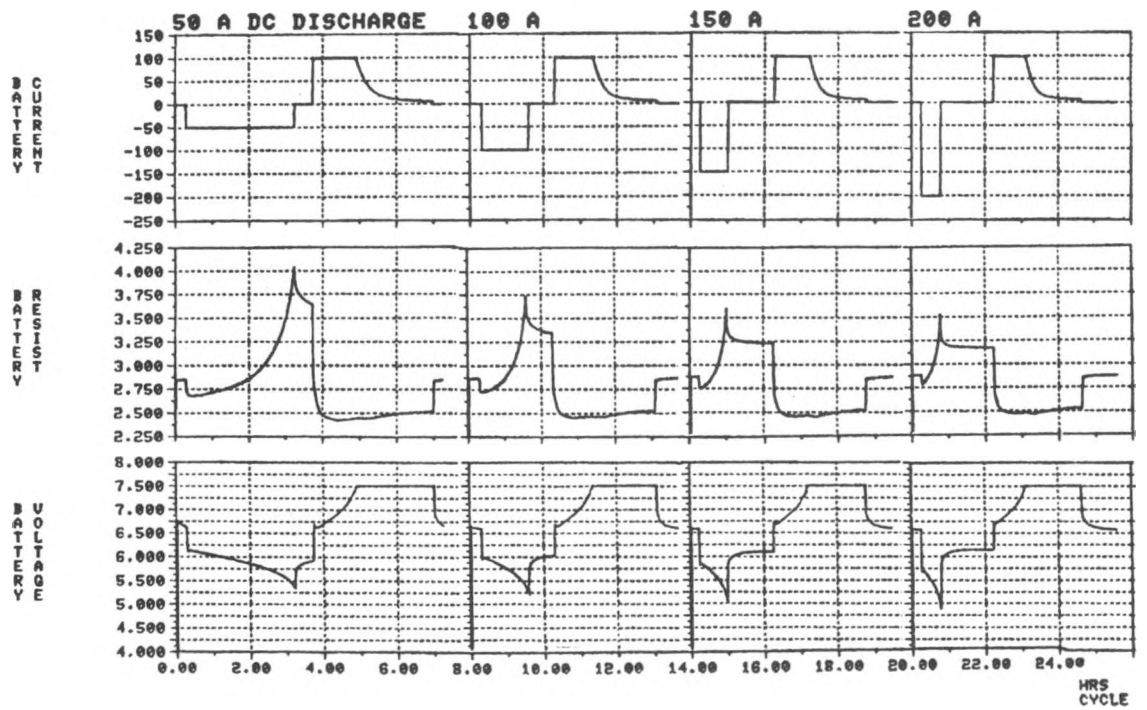

Figure III-11: Internal Resistance of an EV-106 Lead-Acid Battery for Constant-Current Discharge Rates of 50, 100, 150, and 200 A (Average Discharge Internal Resistance, 2.97 ± 0.03 mΩ)

The figure gives computer generated data plots that show battery current, resistance and voltage. For all of the discharge rates shown, the average discharge value of internal battery resistance is 2.97 ± 0.03 mΩ. Additional tests are being developed to evaluate direct battery resistance monitoring and internal "I·R Free" battery voltage derived measurements as a means of battery state of charge indication. Continuous internal resistance measurements are also providing data to enhance battery models for performance prediction.

D. NBTL FY 1981 Advances in Testing Capability

Testing capabilty advances occurred in four areas of the National Battery Testing Laboratory. Software development, hardware expansion and improvement, facility additions and specialized instrumentation all contributed to enhancing the overall operation of the laboratory.

Software

The major software effort was directed at improving the application of simulated driving profiles. Transmission of data from the profile processor to the main NBTL computer allowed unattended operation of driving profile tests. Resulting data is transmitted to the main NBTL computer for reporting and graphical display. The ability to suspend and resume a driving profile test was an equally important addition. The driving profile test station is now a standard operational feature in the NBTL. Other software advances included special programs for temperature compensated charging and the ability to charge a battery using constant power.

Hardware

The major hardware improvement was the installation of the additional NBTL computer. The use of a more powerful processor has reduced the computer response and graphical output time dramatically thereby allowing additional standard and specialized profile tests to be efficiently added to the system. The testing capability of the NBTL was expanded from 32 to 42 test stations - 39 of which are for cells or modules and three are for full-sized batteries. The hydrogen and air-flow safety systems were installed and rendered operational. The CAMAC data acquisition and control system was expanded to the environmental Annex. In addition, the number of stations capable of simulated driving profiles was increased to permit a larger number of life tests based on driving profiles.

Facilities

The Annex environmental testing area was completed and is presently being used to test battery temperature dependence. The testing capacity of the Annex will be expanded as required by the testing program. An additional hood was installed in the main laboratory to provide full-size battery testing capability in that area.

Development

Development of a solid-state battery cell voltage scanner instrument was initiated and an electronic peak power station designed and constructed.

The peak power unit was later interfaced to a microprocessor for stand-alone operation. The peak power station has become yet another standard tool in the operation of the NBTL. The feasibility of using ultrasonics to obtain the specific gravity of battery electrolyte on a non-involved basis was tested and proved feasible in the laboratory tests.

A calibration plan was developed to verify all data acquisition system inputs as well as all instruments used to measure battery voltages. The equipment used in system and instrument calibration are traceable to the National Bureau of Standards.

E. FY 1981 Advances in Battery Components Test (BCT) Laboratory Testing Capability

To acquire the necessary data for evaluating charging techniques, characterizing battery charge acceptance and identifying those parameters that limit battery discharge performance, a versatile computer-based battery testing system with specialized cycling equipment and instrumentation was developed. This system is capable of concurrently cycling up to 15 battery modules under independently controlled and user-defined charge and discharge conditions while also recording battery performance parameter data. Individual operating parameters, such as charge-voltage level, depth-of-discharge, and discharge pulsed-current frequency, can be automatically varied over a range of values during the battery cycling sequence. The ability to define and execute a continuous cycling sequence while systematically varying an operating parameter allows the corresponding effects of that parameter on battery performance to be quantified and recorded. The recorded data from series of single parameter tests may then be used to analyze battery characteristics, evaluate charging methods and assess the effects of discharge conditions imposed by EV propulsion systems.

To perform the above tests requires special, commercially unavailable instrumentation for parameter detection and computer system control of battery cycling conditions. Interface controllers were designed and developed to generate pulsed-current waveform structures by regulating commercially available programmable power supplies and solid-state loads. The interface units also facilitiate computer control of all operating parameter levels. For the pulsed current tests, a wideband power and current detector was developed to obtain signals for computer processing. A battery internal resistance detector/meter was developed that permits computer monitoring of this battery parameter during charge/discharge cycling. Battery resistance and internal "IR Free" voltage are parameters being evaluated for use in measuring state-of-charge.

The test procedures and equipment employed were developed and operationally tested using commercially available batteries (EV-106 and EE-IV). Other battery types, including lead-acid and Ni/Fe improve state-of-the-art cells, are now under test. Other parameter tests and equipment are also being developed to examine the effects of charge-current waveform structures, charge termination conditions, and constant-power discharge levels and profiles on battery performance. The versatility of this computer-based laboratory test system and cycling equipment enhances battery testing, characterization and performance analysis.

IV. ANL TECHNICAL SUPPORT

A. Post-Test Battery Analyses

During FY 1981, the post-test analysis effort has evolved into three distinct types of activity. The first consists of evaluating NBTL test results, initial nondestructive testing, and visual observation of the dissected module. After dissection, the next stage involves analysis of component samples. Among the analytical techniques utilized are individual electrode cycling, SEM examination of crystal structure and X-ray flourescence analysis of active material composition. After exhaustive analysis, the underlying cause of failure may still be unknown. To assist in identifying the mechanisms leading to cell failure, the third activity consists of selected applied research investigations. An example is nickel electrode charge efficiency.

Twenty-five contractor-fabricated modules were analyzed from October 1980 to October 1981. The primary failure modes were generally discovered in the first stage of analysis. A summary of these failure modes for the three aqueous battery systems is shown in Table IV-1.

Visual examination of the nickel/iron module indicated only swelling of the nickel electrode. This swelling suggested loss of electrical contact of the active material to the current collector or pore blockage resulting in electrolyte starvation as possible failure modes. A large increase in ampere-hour capacity was observed when individual nickel electrodes were cycled against inert nickel sheet counter electrodes. Optical and SEM examination showed that the electrode substrate-active material interface was intact and free from corrosion. Furthermore, chemical analysis of electrode samples and X-ray flourescence mapping gave no unexpected results. The electrolyte starvation hypothesis was therefore consistent with the analytical results.

Initial inspections of nickel/zinc modules showed the well known failure mechanisms of shape change and dendritic shorting. The construction of one contractor's modules invariably led to severe zinc electrode shape change and resultant hard destructive shorts. The other contractor's modules avoided hard shorts, but slowly lost capacity due to zinc dendritic separator penetration. Decline of this contractor's nickel electrode capacity was also observed, but not explained.

Lead-acid modules have tended to fail prematurely due to formation procedures or eventually succumb to grid corrosion.

In one series of lead-acid modules, discoloration of the positive electrode indicated that it was the capacity-limiting component. Examination of the crystal structure of the electrode by SEM revealed the presence of inactive lead species. The particular species found indicated that the active material was never completely formed during manufacturing. In another series, negative electrode blistering or heavy mossy deposits limited modules capacities quickly. Normal investigation techniques did not reveal any abnormalities. In related work, techniques are being developed for quantitative measurements of grid corrosion.

Table IV-1

Post-Test Analyses Summary of Primary Failure Modes

Battery Type	Contractor	No. of Modules	Visual Observation of Failure Modes	Analytical Results from Subsequent Studies
Nickel/Iron	A	1	Nickel Electrode Swelling	Electrolyte Stravation/Pore Blockage
Nickel/Zinc	B	4	Separator Penetration by Zinc Dendrites	Nickel Electrode Inactivation
Nickel/Zinc	C	2	Hard Shorts in Areas of Severe Zinc Electrode Shape Change	-
Lead-Acid	D	5	Heavy Mossy Lead Deposits Resulting in Bridging and Shorts	Inactive Negative Electrode Material
Lead-Acid	D	3	Positive Electrode Abnormalities	Incomplete Formation of Positive Active Material
Lead-Acid	E	1	Extensive Positive Grid Corrosion	-
Lead-Acid	E	5	Severe Negative Electrode Blistering	-
Lead-Acid	F	3	Positive Grid Corrosion and Loose Positive Active Material	-

B. Fundamental Electrode Studies

Basic and applied studies to characterize electrodes are performed at ANL in support of the aqueous mobile battery contractors. The efforts are directed toward improving electrode capacity, utilization and cycle life in a manner complementary to the research activities being conducted by the contractors. The particular topics are selected based on need and importance to the progress of the technologies.

Vibrating Electrode Studies

The patent literature indicates that zinc deposited from a caustic solution, onto a vibrating electrode has a much improved morphology. It was on this basis that the Exide Vibrocel™ has been developed. However, during operation of this cell, some problems have been attributed to the zinc electrode. Therefore, efforts were directed to a fundamental analysis of the hydrodynamics and mass transfer characteristics at a vibrating electrode.

The fluid dynamics in a cell with a vibrating electrode were analyzed and found to be governed by the interactions of free-convection, oscillation flow and steady streaming of the electrolyte over the electrode surface. A review of proposed mechanisms and models revealed numerous inconsistencies and lack of supporting experimental data. Therefore, an experimental study of mass transfer at longitudinally vibrating vertical electrodes was carried out.

Since the convective mass transfer properties for copper in acidic sulfate solutions have been thoroughly examined, this system was chosen to experimentally model mass transfer at a vibrating electrode. The 5 cm wide vibrating electrode was partially masked so that only portions of the electrode were active. When such an electrode, with 6.5 cm^2 of active area was stationary in the electrolyte, the predicted 17 ma limiting current was observed. However, when it was vibrated longitudinally at 23.5 Hz at an amplitude of about 0.06 cm, the limiting current and the AC component were observed to depend upon the location of the active portion of the electrode as shown in Figure IV-1. The DC component is attributable to the steady forced convective flow which provides a diffusion layer thickness that increases with increasing distance from the leading edge of the electrode. The AC component, on the other hand, depends upon the symmetry of the flow conditions.

Experiments were run with three electrode active areas, three vibrational amplitudes and several vibrational frequencies ranging from 13 to 36 Hz. It was found that all these data for the DC component could be correlated by using the expression:

$$Sh = C\ Re^{1/2} Sc^{1/3}$$

where Sh, Re and Sc are the Sherwood, Reynolds and Schmidt number respectively. The constant, C, was determined to be 0.52 ± 0.01. This equation is that for the quasi-steady model. It is based upon a boundary layer thickness obtained in a steady stream across the electrode active area. Using the equation, predictions of limiting current (which is related to the Sherwood number) are obtained to within 14% of the observed values.

In summary, the hydrodynamics and mass transfer characteristics of vibrating electrodes provide a basis for increased operating current densities but not basis for improved deposit morphology.

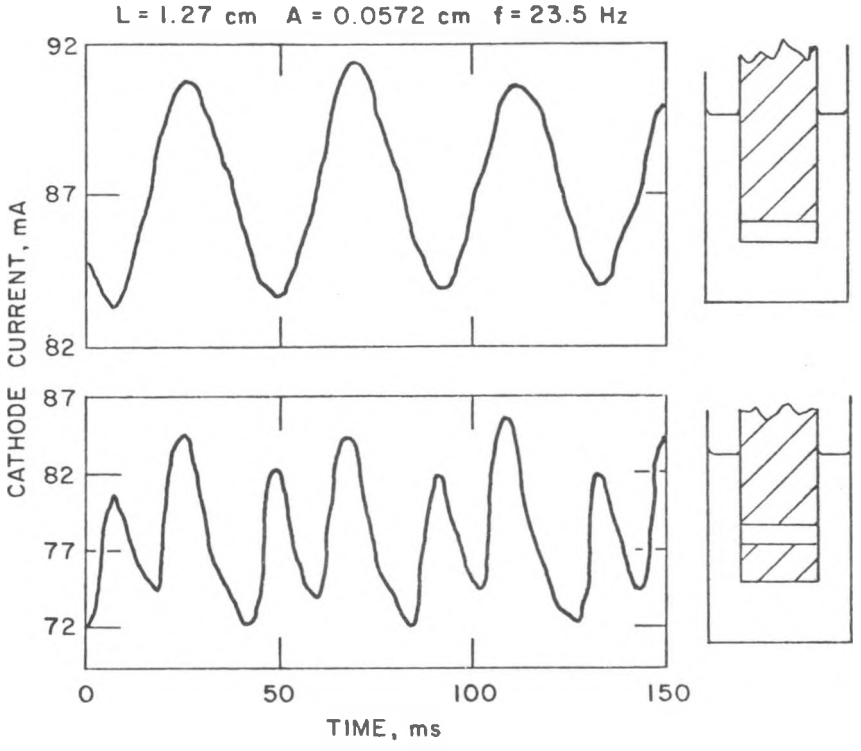

Figure IV-1: Time Dependence of Current on Vibrating Electrodes

Zinc Additive Studies

As presently designed, EV Ni/Zn cells have a shorter than desired cycle life. Frequently, this short life is a result of the formation of zinc dendrites which form electrical conductive paths to the positive nickel electrode. As a result, performance degrades to an unacceptable level. Since the use of organic additives has been found to result in acceptable forms of zinc deposits in the plating of zinc from caustic solution, we initiated a study to evaluate additives for use in Ni/Zn cells. This work supplements the work being carried out by ERC on organic additives.

Figures IV-2a and IV-2b are SEM comparisons of zinc deposited at high current density from a battery electrolyte with and without a commercial additive. It is seen that there is a very striking change in zinc morphology with large dendrites formed when no additive was present and small, rounded zinc particles in the presence of additive. Since a charging cycle is equivalent to a plating cycle, uniform dendrite-free deposition will be possible during charging cycles. However, the stability of the additives must be established.

Magnification = 500x

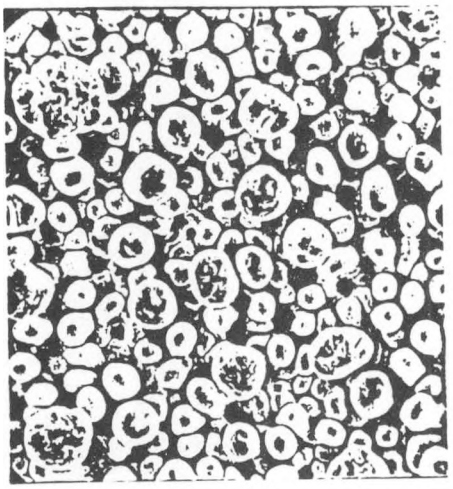

CD = 50 ma/cm^2

Figure IV-2a: SEM Picture of Zinc Deposition from Zincate-Saturated 6 N KOH Electrolyte with Organic Additive at a Current-Density of 50 ma/cm^2 Magnification = 500x

Magnification = 500x

CD = 50 ma/cm^2

Figure IV-2b: SEM Picture of Zinc Deposition from Zincate-Saturated 6 N KOH Electrolyte Without an Additive at a Current-Density of 50 ma/cm^2 Magnification = 500x

In other experiments, it was discovered that cathodic sweep measurements at an amalgamated zinc electrode could be used to detect the presence of an effective additive. When no additive is present a cathodic sweep for zinc deposition peaks at about -1.4 volt vs. a Hg/HgO reference in the same solution (Figure IV-3a). Partially effective additive peaks are seen at more negative potential (Figure IV-3b) and commercially available, very effective additives are displaced so far in the negative direction that no peak is observed up to -1.65 volt (Figure IV-3c). Therefore, it is possible to verify the presence of an additive in the electrolyte by electrochemical means. The next step in these studies will be to use the cathodic sweep technique to monitor additive effectiveness during Ni/Zn cell cycling.

Nickel Electrode Charge Efficiency

One factor inhibiting efforts to improve the performance of nickel electrodes has been the inability to totally characterize the electrode performance with a limited number of experimental measurements. Work carried out last year, led to the conclusion that the state of charge of an electrode and the efficiency of charging are related.

A study of the overall charge efficiency, $\bar{E}$, as a function of the discharge capacity, Q_d, was initiated. Measurements were made on pasted, sintered and pressed metal wool electrodes. The impact of iron contamination was included by cycling the nickel with iron sheet counter electrodes. The data were analyzed using the following two assumptions.

1. The instantaneous charging efficiency, E decreases with increasing state of charge.

2. There is a maximum discharge capacity, $Q_{d,max}$, which is obtained when E goes to zero.

On these bases, and using a normalized capacity, $Q = \frac{Q_d}{Q_{dmax}}$, it was found, see Figure IV-4, that the data for all of the nickel electrodes were correlated by the expression:

$$\ln(1-\bar{E}) = a + bQ_d \qquad (1)$$

where a and b are constants. These results demonstrate that even though Q_{dmax}, for a battery electrode cycled against an iron counter electrode,

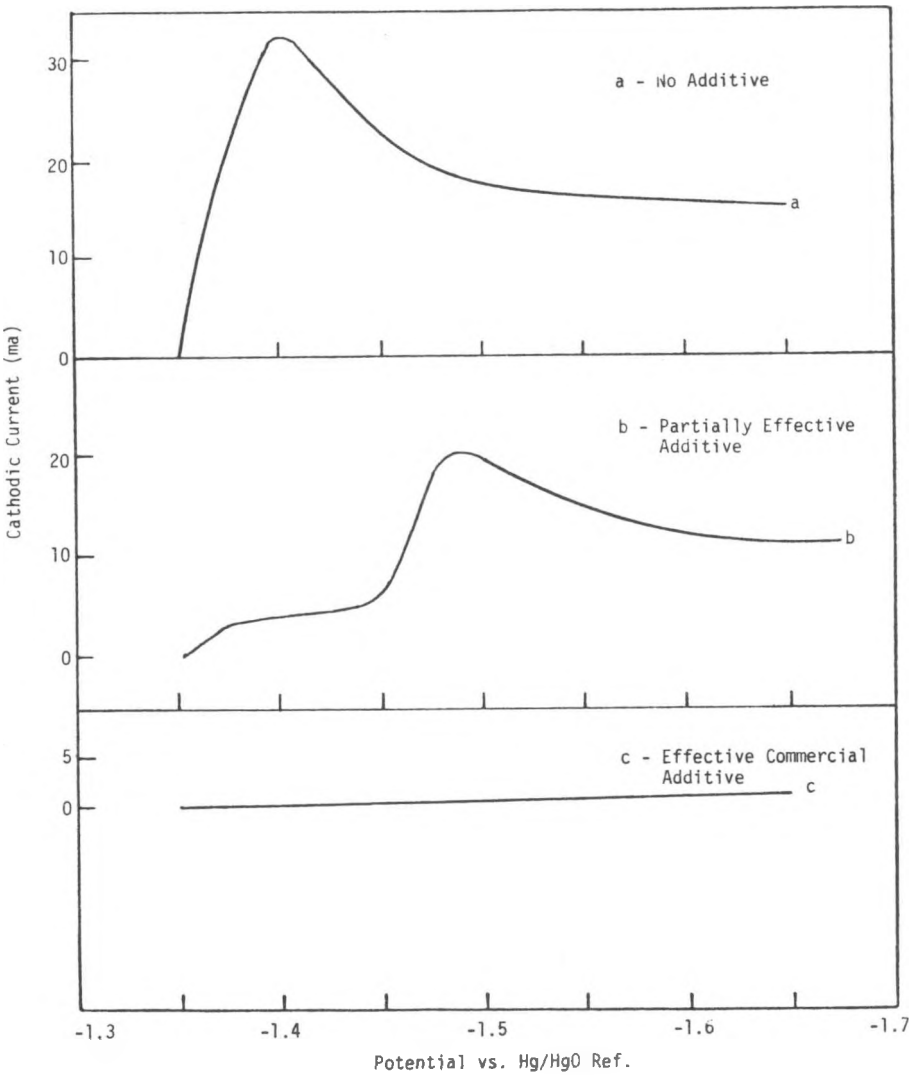

Figure IV-3: Potential Sweep Comparison for
(a) - No Additive
(b) - Partially Effective Additive
(c) - Effective Commercial Additive

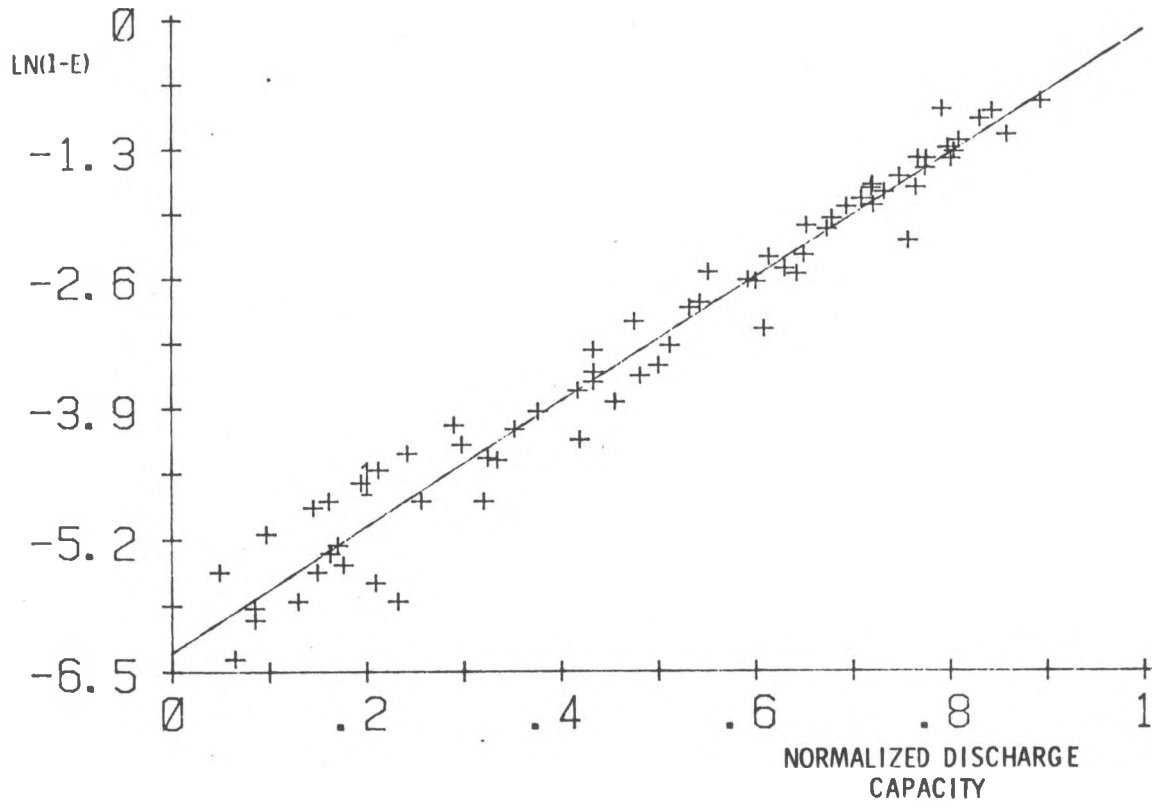

Figure IV-4: Nickel Electrode Average Efficiency vs. Normalized Discharge Capacity

drops to 60 to 70% of its value obtained when cycled against a nickel counter electrode; the correlating equation 1, still characterizes the battery electrodes.

By using equation (1), the instantaneous efficiency, E, can be determined. Figure IV-5 is a plot of E as a function of Q. This result is expected to be useful for estimating thermal effects and water losses by gas evolution during cell operation at various states of charge.

Future studies will investigate the effects of variations in discharge current density and cell operating temperatures. These results are expected to speed the evaluation of modified nickel electrodes by reducing the number of measurements required to characterize them.

Neutron Diffraction Studies on β-PbO_2

The low utilization of lead positive electrodes is major factor limiting lead-acid battery performance. It has been shown that utilization can be increased from about 30% to 60% by establishing the means for electrolyte access to all of the electrode active material. It seems that other factors prevent a greater level of utilization and cause a decline in that level with cycle life. Independent observation indicates that chemically produced β-PbO_2

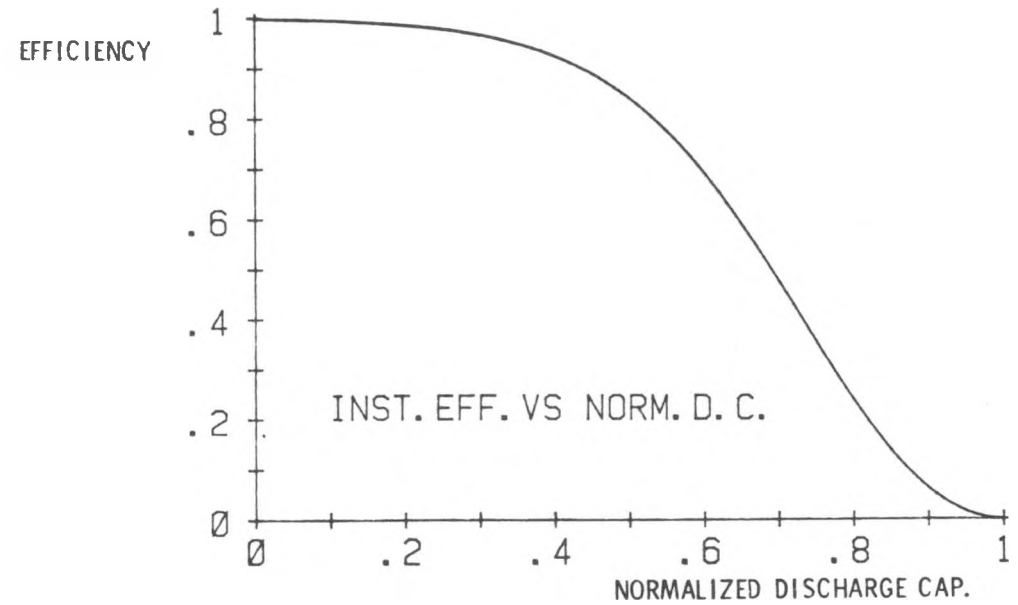

Figure IV-5: Efficiency-Capacity Relationship

is not as active as the electrochemically produced oxide. On this basis, a study with a goal of increased electrochemical utilization was initiated to determine what characterizes the electrochemically active material.

A collaborative effort was initiated with the Solid State Sciences Division in order to make use of their time-of-flight neutron diffractometer as a means for determining the structures and site occupancy in those structures. Commercial batteries were cycled with either H_2SO_4 or D_2SO_4 electrolyte to prepare β-PbO_2-H and β-PbO_2-D. Neutron diffraction spectra were obtained over a d-spacing range of about 0.31 to 1.61 A. Scattering in the low d-spacing range allowed calculation of H and D contents. The diffraction pattern and intensities were analyzed by a computer modeling technique known as the Rietfeld refinement. These analyses indicate the stoichiometry of β-PbO_2-H, to be $H_{0.21}Pb_{0.95\text{-}0.97}O_2$. This is the first work to indicate that battery active lead dioxide is lead-deficient and contains a significant amount of hydrogen. Previous published work had suggested that the material was oxygen deficient. On the other hand, preliminary results seem to indicate that the less active chemically prepared oxide is stoichiometric within the accuracy of the experimental data. The new findings will be of value to workers who are attempting to use additive incorporation to improve electrochemical activity of lead positive active material by modifying the fundamental structure of the β-PbO_2.

C. Nickel/Zinc Battery Separators

Comparative studies of Ni/Zn battery separator materials were continued during the past year. Works performed included the study of zinc penetration failure mechanism of nickel coated Celanese Celgard and nickel salt treated RAI Permion membrane; the effects of membrane electrolyte phase boundary layer resistivity and sequential arrangement of multilayer composite separator system on KOH diffusion flux through the membranes; in-cell cycle life performance tests, and post-test characterization.

An effort was made to examine the zinc penetration resistance of nickel coated separator materials, because it has been reported by several sources that zinc penetration can be greatly retarded by a thin coating of porous nickel on the surface of a separator membrane. The separators used in these tests were nickel coated Celgard 2500 (designated K-317) prepared by Celanese Corp. and NSC-6001 developed by RAI Research Corp. The K-317 separator is Celgard 2500 microporous polypropylene coated with 0.1 mil thick layer of coating consisting of fine nickel powder and cellulose acetate. The NSC-6001 is produced by treating the Permion E-6001 membrane with a nickel salt. E-6001 is a radiation grafted copolymer of methacrylic acid and polypropylene. The zinc penetration test results are shown in Table IV-2.

The zinc penetration test results indicate that nickel coating and nickel salt treatment can improve the zinc penetration factor (ZPF) of the substrate film by about 50% for single layer. In essence, the mechanism of the zinc dendrite barrier consists of the active local action between dendritic zinc anode and the low hydrogen-overvoltage cathodic sites on the nickel layer. The post-test examinations of the failed nickel coated Celgard revealed that the failure of K-317 is attributable to the combined effect of weak spots on the substrate film and the hydrogen gassing caused by the local cell reactions.

Table IV-2. Zinc Penetration Test Data

Temperature: 23°C
Electrolyte: 30% KOH Saturated with ZnO
Overcharging Current: 10 mA

Separator	No. of Layers	Time to Short (min.) (Average Value of 4 Tests)	Zinc Penetration factor (based on a single layer 193 PUDO Cellophane
K-317	1	60 + 30	0.37
K-317	2	240 + 40	1.48
K-317	3	2460 + 330	15.2
E-6001	1	156 + 32	0.96
NSC-6001	1	217 + 62	1.34
NSC-6001	2	265 + 55	1.64
NSC-6001	3	430 + 30	2.65

In a diffusion process, thin films which have concentrations different than that of the bulk solution exist on both sides of the membrane. Thus, the overall diffusion mass transfer resistance of membrane separator to KOH electrolyte diffusion can be separated into membrane and phase boundary components of this resistance. The method of modified Wilson plot[19] was used to separate the components of membrane resistance and to determine if the observed increase in diffusion mass transfer resistance in the 45 to 60% KOH concentration range is attributable to the liquid phase boundary resistances. Typical modified Wilson plots are shown in Figures IV-6 and IV-7. The analytical results are given in Table IV-3.

This analysis indicates that in the range 40-60% KOH electrolyte on one side of the membrane (approximately 0% KOH on the other) (1) the true membrane resistance ($1/K_m = R_m$) for RAI Permion P-2291 40/30 is about twice that for DuPont 193 PUDO cellophane and approximately concentration independent and (2) the phase boundary resistance ($1/k_{b1} + 1/K_{b2} = R_b$) is approximately the same for both materials but is concentration dependent.

Since multi-layers of different separator materials are generally used for the separator systems of alkaline secondary batteries, a mathematical analysis of the multi-layer membrane system, especially with regard to the effect of sequential arrangement of the layers on the KOH diffusion flux, was made. Several series of KOH electrolyte diffusion rate tests were also made on several two-layer systems at various temperatures. The test results confirm the theoretical predictions that in two-layer composite separator system; (1) when both layers are ideal Fickian membranes, the separator system is symmetrical with respect to diffusion in either direction, (2) when either one or both layers contain fixed charges, the permeability of the composite separator will depend on the direction of diffusion. However, as a special case, when the non-linear characteristic parameters such as charge density and the sign of charge of both layers are the same, then the system is symmetrical. Figure IV-8 presents typical diffusion rate test results of a two-layer separator system consisting of a Celanese Celgard 3401 separator which contains no fixed charges, and a RAI Permion P-2291 40/30 separator that contains negative fixed charges. Figure IV-8 shows clearly that the OH^- diffusion flux is much higher (by about 25%) when Celgard 3401 face the dilute side of the diffusion cell.

To establish and evaluate the methodology and procedures of small cell life cycle testing of newly developed separator materials, nickel/zinc cells of 5 Ah capacity were built and tested. The cell tests provide simple, rapid, and effective identification of those separator materials which are worth the effort of full-scale evaluation. The tests with the trielectrode cells were aborted at the 38th-41st cycle as the capacity dropped below 80%. Initial visual inspection of the separators showed no damage. Some zinc dendrites were observed on the separator of one cell.

Post-test characterization indicated that a) the resistance of Celgard 3401 was more than doubled on cycling due to the loss of surfactant activity and b) both separators tested Permion 2291 40/30 membrane and Celgard showed minimal damage over the 40 cycles of test, and also showed no difference between constant current and pulsed charging.

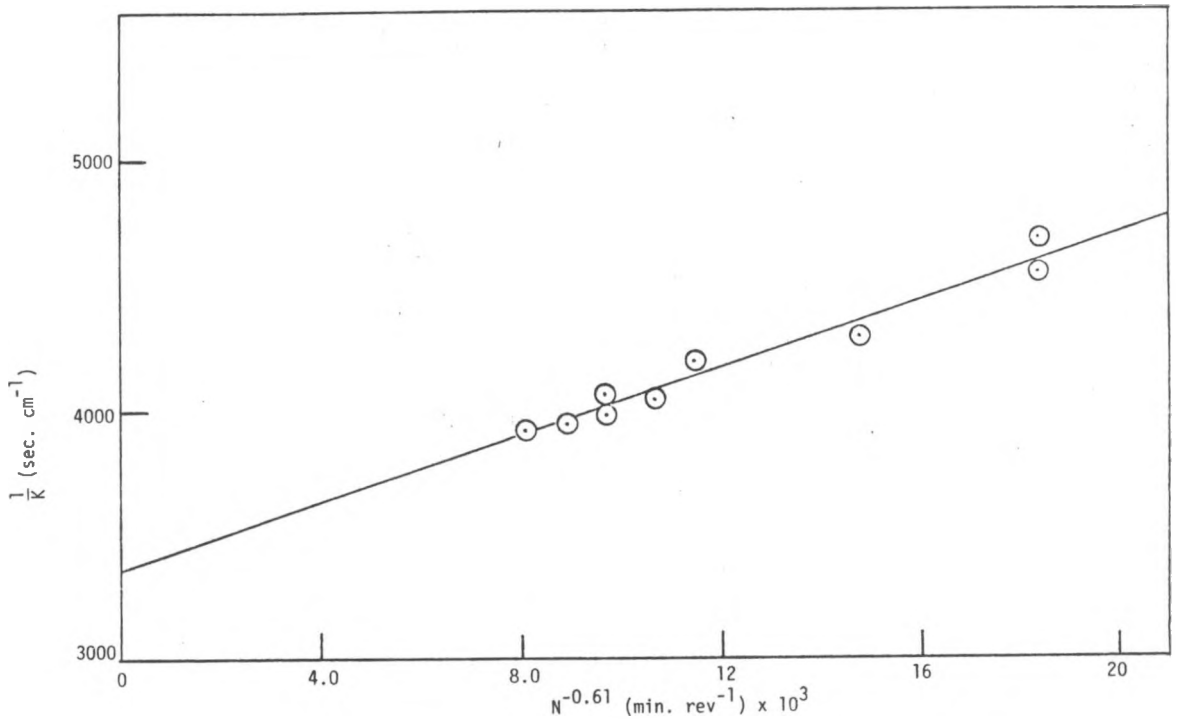

Figure IV-6: Modified Wilson for the Diffusion of 40% KOH Through Permion P-2291 40/30 Membrane

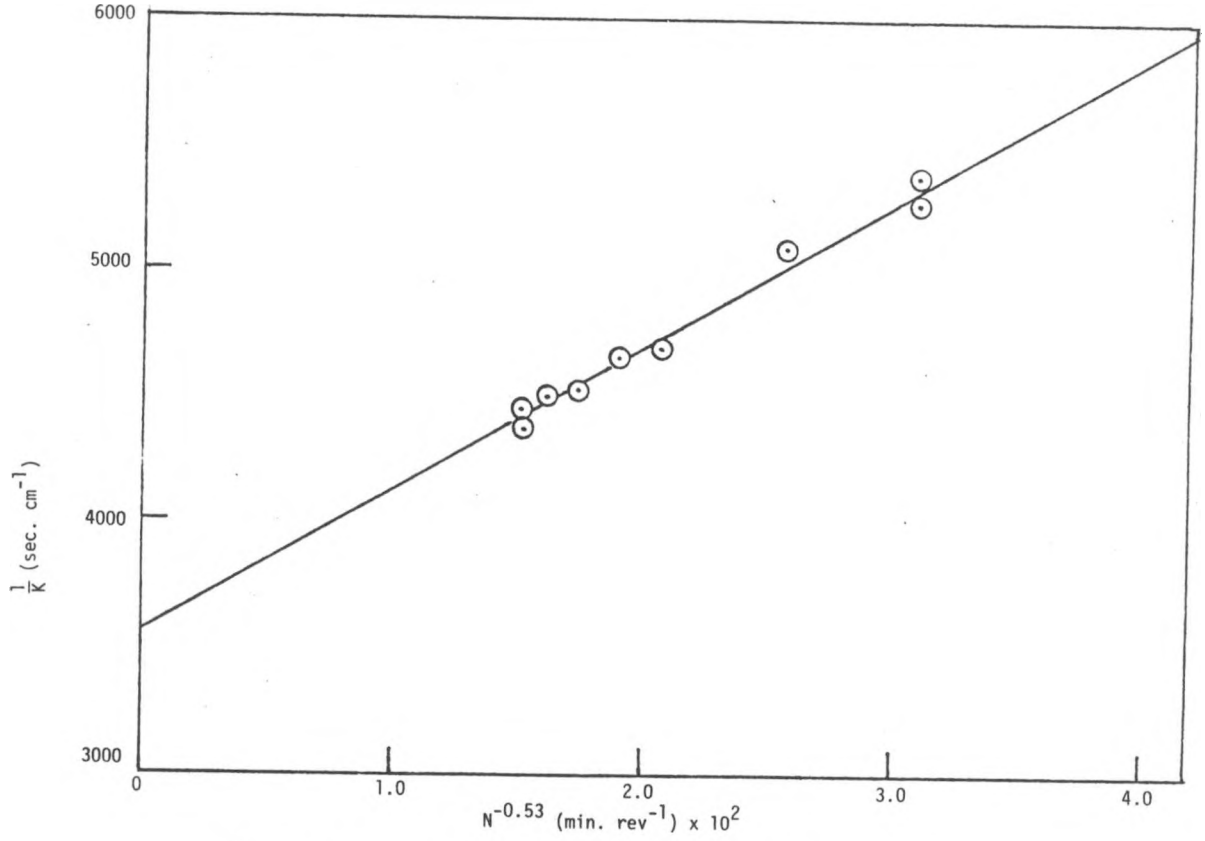

Figure IV-7: Modified Wilson Plot for the Diffusion of 55% KOH Through Permion P-2291 40/30 Membrane

Table IV-3. Modified Wilson Plot Parameters

a) Separator Resistances at 22.5°C
b) Range of Rotational Speed: 700-2,700 r.p.m.

Separator	KOH Concentration Gradient (wt%)	$\frac{1}{k_m} = (R_m)$ (sec. cm^{-1})	$\frac{1}{k_{b1}} + \frac{1}{k_{b2}} (=R_b)$ (sec. cm^{-1})	The Best Fit Values of α
193 PUDO Cellophane	40%	1870	2192	0.63
"	50%	1935	3303	0.55
Permion P-2291 40/30	40%	3373	2146	0.61
"	50%	3560	2968	0.53

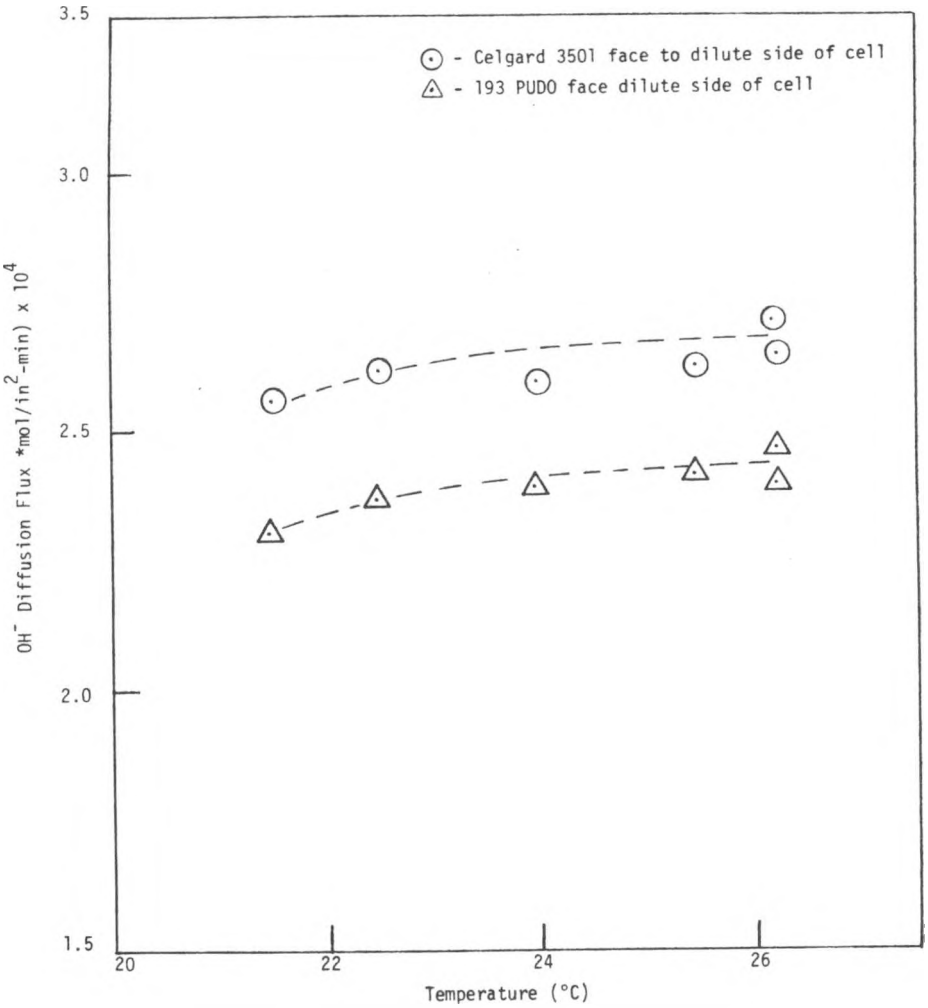

Figure IV-8: OH^- Diffusion Flux Through the Composite Separator System [Celgard 3501 + 193 PUDO]

Professor D. Bennion of Brigham Young University made an assessment of separator materials under an ANL subcontract. His final report[20] on the literature survey included discussion on the role of membranes in zinc/nickel oxide battery technology, possible solutions for problems during battery operation and suggested experiments to characterize membranes.

D. Battery Application Model Development

Computer modeling of battery behavior is aimed at establishing and developing application models which portray battery static/dynamic electrical and thermal behavior during in-vehicle use. These models will provide a basis for evaluating the effects of design variables on battery performance and also assist the understanding of the complex processes which occur within a battery during operation. Research effort was concentrated on the development of a thermal model, a simplified equivalent electrical circuit (EEC) model and a general physicochemical model. These modeling activities are described below.

1. Thermal Modeling of Full-Size EV Batteries

In previous work at ANL, a mathematical model was developed to predict the thermal excursion of a single-module battery.[21,22] For the EV application, however, several modules are needed to power a vehicle of practical size. For example, a full-size battery to be used in a four-passenger sedan consists of eight or more lead-acid modules. Since these modules are compactly packed, as shown in Figure IV-9, the dissipation of heat from a multiple-module battery becomes less efficient, and thus its temperature may be higher than that of a single module. In order to accurately predict and control the temperature of a full-size battery during its operation in a vehicle, a thermal modeling analysis is being carried out by extending the single-module model developed previously.

The thermal behavior of a multiple-module battery can be described by integrating the individual thermal models of all the constituting modules. The equation governing the temperature distribution in an individual module can be written as:

$$\rho C_p \frac{\partial T}{\partial t} = k\nabla^2 T - \rho C_p U \nabla T + \dot{q}$$

where ρ, C_p, k, and U are the average density, the specific heat, the effective thermal conductivity, and the superficial velocity of electrolyte, respectively. The rate of heat production per unit volume,

$$\dot{q} = \dot{q}\,(i, V, \Delta_t, \Delta H, \Delta C_p, \xi, T)$$

has been described in detail in the previous work (21).

The boundary condition at the surface of each module is defined by an energy balance among the heat transfer by conduction, convection, radiation, and the heat accumulation near the surface region of the module, and

is represented mathematically by the following equation:

$$\delta\rho' C_p' \frac{\partial T}{\partial t} = k\nabla T - h(T-T_e) - \sigma\varepsilon(T^4 - T_e^4)$$

where δ, h, σ, ε, and T_e are the boundary thickness, the heat transfer coefficient, the Stefan-Boltzmann constant, emissivity and the temperature of the environment, respectively.

This boundary condition applies equally well to a single-module or multiple-module batteries, with or without gaps between modules except that the definitions of environmental temperature T_e are not the same in the two cases. For a single module, T_e is often set to be the constant ambient temperature, while in the case where modules are placed next to each other, T_e becomes the temperature of the neighboring module. Furthermore, the surrounding air temperature may vary with the location if the number of modules is sufficiently large. Therefore, through the interaction at the boundary, the temperature distributions of a full-size battery may become far more complicated than that of a single module.

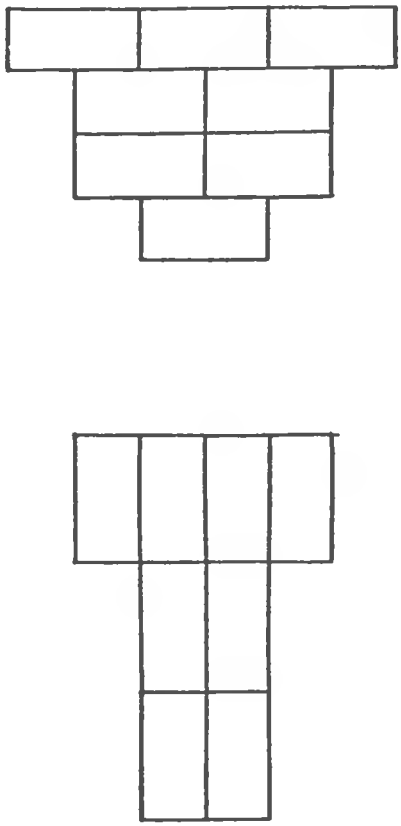

Figure IV-9: Arrangement of Modules in Lead-Acid Battery Pack for a Four-Passenger Car

Another complication arises from the wide variation of the heat transfer coefficient h at various surfaces of modules. Typical methods of evaluating h can be found in the literature concerning the heat transfer in external or internal flow media.[23-25] In general, the heat transfer coefficients are related to the flow conditions, its physical properties, and the temperature gradient by

$h = h\ (Gr, Pr)$	for free convection
$h = h\ (Re, Pr)$	for forced convection
$h = h\ (\delta, k)$	for wall-to-wall conduction
$h = 0$	for insulated boundary

where Gr (Grashof number), Re (Reynolds number), and Pr (Prandtl number) are the dimensionless numbers characterizing the hydrodynamic and thermal domains for the transport environment at each surface.

Once the boundary conditions are formulated, all the three-dimensional governing equations, one for each module, are solved simultaneously by the implicit alternating-direction method.[26] First, the temperature distribution in each module is calculated by alternative iterations in x, y, and z directions. The temperatures of individual modules are then matched at the respective boundaries. Such computations are repeated until the temperatures at all locations converge to a final solution with less than 0.01% deviation from the preceding result. After the solution at a given instant is obtained, the time-dependent parameters are up-dated, and the calculation then proceeds to the next time-step. The entire history of the temperature distribution over a prolonged operation is obtained by the successive time-stepping.

It was found that the numerical method employed in this work is stable, while the number of iterations strongly depends on the rate of heat generation. A typical result of the modeling is shown in Figure IV-10, in which the temperature distributions at the same cross-section of each module of a 3-module lead-acid battery are compared. The result shows that after two hours of charging at the C/3 rate, the average temperatures of modules are approximately 7°C higher than the ambient temperature (25°C), and the temperature difference between the hottest and the coldest spots within each module is about 3°C. It also indicates that the highest temperature exists near the boundaries between modules.

Further refinement of the model is underway. Experimental studies are also planned to verify the accuracy of the calculation. Once the model becomes fully functional, a series of parametric studies are to be carried out to determine the thermal patterns of various types of full-size EV batteries. The effects of the packing arrangement, spacing between modules, as well as the cooling method (e.g., forced air cooling) on the battery temperature distribution are also to be investigated. The results of these studies can provide specific guidelines for designing a thermally stable EV battery.

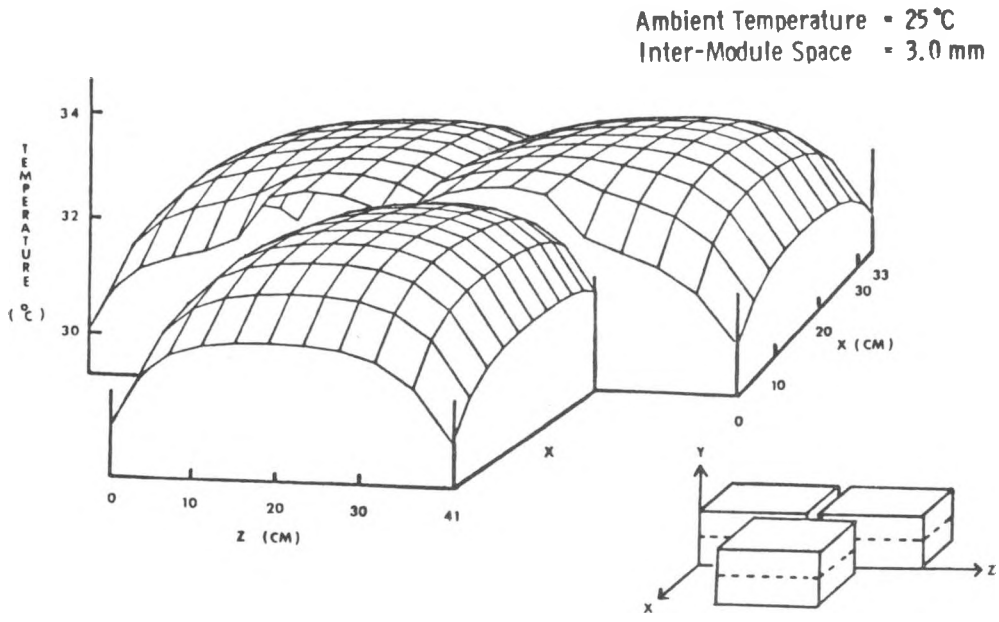

Figure IV-10: Temperature Distribution in a Three-Module Lead-Acid Battery

2. Simplified Equivalent Electrical Circuit Model

The aim of this modeling is the prediction of the voltage-time (V-t) profiles for cells undergoing discharge/charge cycling. The improved version of the equivalent electrical circuit (EEC) that best portrays the electrical behavior of a battery, which is subjected to either the constant current discharge/ charge regime or simplified driving schedule with or without regenerative braking is shown in Figure IV-11. This circuit consists of 3 capacitors and 7 resistors. A conceptual relationship between each branch of the EEC model and physicochemical models can be described as follows: The voltage E_B and the current i_4 represent the output voltage and current of the battery; the capacitor C_1 and resistor R_1 ($R_{1,Dis}$ for discharge and $R_{1,Chg}$ for charge processes) are related to the total quantity of electrode active material and the rate of diffusion of reactive ions from bulk solution to the electrode surface, respectively. The capacitor C_2 is related to the surface concentration of the electroactive species undergoing an electrochemical reaction at a rate that is related to resistance R_2 ($R_{2,Dis}$ being the resistance during discharge of the battery and $R_{2,Chg}$ is the resistance for charging mode). The resistances $R_{1,Dis}$, $R_{1,Chg}$ and $R_{2,Dis}$ vary and depend on the state of charge and the magnitude and direction of the applied current while resistance $R_{2,Chg}$ is invariant. Both C_1 and C_2 capacitors have constant values. The quantity and rate of diffusion of those species present within the body of the electrode to or away from the reaction zone are represented by capacitor C_5 and resistor R_5. These two parameters are assumed to be constant and independent of the state of charge and current. The internal ohmic resistance and the leakage resistance of the battery or cell are represented by resistances R_4 and R_3, respectively. Both of these resistances are also assumed to be invariant. Representative values for an Exide EV-106 six volt lead-acid module are provided in Table IV-4.

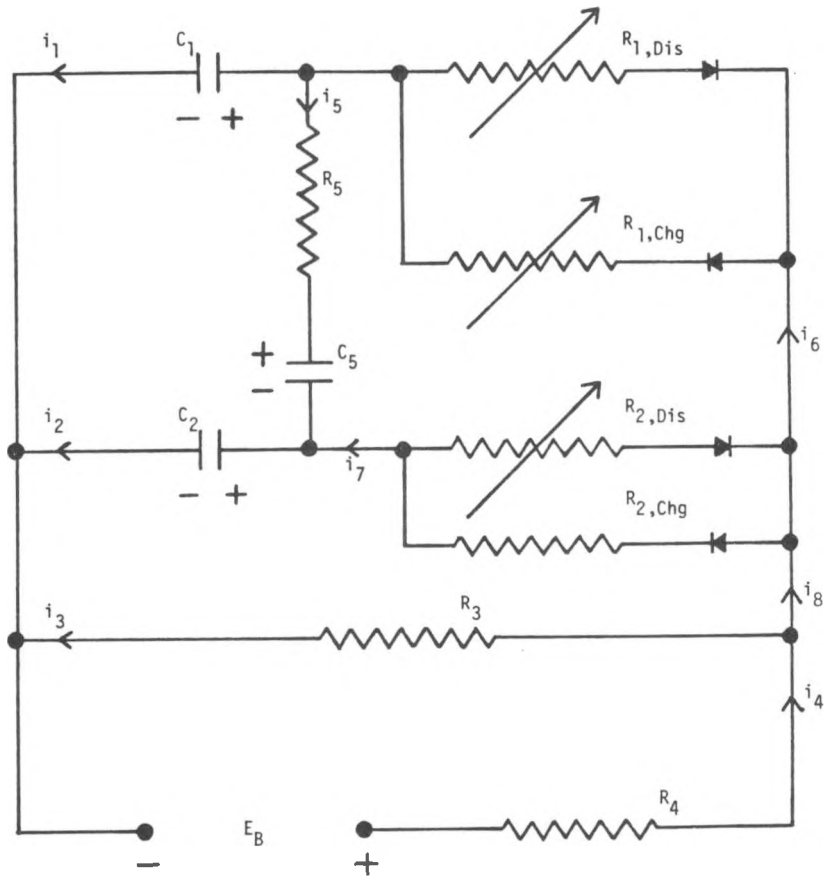

Figure IV-11: Equivalent Electrical Circuit Diagram

Table IV-4 Representative Parameter Values Used for The Simulation of Voltage-Time Profiles

Parameters (Units)	Value
$R_{1,Dis,in}$ (Ω)	3.0×10^{-4}
$R_{1,Chg,in}$ (Ω)	8.0×10^{-4}
$R_{2,Dis,in}$ (Ω)	4.0×10^{-4}
$R_{2,Chg,in}$ (Ω)	6.0×10^{-4}
R_3 (Ω)	10.0
R_4 (Ω)	7.0×10^{-4}
R_5 (Ω)	1.0×10^{-3}
C_1 (F)	2.0×10^{6}
C_2 (F)	1.0×10^{4}
C_5 (F)	1.0×10^{5}
m	1.0
n	1.3
K	2.0×10^{6}
V_{in} (V)	2.0

The results of the computer generated voltage-time (V-t) profiles for constant current discharge/charge regime as well as for driving schedules with and without regenerative braking agree qualitatively very well with the experimental results obtained by NBTL. The addition of capacitor C_5 and resistor R_5 to the EEC model greatly improved the characteristic features of the V-t profiles for constant current discharge/charge regime, especially for open circuit and charging portion of the curves, and the V-t profiles more closely resemble those obtained experimentally.

Recently, research effort was initiated on fitting the EEC model to experimental results. The quantitative comparison of the computer generated V-t curves with the experimental results is based on evaluation of parameter values of the EEC model. Methods for analytical determination of some parameter values of the EEC model from various experiments have been developed. The other component values are determined by employing the parameter optimization methods. Comparison between the results of parameter optimized computer generated V-t profile and a three-cell lead-acid battery data for constant current discharge/charge regime is shown in Figure IV-12. As one can see the approximation of the experimental data using the EEC model is extremely good. The standard deviation between the computed and experimental voltage values at any given time is about 23 mV. At the present time, possibilities of obtaining other parameter values analytically, in order to reduce as much as possible the number of parameter values that have to be determined using the parameter optimization methods, are being explored. The future goal of the project is to be able to predict the battery behavior over an extended time period and possibly its lifetime from a few specific tests.

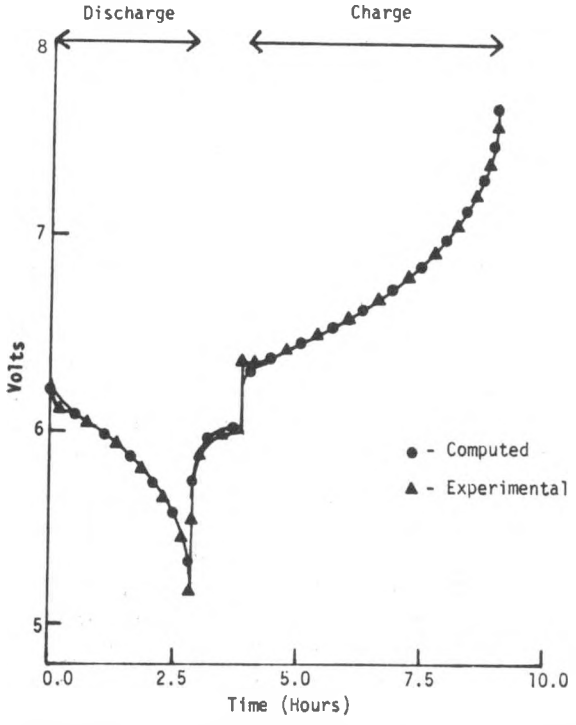

Figure IV-12: Comparison of Voltage-Time Profile Calculated from the EEC Model with Experimentally Measured Profile

3. Generalized Electrical Models

During 1981, an approximate physicochemical battery model was developed and programmed for computer solution. The model, which is actually a single cell model, is intended for use with vehicle simulations and for the processing of battery test and utilization data. Verification and refinement of the model are in progress and preliminary results are promising, as suggested by the comparison of model results with NBTL test data in Figure IV-13.

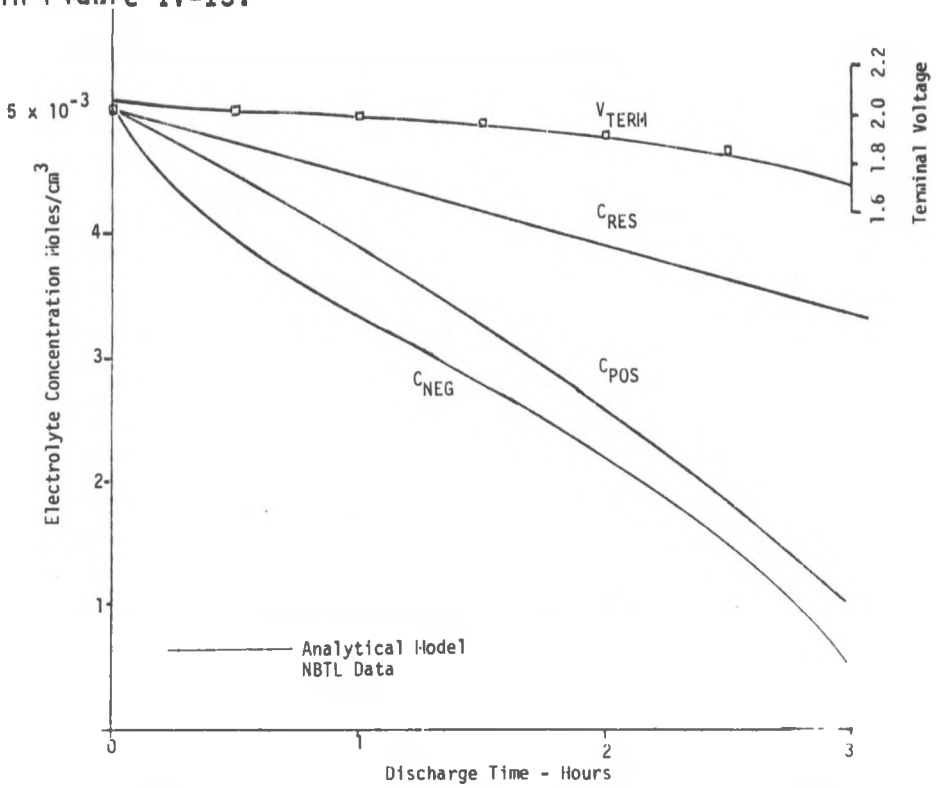

Figure IV-13: Simulated Constant Current (C/3) Discharge of a Lead-Acid Cell

The battery model was developed from the basic equations that describe cell behavior, as presented in the literature[27] and it is not dependent upon empirical data other than that which describes the basic physical properties of the materials and basic electrode behavior. However, some sacrifice of internal detail was thought necessary in order to limit the complexity of the model. Figure IV-14 shows how a section of a typical cell between the center lines of adjacent positive and negative electrodes has been divided into six distinct regions. These are the active and passivated regions of both electrodes, the reservoir space and a single separator. Within each region, porosity (volume fraction occupied by electrolyte) is assumed to be uniform and in the two active regions (only) porosity varies with time. The concentration is uniform but varies with time in the two active regions and in the reservoir. Concentration is assumed to vary linearly through the two passivated regions and the separator, as shown. The thickness dimensions of the two active electrode regions also vary with time. Accordingly, the model comprises seven first order differential equations which determine the timewise behavior of three concentrations, two porosities, and two thickness dimensions.

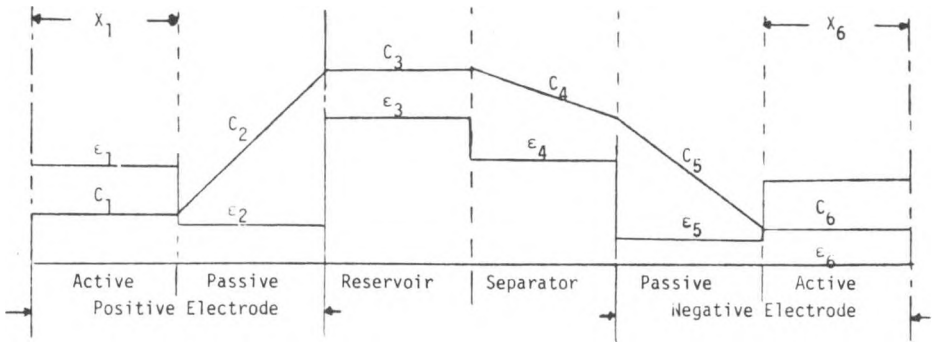

Figure IV-14: Electrolyte Concentration (C) and Porosity (ε) Distributions in Idealized Cell

Additional equations are used to describe electrode current distribution and overpotential, as well as average diffusivity and conductivity in each region. The differential equations are integrated by means of preprogrammed software with battery current as the independent variable. Terminal voltage is computed as needed from tabulations of electrode potential, as well as equations which account for concentration gradient, power losses due to heating of the electrolyte, electrode resistance, and overpotential at the active-passive interfaces.

A particular feature of the battery model, which leads to considerable simplification, is the method used to divide total cell current into two parts, one of which is assumed to act uniformly through an active electrode region to decrease the porosity. The remaining portion is assumed to act entirely at the active-passive interface, causing the thickness of the active region to change with time. Assuming uniform porosity, uniform electrolyte concentration and an exponential (Tafel) relationship between reaction rate and overpotential, the reaction rate distribution can be found in the form of a secant squared function[28]. The value of this function midway between the electrode centerline and the active-passive interface is used to determine a uniform porosity change in the active region. The remaining current, which is in the form of a spike near the interface, is used to determine rate of movement of the interface. This rather arbitrary approximation appears to work well in terms of external battery behavior prediction but its utility is subject to further evaluation.

Future development of the model should include evaluation of its prediction accuracy under variable loading conditions, e.g., driving patterns. Further simplification of the model should be studied and its incorporation into a parameter determination system considered. The latter would facilitate the evaluation of battery performance in the field and its comparison with laboratory testing results.

E. In-Vehicle Test Monitoring Support

1. In-Vehicle Battery Testing

Testing of developmental batteries in vehicles has been carried out primarily by the Jet Propulsion Laboratory (JPL), who will issue separate reports on the test data gathered from the different batteries. During

FY 1981, two full-sized (23.4 kWh, 96-V) Globe lead-acid EV batteries were tested in in-vehicle tests at JPL. These batteries, which consisted of eight 12-V modules, were first sent to NBTL for a characterization test. The characterization test, requiring about 20 discharges, consisted of constant-current and constant-power discharges, as well as discharges simulating driving profiles. Both batteries performed reliably and were promptly shipped to JPL for in-vehicle testing.

During FY 1980 and FY 1981, JPL purchased two full-sized Westinghouse Ni/Fe batteries equipped with a central electrolyte and gas management system (EMS). Testing of these batteries was hampered by problems associated with the EMS (also encountered in previous NBTL module tests). A third battery was assembled by Westinghouse personnel from the best cells of the two batteries. This battery exhibited low capacity and leaks in the EMS, and only limited testing was done.

Testing of an EPI Ni/Fe battery at JPL was quite successful, with performance in accordance with expectations based upon prior NBTL module tests. At JPL, a range of 96 miles at 50 mph was obtained. Testing at other speeds was hampered by problems related to the vehicle motor and controller.

2. Demonstration Results Monitoring

A major activity in the DOE Electric and Hybrid Vehicle Program is the Private Sector Evaluation Project which involves the use of electric vehicles in fleet service by various companies. The purpose of this evaluation project is to generate an overall public awareness of the utility of electric vehicles and to provide the industrial community with the information necessary to make production commitments. In this regard, ANL/OEPM is continually monitoring the results of the private sector evaluation tests to identify problem areas and concerns related to battery performance, safety, and reliability in order to establish if changes are required in the battery R&D program. Frequent communication is also maintained with other electric vehicle demonstration programs, specifically the programs currently sponsored by the Electric Power Research Institute and the U.S. Postal Service.

As of September 1981, the private sector evaluation project involved 16 site operators with 392 vehicles in operation. These operators have generally been satisfied with the performance of the vehicle fleet when operational, but several chronic problems have developed that have kept vehicles out of service for extended periods. Many of the problems have been associated in one way or the other with the performance of the battery. These problems can be classified into three categories: (1) Performance of chargers and charging procedures--particularly the inability of chargers to return the battery to the prescribed capacity. (2) Battery thermal management--chronic overheating of the battery (>130°F) during charge and discharge operations. Conditions identified as leading to this situation have been inadequate ventilation (either by improper design or by equipment malfunction) and improper electrolyte maintenance. (3) Malfunction and meltdown of battery terminals and interconnecting cables. Loose terminal connections, faulty battery module retention systems, improper torque on connectors, improperly sized cables, and extensive corrosion of terminals and connectors are examples of conditions leading to problems associated with terminals and connectors. To help address these and other issues, the Private Sector

Evaluation Project has convened a task force, constituted in part of representatives from the site operators, to determine what must be done to improve battery-vehicle reliability.

Other problems reported by the site operators have mainly related to instances of battery abuse (e.g. driving batteries to >80% DOD on a day-by-day basis) and inadequate maintenance. The implementation of a comprehensive maintenance schedule has been instrumental in minimizing vehicle down times. One of the site operators has achieved a very high vehicle use factor by adopting a maintenance schedule that includes a detailed examination of the vehicle battery and interface equipment on a biweekly basis.

Future plans by several site operators include evaluation of the nickel/iron battery in fleet service. As of October 1981, Northrop Corporation, General Telephone and Electronics Corporation, and AT&T have entered into agreements to retrofit electric vehicles with nickel/iron batteries. In a related activity, the Electric Power Research Institute is planning to test and evaluate the nickel/iron system in fleet service at their TVA site late in 1982. The information obtained in this program will be compared against baseline data now being acquired at TVA with lead-acid powered vehicles.

F. Hybrid Vehicle Battery Requirements Assessment

The performance characteristics of batteries designed for use in electric-internal combustion engine hybrid vehicles are expected to differ significantly from those designed for vehicles with electric propulsion only. The principal goals of this study were; (1) the identification of a range of battery performance parameters, i.e., specific energy and specific power, that tend to maximize petroleum displacement for a chosen baseline hybrid vehicle and mission; (2) examination of the effects of these parameters, along with battery cycle life, on the breakeven battery cost of the baseline hybrid vehicle relative to an internal combustion engine (ICE) vehicle of similar performance capability; (3) determination of the sensitivity of petroleum displacement and breakeven battery cost to variations of battery performance parameters; and (4) examination of the combined effect of battery performance parameter and battery mass fraction variations on vehicle performance. The final result of this effort was a set of battery design goals which will assist in the preparation of a Request for Proposal (RFP) addressed to the various battery manufacturers. This RFP will specify battery cost and design tradeoff studies leading to hybrid vehicle specific battery designs which optimize vehicle performance in terms of items (1) and (2) above.

The study began with a search of the available literature, including proposals and reports from the DOE Near-Term Hybrid Vehicle (NTHV) Development Program. Preliminary estimates of minimum required battery specific power and specific energy were obtained. Following this initial effort, a comprehensive study of the effects of battery performance variations on vehicle performance was undertaken, using the NTHV as a baseline vehicle design. A mathematical model was developed which incorporated an energy flow characterization of the NTHV, along with a special battery model and statistical computations which evaluated average vehicle performance over daily urban travel distance distributions.

The baseline vehicle used in the parametric study is similar to the NTHV design which is a five passenger sedan of medium size and weighing 2023 kg fully loaded. Propulsion is by means of a 34 kw electric motor and a 50 kw ICE. NTHV control strategy makes maximum use of stored electrical energy by utilizing the electric system as the primary power source. When additional power is needed to meet the performance requirement the heat engine and electric motor are used together in a 50/50 power split. When battery depth of discharge (DOD) reaches 70 percent, the heat engine is used as the primary energy source and the battery energy is saved for power augmentation.

The battery model used in this study utilizes an empirical peak power versus depth of discharge function derived from NBTL test data. This function is used to limit available peak power and to determine a battery efficiency factor relating power at the battery terminals to the internal chemical energy conversion rate. Depth of discharge is found by accumulating battery utilization time, computing average discharge power and using it to find the total available chemical energy from a modified watt Hour/Kg versus watt/Kg curve which has been corrected for battery losses. Depth of discharge (DOD) is computed as the ratio of stored chemical energy to available chemical energy. The baseline battery characteristics, which are based upon ISOA lead-acid test results, were scaled around the C/3 energy density and the 50% DOD peak power point to provide a parametric family of realistic battery designs for the study. An idealized battery system with constant peak power and energy density was also used in the study to represent future battery technology. Results with the realistic and idealized models were not markedly different.

Evaluation of vehicle performance for each set of battery parameters was accomplished by finding the expected values of certain performance indices over a daily travel distance distribution. The latter was derived from published data to be representative of average urban daily vehicle usage. The Federal Urban Driving Cycle (EPA) was used throughout the study. An average equivalent petroleum consumption index, reflecting utility wall plug energy consumption as well as hydrocarbon fuel consumption, was derived by this method and used as a primary performance indicator.

The data shown in Figure IV-15 illustrates how NTHV equivalent petroleum consumption is affected by battery specific power and specific energy in urban driving. As expected, increased energy storage capability extends the electric range of the vehicle and results in a decrease in fuel consumption, although a definite diminishing returns effect is apparent. At low specific power levels, hydrocarbon fuel consumption is high because of the need to make up the electric power deficit with the ICE. As specific power increases above 100-120 w/kg, the effect on petroleum consumption decreases (solid curves). This suggests this specific power range might be adequate for the hybrid application and that one of the EV battery designs shown could be used. In the case of the NTHV, however, it was necessary to design to a higher power level (146 W/kg) in order to meet the propulsion power to weight ratio requirement of a conventional ICE vehicle. This constraint was achieved by limiting battery DOD, in each case, to a value which insured that sufficient power was always available. The consequent reduction in available energy due to the limited DOD caused a marked increase in petroleum consumption below the 145-150 W/ kg level (dashed curves). Note that the NTHV battery has been designed to meet this power requirement.

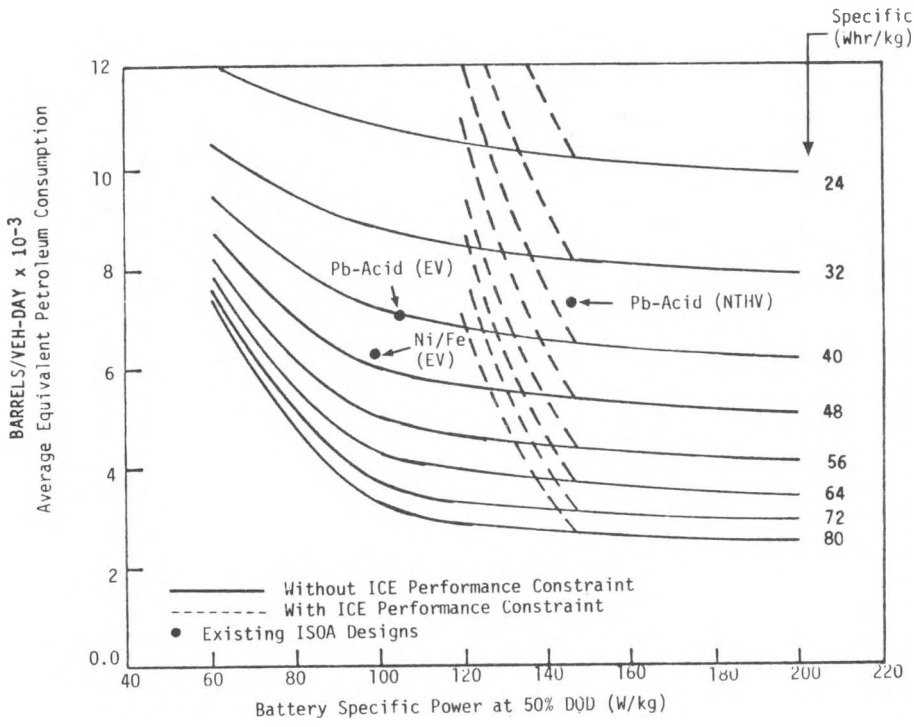

Figure IV-15: Effect of Battery Parameters on NTHV Fuel Consumption (Urban Driving Only)

Hybrid vehicle acceptance will depend to a great extent on how operating cost compares with that of a conventional vehicle. Because battery price is a significant part of hybrid vehicle operating cost, the impact of battery performance parameters on cost was examined by comparing the NTHV lifetime operating cost with that of an ICE vehicle of comparable size and performance. Gasoline and wall plug electricity costs, initial and replacement battery costs, vehicle costs with financing and salvage values for vehicles and battery were included in the analysis. Using the replacement method, a breakeven battery cost was determined for each battery parameter combination. Battery lifetime as a function of DOD was modeled with an empirical function relative to the 80% DOD lifetime. Typical results are shown in Figure IV-16 for the gasoline and electricity costs indicated.

Figure IV-16 suggests that an increase of specific power above the 150 W/kg level will not improve operating cost significantly. However, increasing specific energy above the 60 Wh/kg level or otherwise improving battery lifetime has a significant effect because only two battery packs are required over the twelve year vehicle lifetime. At low specific power levels, improved battery life fails to counteract the increased cost of hydrocarbon fuel.

On the basis of this study, battery design goals of 150 w/kg specific power, 60-70 wh/kg specific energy, and $80/KwH cost with an 80% DOD cycle life in excess of 800 cycles, is appropriate when vehicles in the size and weight class of the NTHV are considered. Further study to determine the applicability of these goals to smaller vehicles is indicated.

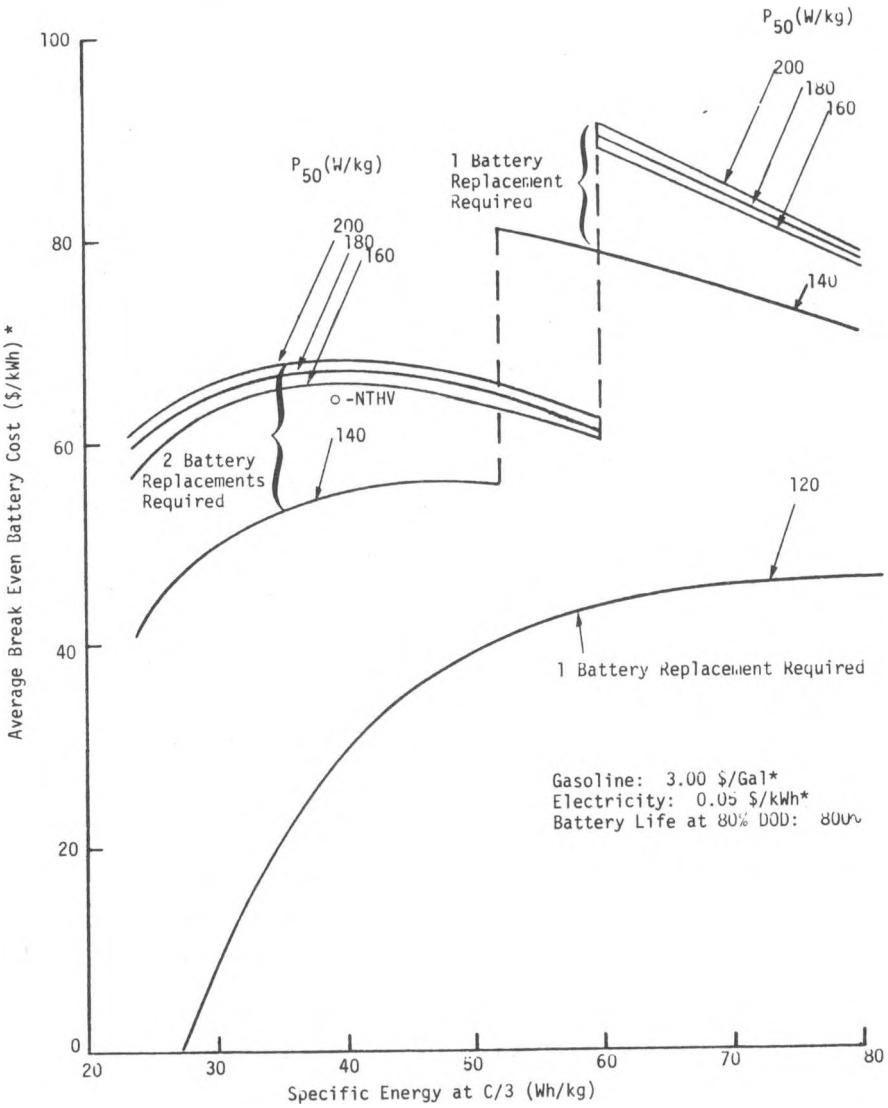

Figure IV-16: Effect of Battery Parameters on Breakeven Battery Cost
* - 1980 Dollars

G. Materials Availability/Cost Studies

A critical question in the future commercialization of battery powered electric vehicles is their impact on the price and distribution network of various materials. Significant price increases on changes in distribution from relatively stable sources to unstable suppliers could alter commercialization of these vehicles (increase their cost relative to other vehicles) and magnify current balance of payments problems. Argonne National Laboratory has developed the Materials Economic Technology Assessment Link (METAL) to assess material price and distributional flow impacts that result from new energy technologies.

The METAL model is a quadratic program based model which traces the least cost pattern of material flow along traditional and future World distribution networks. The model determines the material price and flows which result from commercialization scenarios in a competitive market.

An extreme case commercialization of nickel/zinc powered vehicles was examined for nickel, cobalt, and zinc. Lead-acid battery powered vehicles using the same sales were used to examine lead. The scenarios assumed 500,000 vehicles sold per year from 1985-1989, 1,000,000 vehicles per year from 1990 to 1994, and 3 million per year from 1995-1999. A 25 kilowatt hour nickel/zinc battery per vehicle with 3.5 kilograms per kWh of nickel, 0.175 kg/kWh of cobalt, 1.9 kg/kWh of zinc, was assumed. In parallel, a 25 kWh lead-acid battery per vehicle with 13.6 kg/kWh of lead was also assumed. In addition to a base case assuming no EV commercialization through the year 2000, no recycling and no stockpiling, six scenarios were run for each metal (nickel, cobalt, lead and zinc): These include: (1) an EV case with EV's introduced; (2) an EVS scenario which assumes no recycling but assumes the U.S. Government fills and maintains its stockpile goals (203,000 short tons of nickel, 22,000 short tons of cobalt, 875,000 short tons of lead, and 1,313,000 short tons of zinc) through 1994 and fully releases the stockpile between 1995-1999, (3) an EVSH scenario that assumes all the EVS characteristics but only a release of one-half the stockpile between 1995-1999; (4) an EVRS which has the EVS characteristics plus 95% recycling of EV material between 1990 and 2000; (5) an EVRSH scenario which is the same as EVSH plus recycling, and (6) EVR which assumes the EV characteristics plus recycling. The following paragraphs summarize the results of this analysis.

In the extreme case, the real cost of nickel (1978) dollars in the nickel/zinc EV would be $843 per vehicle or $33.72 per kWh in the year 2000. This represents an increase of $6.80 per kWh or $170 per vehicle over the base case. If the United States exercises proper foresight and planning (recycling and stockpiling) there will be no significant changes in distributional flows or real prices of nickel. High commercialization without proper planning will result in U.S. dependence on Russia and Africa to meet significant portion of increased demand in 2000. With recycling and stockpile release, U.S. demand would be met by Canada. Changes in European demand would be met by Oceania (New Caledonia and Japan). In most cases, the EV demand for nickel is not likely to create distributional flow or price upheavals in domestic and foreign markets.

In the extreme case the real cost of cobalt (1978 dollars) in the nickel/zinc EV would be $203.93 per vehicle or $8.16 per kWh. This is the same as the base case. Thus, if no monopoly power is exerted by African suppliers the real competitive price of cobalt will not be changed by nickel/zinc powered EV's. Unfortunately, the distribution patterns and past history of traditional suppliers (Zaire, Zambia) indicate price control and complete shut-off of cobalt is possible. Under all scenarios the U.S. will rely on African ore and metal to supply its cobalt needs with or without EV's. Recycling and stockpiling will decrease import requirements but not eliminate them. Recycling and stockpiling will not significantly alter the possibility of shut-off and monopoly price changes. Ocean sea mining and the development of viable substitutes for cobalt appear to be the only feasible solution.

In the extreme case the real cost of lead (1978 dollars) in the lead-acid EV would be $809.73 per vehicle or $32.39/kWh. The introduction of electric vehicles in the extreme case raises the price of lead 45%. Distributional flows change very little. Canada and the United States supply increased ore and metal to the U.S. refineries. Mexico decreases its refined product sales to the South American market and meets the rest of U.S. EV

In the extreme case the real cost of zinc (1978 dollars) in the nickel/zinc EV would be $81.00 per vehicle or $3.23/kWh. The introduction of EV's changes the world distribution flows very little. The United States and Canada supply most of the ore and metal needs required by EV commercialization. Some additional metal is supplied by Mexico. It is important to note that EV introduction will increase reliance on foreign suppliers. A final report[29] summarizing this information has been completed.

V. RELEVANT NON-ANL SUPPORT RESEARCH

In addition to the battery research and development activities carried out under the direction of ANL, DOE supports other research efforts on electric vehicle batteries. Of particular interest are a number of basic research topics grouped under the Applied Battery and Electrochemical Research Program managed by The Lawrence Berkeley Laboratory. The pertinent topics are described briefly in the following paragraphs.

A. Research on Lead-Acid Battery Electrodes

The work of Caulder and Simon at the Naval Research Laboratory was completed and the final report[30] was issued. The capacity loss of the positive plate was attributed to a dense coralloid structure which developed during charge/discharge cycling. Failure of tubular positive plates was attributed to the formation of high volume corrosion products on the lead spline.

B. Supported Liquid Membrane Battery Separators

Pemsler of Castle Technology began a study of supported liquid membranes for use as battery separators. At the present time, the effort is focused on separators for the Ni/Zn system. This work is intended to address three objectives: 1) Screening of liquid ion exchange reagents for stability and for optimal hydroxyl ions exchange capacity; 2) Measurements of hydroxyl ion transport rates through this type of separator; and 3) Determination of the effects of using this type of separator on the behavior of zinc electrodes.

Ambient temperature studies have found that the activity of the liquid ion exchange reagent systems does not decrease over periods of at least two months. Elevated temperature stability tests have also shown no degradation after 6 weeks at 50°C. Hydroxyl ion transport in these separators are about 2 to 3 times lower than in the supporting separator membrane itself. Cycling of cells using this type of separator is underway to evaluate the effect on the zinc electrode.

C. Development of a High Rate Insoluble Zinc Electrode for Alkaline Batteries

This program conducted by Charkey at ERC concentrates on the development of Zn electrode/electrolyte formulations which result in insoluble discharge products and the development of activated ZnO samples which are insoluble and/or have the ability to form a more conductive anodic film upon cycling. The latter property of the activated ZnO may permit the use of dilute KOH (15-20%) as the battery electrolyte in which ZnO solubility is limited.

To carry out this work, the zinc electrode is doped with another element, the solubility of the resulting oxide is determined and electrode polarization is measured to determine its suitability as a battery electrode. During the past year, Ce, Pb, Al, La and Cd have been used to dope zinc electrodes. In general, electrode polarization is found to increase as zinc solubility decreases.

D. Concentration Changes in a Zinc Anode Compartment Under Conditions of Severely Limited Convective Flows

Hamby of Linfield Research Institute continued his work on the evaluation of predictions of hydroxyl ion depletion as a failure mode for porous zinc electrodes. A cell was designed to permit sampling of the anolyte within less than one minute of the termination of discharge. The data obtained using this cell indicate that the rate of depletion of hydroxide ion is significantly less than predicted. For example, a 40% drop in hydroxide ion concentration was observed after a 40 minute discharge at 20 ma/cm^2; whereas, a drop of 75% was predicted. It is hypothesized that this difference arises from the neglect of pressure and zinc concentration gradients by the theoretical expressions used to predict the composition changes. In any case, the extent of hydroxide ion depletion is very great when convective mass transport is eliminated.

E. Basic Development of Nickel/Zinc Electrodes

The goal of the work by Katan at Lockheed Missiles and Space Company is to generate basic data to aid development of zinc/nickel oxide batteries for electric vehicles. Experiments are performed in several analog single pore cell designs. During the past year, there were five major accomplishments:

1. Displacement velocities proportional to current density and morphological forms dependent on current density for isolated zinc particles were observed for several current densities.

2. A method for using suspended zinc particles to evaluate dendrite penetration resistance of separator materials was developed.

3. The rate of growth of mossy zinc deposits was measured.

4. Potential profiles in a single zinc pore were determined and found to drop rapidly with depth in the electrode.

5. By varying the overcharge time and current density of a nickel electrode, a charging condition was determined which resulted in capacity nearly double that at higher current densities.

F. An Electrochemical and Morphological Study of the Effect of Temperature on the Restructuring and Loss of Capacity of Alkaline Battery Electrodes

MacDonald at Ohio State University is continuing to investigate the capacity loss on cyclic charging/discharging of porous iron, nickel, and zinc electrodes in alkaline electrolytes. The loss of charge capacity can be attributed, in part, to a degradation of particle-particle electronic contact caused by the cyclic formation and reduction of oxidation products. The goal

of this program is to identify the mechanism(s) of charge capacity loss with emphasis on studying the effect of temperature on those processes which lead to restructuring of the porous electrode and degradation of interparticle contacts.

The work, which has focussed on the nickel electrode has emphasized the collection of impedance data for a variety of operating current densities and temperatures. One finding of these studies is that the anodic oxide film on nickel grows in accordance with the inverse logarithmic law. Efforts are continuing for the purpose of curve fitting data to the transmission line model for porous electrodes.

G. Thermodynamic Framework for Estimating the Efficiencies of Alkaline Batteries

MacDonald of Ohio State University began a project to develop thermodynamic information for alkaline batteries. The aim of this project is to define the thermodynamic properties of concentrated aqueous solutions of LiOH, NaOH and KOH over the temperature range of -20°C to 120°C and those of the metals Li, Al, Fe, Ni and Zn in these alkaline environments. This information is required to assess the overall efficiencies of alkaline battery systems. As a first step, data were collected and equations are being developed to calculate the pH of the hydroxide solutions as a function of temperature and concentration, including the effect of ion pair formation.

H. Temperature Limitation of Primary and Secondary Battery Electrodes

The previous studies of McKubre at SRI International have been on the temperature limitations of Ni, Fe and Zn electrodes in aqueous NaOH electrolyte. He has now extended these studies to include the KOH electrolyte. Particular emphasis was directed towards determining the influence of lithium concentration on the charge/discharge characteristics of iron and nickel oxide electrodes in KOH electrolytes. Slow sweep potentiodynamic studies on the nickel oxide electrode yielded curves lacking reproducibility. This lack was attributed to a variable carbonate level which ranged up to 5% in the working electrolyte.

The following R&D efforts on aqueous electric vehicle batteries were partially funded by DOE through ANL.

I. High Cycle Life, High Energy Density, Nickel/Zinc Batteries

Wagner of U.S. Army ERADCOM reported on his charging studies on maintenance-free nickel/zinc cells at the October 1981 Electrochemical Society Meeting in Denver CO. In this report, he concluded, in contrast to constant current charging, that an interrupted current charge with a rest interval of 150 to 250 milliseconds and a maximum pulse interval of 50 to 60 milliseconds at a frequency of 3 to 5 Hertz will completely prevent zinc penetration through Celgard 3400 separator. Nominal 5 Ah cells, with an initial capacity of 7.2Ah were maintaining 6.4 to 6.7 Ah capacity at 500 cycles. The cycling consisted of repetetive cycles of twenty-five, 4 Ah discharges and 2 deep discharges each consisting of two steps 1) discharge at a 2A rate to a 1.0 volt cut-off, 2) followed immediately by discharge at 1A to a 1.0 volt cutoff.

J. Pulsed Discharge of Electric Vehicle Batteries

Simon, Caulder (Naval Research Laboratory) and Dowgiallo (U.S. Army MERADCOM) examined the effects of pulsed discharge on the capacity and life of lead-acid batteries. The microstructure of the lead-acid battery was found to be converted to the inactive corolloid structure more rapidly under pulsed discharge conditions. The capacity of the battery was consequently reduced.

VI. REFERENCES

1. Yardney Electric Corporation, "Final Report - Design and Cost Study Zinc/Nickel Oxide Battery for Electric Vehicle Propulsion", ERDA Report No. ANL-K-76-3453-1, October 1976.

2. Energy Research Corporation, "Final Report - Design and Cost Study of Nickel/Zinc Batteries for Electric Vehicles", ERDA Report No. ANL-K-76-3541-1, October 1976.

3. Gould Inc., "Develop Nickel/Zinc Battery Suitable for Electric Vehicle Propulsion", ERDA Report No ANL-K-77-3558-1, February 1977.

4. Eagle-Picher Industries Inc., "Design and Cost Study for Nickel/Zinc Battery Manufacture, Electric Vehicle Propulsion Batteries", ERDA Report No. ANL-K-77-3542-1, June 1977.

5. ESB Incorporated, "Cost and Design Study to Develop Lead-Acid Batteries for Electric Vehicle Propoulsion", ERDA Report No. ANL-K-77-3621-1, February 1977.

6. Globe-Union Inc., "Design and Cost Study for Development of Lead-Acid Batteries Suitable for Electric Vehicle Propulsion", ERDA Report No. ANL-K-77-3624-1, August 1977.

7. Eltra Corporation, "Final Report, Task A, Design and Cost Study Development of a Lead-Acid Battery Suitable for Electric Vehicle Propulsion", ERDA Report No. ANL-K-77-3628-1, August 1977.

8. Gould Inc., "Final Report on ANL Contract No. 31-109-38-3639, State-of-the-Art Lead-Acid Vehicle Batteries", ERDA Report No. ANL-K-77-3639-1, August 26, 1977.

9. Westinghouse Electric Corp., "Final Report - Design and Cost Study of a Nickel/Iron Oxide Battery for Electric Vehicles, Volume II: Public Report", ERDA Report No. ANL-K-77-3723-1, August 23, 1977.

10. "Annual Report for 1981 on Research, Development, and Demonstration of Lead-Acid Batteries for Electric Vehicle Propulsion", ANL Contract No. 31-109-38-4206, Eltra - C&D Batteries Division, ANL/OEPM-81-8, March 1982.

11. "Annual Report for 1981 on Research, Development, and Demonstration of Lead-Acid Batteries for Electric Vehicle Propulsion", ANL Contract No. 31-109-38-4207, Exide Management & Technology Company, ANL/OEPM-81-9, March 1982.

12. "Annual Report for 1981 on Research, Development, and Demonstration of Lead-Acid Batteries for Electric Vehicle Propulsion", ANL Contract No. 31-109-38-4205, Johnson Controls Inc. - Globe Battery Division, ANL/OEPM-81-10, March 1982.

13. "Annual Report for 1981 on Research, Development, and Demonstration of Nickel/Zinc Batteries for Electric Vehicle Propulsion", ANL Contract No. 31-109-38-4248, Energy Research Corporation, ANL/OEPM-81-11, March 1982.

14. "Annual Report for 1981 on Research, Development, and Demonstration of Nickel/Zinc Batteries for Electric Vehicle Propulsion", ANL Contract No. 31-109-38-4448, Exide Management & Technology Company, ANL/OEPM-81-12, March 1982.

15. "Annual Report for 1981 on Research, Development, and Demonstration of Nickel/Iron Batteries for Electric Vehicle Propulsion", ANL Contract No. 31-109-38-4292, Eagle-Picher Industries, ANL/OEPM-81-13, March 1982.

16. "Annual Report for 1981 on Research, Development, and Demonstration of Nickel/Iron Batteries for Electric Vehicle Propulsion", ANL Contract No. 31-109-38-4141, Westinghouse Electric Corporation, ANL/OEPM-81-14, March 1982.

17. N. P. Yao et al., "Development of Aqueous Batteries for Electric Vehicles - Summary Report, October 1977-September 1979," ANL/OEPM-80-5, June 1980.

18. N. P. Yao et al., "Development of Aqueos Batteries for Electric Vehicles - Summary Report, October 1979-September 1980," ANL/OEPM-81-5, February 1981.

19. T. G. Kaufmann and E. F. Leonard, "Modified Wilson Plots", Journal AIChE, 14, 110 and 421 (1968).

20. D. Bennion, "Literature Study of Separator Materials", under publication.

21. K. W. Choi and N. P. Yao, "An Engineering Analysis of Thermal Phenomena for Lead-Acid Batteries During Recharge Processes", ANL-77-24 (1977).

22. K. W. Choi and N. P. Yao, "Heat Transfer in Lead-Acid Batteries Designed for Electric Vehicle Propulsion Application", J. Electrochem. Soc., 126, 1321-1328 (1979).

23. W. M. Kays, "Convective Heat and Mass Transfer", McGraw-Hill, New York (1966).

24. J. P. Holman, "Heat Transfer", 5th Edition, McGraw-Hill, New York (1981).

25. Y. Jaluria, "Natural Convection Heat and Mass Transfer", Pergamon Press, New York (1980).

26. B. Carnaham, H. A. Luther, and J. O. Wilkes, "Applied Numerical Methods", John Wiley and Sons, New York (1969).

27. W. H. Tiedemann, and J. Newman, "Mathematical Modeling of Lead-Acid Cell", Unpublished, Globe Battery Division of Johnson Controls, Milwaukee, WI, Date Unknown.

28. J. S. Newman and C. W. Tobias, "Theoretical Analysis of Current Distribution in Porous Electrodes", Journal of the Electrochemical Society, 109, 1185 (1962).

29. L. G. Hill, C. M. Macal and F. R. Wyant, "An Evaluation of Nickel, Cobalt, Lead and Zinc Price and Distributional Flow Changes Assuming High Commercialization of Nickel/Zinc and Lead-Acid Electric Vehicles", ANL-OEPM-82-1, January 1982.

30. NRL Memorandum No. 4751, "Research on Lead-Acid Battery Electrodes", February 1982.

VII. PUBLICATIONS

1. "Development of Near-Term Batteries for Electric Vehicles - Summary Report, October 1977-September 1979", N. P. Yao, et al., ANL/OEPM-80-5, June 1980.

2. "Transient Current Distributions in Porous Zinc Electrodes in KOH Electrolyte", M. B. Liu, Y. Yamazaki, G. M. Cook, and N. P. Yao, ANL/OEPM-80-6, February 1981.

3. "Annual Report for 1981 on Research, Development, and Demonstration of Lead-Acid Batteries for Electric Vehicle Propulsion", ANL Contract No. 31-109-38-4206, Eltra - C&D Batteries Division, ANL/OEPM-81-8, March 1982.

4. "Annual Report for 1981 on Research, Development, and Demonstration of Lead-Acid Batteries for Electric Vehicle Propulsion", ANL Contract No. 31-109-38-4207, Exide Management & Technology Compnay, ANL/OEPM-81-9, March 1982.

5. "Annual Report for 1981 on Research, Development, and Demonstration of Lead-Acid Batteries for Electric Vehicle Propulsion", ANL Contract No. 31-109-38-4205, Johnson Controls Inc. - Globe Battery Division, ANL/OEPM-81-10, March 1982.

6. "Annual Report for 1981 on Research, Development, and Demonstration of Nickel/Zinc Batteries for Electric Vehicle Propulsion", ANL Contract No. 31-109-38-4248, Energy Research Corporation, ANL/OEPM-81-11, March 1982.

7. "Annual Report for 1981 on Research, Development, and Demonstration of Nickel/Zinc Batteries for Electric Vehicle Propulsion", ANL Contract No. 31-109-38-4448, Exide Management & Technology Company, ANl/OEPM-81-12, March 1982.

8. "Annual Report for 1981 on Research, Development, and Demonstration of Nickel/Iron Batteries for Electric Vehicle Propulsion", ANL Contract No. 31-109-38-4292, Eagle-Picher Industries, Inc., ANl/OEPM-81-13, March 1982.

9. "Annual Report for 1981 on Research, Development, and Demonstration of a Nickel/Iron Battery for Electric Vehicle Propulsion", ANL Contract No. 31-109-38-4141, Westinghouse Electric Corporation, ANL/OEPM-81-14, March 1982.

10. "Annual Synopsis of Battery Support Research, Fiscal Year 1980", ANL Office for Electrochemical Project Management, ANL/OEPM-81-3, May 1981.

11. R. Varma, G. N. Cook, and N. P. Yao, "Stibine/Arsine Emissions from Lead-Acid Batteries", Second U.S. DOE Environmental Control Symp., Reston, VA, March 17-19, 1980, Proc. Vol. 2, Nuclear Energy Conservation and Solar Energy, U.S. DOE Report CONF-800334/2, pp. 709-719, June 1980.

12. N. P. Yao, "Heat Transfer Modeling and Thermal Management of Batteries", AIChE Symp. Ser. 77 (204), 129-137 (1981).

13. R. Varma, G. Cook, W. Molinarolo, and N. P. Yao, "In-Situ Monitoring of Electrode Surface Phases by Laser Raman Spectroscopy During Anodization and Sulfation of Tetrabasicleadsulfate in Sulfuric Acid", Extended Abstracts Electrochem. Soc. Meeting, Minneapolis, MN, May 10-15, 1981, Vol. 81-1, pp. 902-905 (1981).

14. M. Liu, B. Faulds, G. Cook, and N. P. Yao, "Current Distribution in Porous Zinc Electrode II. The Effect of Electrolyte Conductance", Extended Abstracts Electrochem. Soc. Meeting, Minneapolis, MN, May 10-15, 1981, Vol. 81-1, pp. 14-16 (1981).

15. R. Varma, G. Cook, and N. P. Yao "Anodization and Sulfation of Tetrabasicleadsulfate in Sulfuric Acid: In-Situ Monitoring of Electrode Surface Phases by Laser Raman Scattering", J. Electrochem. Soc. 128(5), 1166-1168 (1981).

16. N. P. Yao, C. C. Christianson, and F. Hornstra, "Prospect of Advanced Lead-Acid, Nickel/Iron and Nickel/Zinc Batteries for Electric Vehicle Application", Proc. 16th Intersociety Energy Conversion Engineering Conf., Atlanta, GA, August 9-14, 1981, Paper No. 819320, Vol. 1, pp. 641-644 (1981).

17. W. H. DeLuca, R. L. Biwer, and N. P. Yao, "Effects of Constant-Current/ Constant Voltage Charge Parameters on Lead-Acid Traction Cell Performance" Proc. 16th Intersociety Energy Conversion Engineering Conf., Atlanta, GA, August 9-14, Paper No. 819331, Vol. 1, pp. 674-679 (1981).

18. M. B. Liu, G. M. Cook, and N. P. Yao, "Passivation of Zinc Anodes in KOH Electrolytes", J. Electrochem. Soc., 128(8), 1663-1668 (1981).

19. Y. Yamazaki and N. P. Yao, "Current Distributions in Soluble Battery Electrodes I. Theoretical", J. Electrochem. Soc., 128(8), 1655-1658 (1981).

20. Y. Yamazaki and N. P. Yao, "Current Distributions in Soluble Battery Electrodes II. Experimental", J. Electrochem. Soc. 128(8), 1658-1662 (1981).

21. Mark B. Knaster, "Vibrating Zinc Electrode in Alkaline Electrolyte", Extended Abstracts Electrochem. Soc. Meeting, Hollywood, FL, October 5-10, 1980, Vol. 80-2, pp. 250-252 (1980).

22. Basanta K. Mahato, "Lead-Acid Battery Expander II. Efficacy of the Microelectrode Technique in Predicting the Expander Activity on the Pasted Electrode Performance", Extended Abstracts Electrochem. Soc. Meeting, Hollywood, FL, October 5-10, 1980, Vol. 80-2, pp. 275-277, (1980).

23. G. L. Wierschem and W. H. Tiedemann, "Cycling Behavior of Lead-Acid Batteries for Electric Vehicles", Extended Abstracts Electrochem. Soc. Meeting, Hollywood, FL, October 5-10, 1980, Vol. 80-2, pp. 278-281, (1980).

24. J. F. Jackovitz and Joseph Seidel, "Structural Studies of Alkaline Nickel Electrode Powders", Extended Abstracts Electrochem. Soc. Meeting, Denver, Colorado, October 11-16, 1981, Vol. 81-2, pp. 66-67 (1981).

25. R. Rosey, "Westinghouse Nickel/Iron Battery Performance--1981", Proc. EVC Symp. VI, Baltimore, MD, October 21-23, 1981; Electric Vehicle Council, Washington, DC, 1981, Paper EVC No. 8103.

26. N. J. Maskalick, "Alkaline Nickel Electrode Voltage vs. Current Performance", Extended Abstracts Electrochem. Soc. Meeting, Denver, CO, October 11-16, 1981, Vol. 81-2, pp. 90-91 (1981).

27. Ray Hudson, "The Nickel/Iron Battery for Electric Vehicle Propulsion", Electric Vehicle News, Vol. 10, No. 4, pps. 12-17, November 1981.

28. S. Thornell and E. Pearlman, "Performance of Nickel Cathodes as Free Standing Electrodes in the Ni-Zn Vibrocel™", Extended Abstracts Electrochem. Soc. Meeting, Denver, CO, October 11-16, 1981, Vol. 81-2, pp. 103-105 (1981).

29. M. Klein, A. Leo, A. Charkey, "Simulated Vehicle Testing of Ni/Zn Batteries", Proc. EVC Symp. VI, Baltimore, MD, October 21-23, 1981; Electric Vehicle Council, Washington, DC, 1981; Paper EVC No. 8104.

30. B. K. Mahato, "Lead-Acid Battery Expander II. Expander Activity Correlation Between Microelectrode and Pasted Electrode", J. Electrochem. Soc. 128(7): 1416-1422 (July 1981).

31. Robert O. Carr, "National Battery Test Laboratory (NBTL)" American Laboratory, under publication.

32. Exide Management and Technology Company, "Exide Ni/Zn VIBROCEL™ Program", American Metals Market, under publication.

33. R. Hudson, "The Nickel/Iron Battery for Electric Vehicle Propulsion", EVC Symp. VI, sponsored by the Electric Vehicle Council, Baltimore, MD, October 21-23, 1981.

34. L. E. Vaaler, E. W. Brooman, and H. Fuggiti, "Design of Positive Electrodes for Lead-Acid Batteries to Minimize Weight and Voltage Losses", Symposium on Electrochemical Engineering and Optimization of Batteries for Electric Vehicles AIChE, Detroit, MI Conference, Aug. 16-18, 1981.

35. K. Gentry and R. Hudson, "Ni/Fe Batteries--An Alternate to Lead-Acid Electric Vehicle Propulsion", Proc. 16th Intersociety Energy Conversion Engineering Conference (IECEC) Atlanta, GA, August 9-14, 1981, pp. 674-679 (1981).

36. D. E. Bowman, "Globe Lead-Acid Battery", 4th DOE Battery & Electrochemical Contractors' Conference, Washington, DC, June 2-4, 1981.

37. R. Hudson, "Eagle-Picher Nickel/Iron Technology Features", 4th DOE Battery & Electrochemical Contractors' Conference, Washington, DC, June 2-4 1981.

38. R. Rosey, "Westinghouse Nickel/Iron Technology Features", 4th DOE Battery & Electrochemical Contractors' Conference, Washington, DC, June 2-4, 1981.

39. E. Pearlman, "Exide Long-Life Nickel/Zinc Vibrocel Battery", 4th DOE Battery & Electrochemical Contractors' Conference, Washington, DC, June 2-4, 1981.

40. H. Espig, "Gould Nickel/Zinc Battery", 4th DOE Battery & Electrochemical Contractors' Conference, Washington, DC, June 2-4, 1981.

41. D. T. Ferrell, "Exide Lead-Acid Battery", 4th DOE Battery & Electrochemical Contractors' Conference, Washington, DC, June 2-4, 1981.

42. H. R. Cash, "Eltra Lead-Acid Battery", 4th DOE Battery & Electrochemical Contractors' Conference, Washington, DC, June 2-4, 1981.

43. Anthony Leo, Martin Klein, and Allen Charkey, "Development of Low Cost Ni/Zn Electric Vehicle Batteries", 4th DOE Battery & Electrochemical Contractors' Conference, Washington, DC, June 2-4, 1981.

44. L. Ojefors, B. Anderson, and R. Hudson, "Nickel/Iron Batteries - Recent Results", New Energy Conservation Technologies and Their Commercialization Conference, sponsored by the International Energy Agency, Berlin, Federal Republic of Germany, April 6-10, 1981.

45. R. Hudson and E. Broglio, "Development of the Nickel/Iron Battery System for Electric Vehicle Propulsion", Proc. 29th Power Sources Conf., Atlantic City, NJ, June 9-12, 1980, published by the Electrochemical Soc., NJ, pp. 259-261 (1981).

46. C. C. Christianson, N. P. Yao, and F. Hornstra, "Near-Term Batteries for Electric Vehicles", Energy Technology VIII, Proc. Eighth Energy Technology Conf., Washington, DC, March 9-11, 1981, Government Institutes, Inc., Rockville, MD, pp. 616-623 (1981).

47. F. Hornstra, E. Berrill, P. Cannon, D. Corp, W. DeLuca, D. Fredrickson, L. Singer, C. Swoboda, C. Webster, C. Christianson, and N. P. Yao, "Battery Testing Results at the National Battery Test Laboratory", Fourth U.S. Dept. of Energy Battery and Electrochemical Contractors' Conf., Washington, DC, June 2-4, 1982, U.S. Dept. of Energy Report CONF-810642, pp. 65-71 (June 1981).

48. F. Hornstra, C. C. Christianson, P. Cannon, D. Fredrickson, C. Swoboda, C. Webster, and N. P. Yao, "The Impact of Regenerative Braking on Battery Performance and Energy Cost in Electric Vehicles in Urban Driving Patterns", Proc. Electric Vehicle Council Symp. VI, Baltimore, MD, October 21-23, 1981 (1981); Paper EVC No. 8106. Also publ. in Electric Vehicle News 10(4):8-11 (November 1981).

49. W. H. DeLuca, F. Hornstra, G. H. Gelb, B. Berman, and L. Moede, "System and Method for Charging Electrochemical Cells in Series", U.S. Patent No. 4,238,721, Dept. of Energy Case No. S-50,999, Issued December 9, 1980.

50. R. Varma, G. M. Cook, and N. P. Yao, "Anodization and Sulfation of Tetrabasicleadsulfate in Sulfuric Acid: In Situ Monitoring of Electrode Surface Phases by Laser Raman Scattering", J. Electrochem. Soc. 128(5), 1165-1168 (1981).

51. N. P. Yao "Electrochemical Technology for Energy and Resource Savings", Fourth U.S. Dept. of Energy Battery and Electrochemical Contractors' Conf., Washington, DC, June 2-4, 1981, U.S. Dept. of Energy Report CONF-810642 (Summ.), pp. 196-199 (June 1981).

52. N. P. Yao, "Near-Term Battery Support", Fourth U.S. Dept. of Energy Battery and Electrochemical Contractors' Conf., Washington, DC, June 2-4, 1981, U.S. Dept. of Energy Report CONF-810642 (Summ.), pp. 30-35 (June 1981).

53. N. P. Yao, "Near-Term Electric Vehicle Batteries", Fourth U.S. Dept. of Energy Battery and Electrochemical Contractors' Conf., Washington, DC, June 2-4, 1981, U.S. Dept. of Energy Report CONF-810642 (Summ.), pp. 3-6 (June 1981).

54. N. P. Yao, C. C. Christianson, R. C. Elliott, and J. F. Miller, "Status of Nickel/Zinc and Nickel/Iron Battery Technology for Electric Vehicle Applications", Proc. Nickel Secondary Batteries Session of the 29th Power Sources Symp. Electrochem. Soc., Atlantic City, NJ, June 10-12, 1980, pp. 247-256 (1981).

55. N. P. Yao, C. C. Christianson, and T. S. Lee, "Improved Lead-Acid Batteries -- The Promising Candidate for Near-Term Electric Vehicle", Proc. Secondary Batteries Session of the 29th Power Sources Symp., Electrochem. Soc., Atlantic City, NJ, June 10-13, 1980, pp. 261-265 (1981).

56. N. P. Yao, C. C. Christianson, T. S. Lee, J. F. Miller, and J. B. Rajan, "DOE's Electric Vehicle Battery Program -- Status of Improved Lead-Acid, Nickel/Iron and Nickel/Zinc Battery Developments in 1981", Proc. Electric Vehicle Council Symp. VI, Baltimore, MD, October 21-23, 1981; Paper EVC No. 8101 (1981).

57. N. P. Yao, C. C. Christianson, T. S. Lee, J. F. Miller and J. Rajan, "Near-Term EV Battery Project", Fourth U.S. Department of Energy Battery

and Electrochemical Contractors' Conference, Washington, DC, June 2-4, 1981, U.S. Dept. of Energy Report CONF-810642 (Absts.), pp. 7-13 (June 1981).

58. C. A. Swoboda, P. H. Cannon, F. Hornstra, R. J. Kmiec, and N. P. Yao, "Solid-State High Common-Mode Battery Cell Voltage Scanner", ANL/OEPM-81-7, 1981.

59. N. P. Yao, C. C. Christianson, F. Hornstra, G. Cook, W. DeLuca, T. Lee, J. Miller, J. Rajan, and C. Swoboda, "Development of Aqueous Batteries for Electric Vehicles -- Summary Report October 1979-September 1980", ANL/OEPM-81-5.

Distribution for ANL OEPM-82-5

Internal:

J. Arntzen
M. H. Bhattacharyya
J. Becker
E. S. Beckjord
M. Bernard
R. Biwer
R. Breyne
L. Burris
E. Carothers
A. A. Chilenskas
C. C. Christianson
K. Choi
G. Cook
D. Corp
W. DeLuca
F. Foster
D. Fredrickson
B. R. T. Frost
E. C. Gay
J. Geller
E. Hayes
F. Hornstra
R. Hogrefe
R. Kmiec
S. J. LaBelle
J. Lee
T. S. Lee
J. Marr
J. Miller
P. A. Nelson
D. Poa
J. Rajan
J. J. Roberts
H. Shimotake
T. K. Steunenberg
A. Tummillo
R. Varma
G. Vasilopulos
J. Weber
C. Webster
N. P. Yao (25)
ANL Contract File
ANL Libraries (2)
TIS Files (6)
ANL Patent Dept.

External:

DOE-TIC, for distribution per UC-94ca (281)
Manager, Chicago Operations Office, DOE
R. Gariboldi, DOE-CH
Chemical Engineering Division Review Committee Members:
   C. B. Alcock, U. Toronto
   S. Baron, Burns and Roe, Inc., Oradell, N. J.
   T. Cole, Jet Propulsion Lab.
   W. L. Worrell, U. Pennsylvania
E. P. Ames, TRW, Redondo Beach, CA
S. J. Angelovich, Duracell Inc., Tarrytown, NY
R. R. Aronson, Electric Transportation Mgmt, Inc., Ft. Lauderdale, FL
B. A. Askew, EPRI, Palo Alto, CA
R. Banes, Jet Propulsion Lab., Pasadena, CA
K. F. Barber, Office of Vehicle & Engine R&D, U.S. DOE, Washington, DC
S. Baron, Burns & Roe, Inc., Oradell, NJ
D. Barron, Delco Remy, Div. of GMC, Anderson, IN
R. R. Bassett, Sandia National. Labs., Albuquerque, NM
W. Bauer, KW Battery Co., Skokie, IL
E. S. Buzzelli, Westinghouse, Pittsburgh, PA
W. C. Beasley, Union Carbide Corp., Danbury, CT
D. H. Beilstein, St. Joe Lead Co., Clayton, MO
H. Bell, Arizona Public Service Co., Phoenix, AZ
J. Bene, NASA-Langley Research Center, Hampton, VA
J. R. Birk, EPRI, Palo Alto, CA
D. N. Bennion, Brigham Young Univ., Provo, UT
D. P. Boden, C & D Batteries, Plymouth Meeting, PA
B. Borisoff, Borisoff Engineering Co., Van Nuys, CA

J. Brennand, General Research Corp., Santa Barbara, CA
A. F. Brewer, Brewer Associates, Malibu, CA
P. Bro, Hyde Park Estates, Santa Fe, NM
J. Broadhead, Bell Labs., Murray, Hill, NJ
J. Brogan, Office of Energy Systems Research, U.S. DOE, Washington, DC
E. P. Broglio, Eagle-Picher Ind. Inc., Joplin, MO
P. J. Brown, Office of Vehicle & Engine R&D, U.S. DOE, Washington, DC
R. A. Brown, Eagle-Picher Industries, Joplin, MO
J. Bryant, Jet Propulsion Lab., Pasadena, CA
A. J. Burgess, Lucas Industries Inc., Troy, MI
R. Burns, Marathon Battery Co., Waco, TX
D. M. Bush, Sandia National Lab., Albuquerque, NM
W. P. Cadogan, Emhart Corp, Hartford, CT
E. J. Cairns, Lawrence Berkeley Lab., Berkeley, CA
E. A. Campbell, Electric Vehicle Consultants, Inc., New York, NY
A. J. Catotti, General Electric Co., Gainesville, FL
R. Clark, Sandia National Lab., Albuquerque, NM
R. A. Crawford, PPG Industries, Inc., Barberton, OH
S. DeGrey, Jet Propulsion Lab., Pasadena, CA
A. N. Dey, Duracell Inc., Burlington,MA
A. Dicker, Boyertown Auto Body Works, Boyertown, PA
W. J. Dippold, Office of Vehicle & Engine R&D, U.S. DOE, Washington, DC
T. P. Dirkse, Calvin College, Grand Rapids, MI
F. Donahue, Univ. of Michigan, Ann Arbor, MI
D. L. Douglas, EPRI, Palo Alto, CA
D. Dunoye, Reston, VA
M. Eisenberg, Electrochimica Corp., Mountain View, CA
C. English, Tech. Application Ctr., Albuquerque, NM
E. C. Essig, Long Island Lighting Co., Mineola, NY
G. H. Farbman, Westinghouse Electric Corp., Pittsburgh, PA
D. T. Ferrell Jr., Huntingdon Valley, PA
W. Feduska, Westinghouse Elec. Corp., Pittsburg, PA
R. J. Ferraro, Electric Power Research Inst., Palo Alto, CA
E. C. Fiss, Duke Power Co., Charlotte, NC
A. Fleischer, Orange, NJ
C. W. Fleischmann, C & D Batteries Div., Plymouth Meeting, PA
R. F. Fogle, Rockwell International, Anaheim, CA
L. R. Foote, Ford Motor Co., Dearborn, MI
J. S. Fordyce, NASA - Lewis Research Center, Cleveland, OH
H. A. Fuggiti, Exide Corp., Yardley, PA
B. Ganji, KW Battery Co., Skokie, IL
M. Genge, IIT Research Inst., Chicago, IL
J.H.B. George, George Consulting International, Inc., Concord, MA
L. J. Gerlach, USPS, R&D Labs., Rockville, MD
R. T. Gersteinberger, Northrop Corp. Aircraft Div., Hawthorne, CA
W. M. Gillespie, Tulsa, OK
J. R. Gilmore, Ford Motor Co., Dearborn, MI
G. Goodman, Johnson Controls, Inc., Milwaukee, WI
E. E. Gough, Lucas Industries Inc., Troy, MI
J. Gould, Unique Mobility Inc., Englewood, CO

L. B. Gratt, IWG Corp., San Diego, CA
G. Greenberg, EV/BT, Stamford, CT
D. Greider, Solar Central, Mechanicsburg, OH
P. P. Groumpos, Cleveland State Univ., Cleveland, OH
R. G. Gunther, General Motors Res. Lab., Warren, MI
R. Hall, Aerospace Corp., Washington, DC
W. Hamilton, General Research Corp., Santa Barbara, CA
K. Hardy, Jet Propulsion Lab., Pasadena, CA
G. S. Hartman, Exide Corp., Yardley, PA
J. L. Hartman, General Motors Res. Lab., Warren, MI
W. W. Harvey, Arlington, MA
E. A. Heintz, Airco Carbon, Niagara Falls, NY
E. Hellmann, Energy Development Associates, Madison Heights, MI
R. Hewitt, Jet Propulsion Lab., Pasadena, CA
A. Himy, Hyattsville, MD
J. S. Hodgman, General Electric Co., Gainesville, FL
R. Hudson, Eagle-Picher Industries, Inc., Joplin, MO
J. Hooker, Electric Motor Cars, Richardson, TX
H. R. Ivey, Wood-Ivey Systems Corp., Winter Park, FL
G. J. Janz, Rensselaer Polytechnic Institute, Troy, NY
J. Keith, Kaman Sciences, Colorado Springs, CO
J. J. Kelley, Willingboro, NJ
R. A. Keyes, Robert A. Keyes Associates, Martinsville, IN
R. S. Kirk, Office of Vehicle & Engine R&D, U.S. DOE, Washington, DC
A. R. Landgrebe, Office of Energy Systems Research, U.S. DOE, Washington, DC
C. M. Langkau, Union Carbide Corp., Westlake, OH
H. Lauve, Grosse Pointe, MI
D. Linden, Little Silver, NJ
E. Ling, Revere Research, Inc., Edison, NJ
J. E. Long, Jet Propulsion Lab., Pasadena, CA
J. S. Makulowich, Electric Vehicle Council, Washington, DC
L. Mapa, KW Battery, Skokie, IL
L. Marcoux, Tustin, CA
D. P. Martus, SAE, Warrendale, PA
V. R. Matricardi, Aerospace Corp., Washington, DC
C. E. May, NASA - Lewis Research Center, Cleveland, OH
E. Meeks, Derl Manufacturing Co., Compton, CA
L. F. Mercantanti, Advanced Vehicle Technology, Inc., Princeton, NJ
R. W. Meyerhoff, IAPC Research Center, Suffern, NY
R. P. Mikkelson, General Dynamics, Convair Aerospace Div., San Diego, CA
D. K. Miner, Copper Development Association Inc., Birmingham, MI
R. Miner, Office of Vehicle & Engine R&D, U.S. DOE, Washington, DC
L. G. Morin, Tarrytown, NY
D. R. H. Muller, Lawrence Berkeley Lab., Berkeley, CA
F. McLarnon, Lawrence Berkeley Lab., Berkeley, CA
J. S. Newton, Glen Ellyn, IL
A. O. Nilsson, SAB NIFE Inc., Lincoln, RI
L. G. O'Connell, Lawrence Livermore National Lab., Livermore, CA
J. M. Olsen, Detroit Edison, Detroit, MI
E. I. Onstott, Los Alamos National Lab., Los Alamos, NM
J. P. Overman, Hammond Lead Products, Inc., Hammond, IN

J. E. Pavlosky, NASA/Lyndon B. Johnson Space Center, Houston, TX
J. P. Pemsler, Castle Technology Corp, Woburn, MA
H. L. Recht, Rockwell International, Downey, CA
R. A. Rizzo, Johnson Controls, Inc., Milwaukee, WI
R. Rosey, Westinghouse Electric Corp., Pittsburg, PA
J. Rowlette, Jet Propulsion Lab., Pasadena, CA
C. J. Rowan, Philadelphia Electric Co., Philadelphia, PA
H. E. Ruskie, Naval Liason Unit, New York, NY
R. T. Schneider, RTS Laboratories, Gainesville, FL
H. N. Seiger, Harvey N. Seiger Associates, Waterford, CT
J. Seliber, Fluid Drive Engineering Co., Chicago, IL
E. T. Seo, The Gates Corp., Denver, CO
E. J. Steeve, Commonwealth Edison Co., Chicago, IL
I. Stein, JPL, Pasadena, CA
R. Strauss, Comsat Labs., Clarksburg, MD
J. Swisher, Office of Energy Systems Research, U.S. DOE, Washington, DC
P. C. Symons, Energy Development Associates, Madison Heights, MI
R. Thacker, General Motors, Warren, MI
G. Thiess, Turbo Electric, Richardson, TX
W. H. Tiedemann, Johnson Controls, Inc., Milwaukee, WI
H. A. Toulmin, Bloomfield Hills, MI
J. Trocciola, United Technologies, South Windsor, CT
G. W. Tuffnell, The International Nickel Co., Inc., Troy, MI
H. B. Urbach, David W. Taylor Navel Ship R&D Center, Annapolis, MD
G. Van Ommering, Ford Aerospace & Communications Corp., Palo Alto, CA
C. J. Venuto, C&D Batteries, Plymouth Meeting, PA
S. W. Vreeland, General Dynamics, San Diego, CA
G. J. Walker, Office of Vehicle & Engine R&D, U.S. DOE, Washington, DC
C. H. Waterman, U. S. Electricar Corp., Athol, MA
G. Way, Troy, MI
R. E. Weber, Kimberly-Clark Corp., Roswell, GA
C. E. Weinlein, Johnson Controls, Inc., Milwaukee, WI
H. B. West, McGraw-Edison Co., Bloomfield, NJ
R. Wilks, Lavelle Aircraft Co., Newtown, PA
G. A. Woolridge, Boeing Aerospace Co, Seattle, WA
V. Wouk, New York, NY
W. B. Wylam, Delco Remy Div, GMC, Anderson, IN
R. A. Wynveen, Life Systems, Inc., Cleveland, OH
Chloride Technical Ltd., Library, Manchester, England